NASA Conference Publication 2122
Part II


# Cryogenic Technology

Proceedings of
a conference held at
Langley Research Center
Hampton, Virginia
November 27-29, 1979



NASA

NASA Conference Publication 2122
Part II

# Cryogenic Technology

Proceedings of
a conference held at
Langley Research Center
Hampton, Virginia
November 27-29, 1979

National Aeronautics
and Space Administration

**Scientific and Technical
Information Office**

1980

## PREFACE

The proceedings of the NASA Conference on Cryogenic Technology held at Langley Research Center on November 27-29, 1979, are in this NASA Conference Publication.

The purpose of the conference was to provide early dissemination of new cryogenic technology generated by the design and construction of the National Transonic Facility and review of plans and programs essential to its operation and utilization. This was the first conference held specifically for this purpose.

The technical papers reported resulted from in-house efforts and covered a wide variety of subjects where new technology had evolved as a consequence of the cryogenic test environment. The general areas covered by sessions were:

I. Overviews
II. Mechanical/Structural Design
III. Systems Design
IV. Instrumentation
V. Model/Sting Technology

The efforts of the review committee, session chairmen, and speakers contributing to the technical excellence and professional character of the conference are especially appreciated.

Certain commercial materials are identified in the proceedings in order to specify adequately the materials investigated in the developmental work. In no case does such identification imply recommendation or endorsement of the product by NASA, nor does it imply that the materials are necessarily the only ones or the best ones available for the purpose. In many cases equivalent materials are available and would probably produce equivalent results.

Robert R. Howell
Conference Chairman

CONTENTS

Part I*



*Papers 1 to 16 are presented under separate cover.

SESSION III - SYSTEMS DESIGN
Chairman: Walter E. Bruce, Jr.



PART II

SESSION IV - INSTRUMENTATION
Chairman: Joseph F. Guarino

SESSION V - MODEL/STING TECHNOLOGY
Chairman: Clarence P. Young, Jr.

# SESSION IV - INSTRUMENTATION

# INSTRUMENTATION SYSTEMS FOR THE NATIONAL TRANSONIC FACILITY

Joseph F. Guarino
Langley Research Center

## OVERVIEW

Instrumentation and measurement systems are important elements in any complex research facility. The National Transonic Tunnel with its unique operational characteristics is clearly a complex facility and as such represents a significant challenge to wind tunnel instrument designers. This paper will briefly describe the instrument requirements imposed by the new testing environment, the instrument systems being provided for facility calibration and operation, and the research and development activities directed at meeting overall instrument and measurement requirements.

### New Design Requirements

The approach taken to achieve high Reynolds number test capability in the NTF was through a combination of cryogenic operation and increased pressure. These factors singly or together affected all instrument designs and in some instances created new measurement requirements. The impact of this new operating environment is clearly illustrated by the typical NTF operating envelope shown in figure 1. As a point of reference, the shaded area at the lower left depicts the operating range of existing transonic tunnels. The vertical scale is essentially proportional to temperature and covers a range varying from ambient down to 77 K (140°R). The cryogenic environment requires that instruments be developed capable of obtaining accurate data by direct operation at cryogenic conditions or by providing instruments with thermally controlled and conditioned enclosures. Both approaches have been pursued with success. Force balances have been developed and evaluated at cryogenic temperatures with extremely good results. Pressure instrumentation, on the other hand, requires a thermally controlled environment for successful operation at reduced temperature. High tunnel operating pressure, represented by the horizontal scale on figure 1, results in significantly increased model loads. This requires that force balances be designed with extremely high capacities--up to 85 000 N (19,000 pounds) of normal force as an upper limit. The high anticipated model loads also dictate the need for a model deformation measurement system which represents both a new and very difficult measurement requirement. Instrument design is further impacted by the wide operating range achievable in NTF represented by the area of the operating envelope in figure 1. This may require, for example, that more than one balance is needed to cover a particular test program if data accuracy is to be maintained. Although only the extreme and most severe test conditions and requirements have been discussed to this point, it should be emphasized that the tunnel can and will be operated at significantly less demanding conditions resulting in a less severe instrument design problem.

## NTF Instrumentation Systems

A new, complex wind tunnel such as NTF requires a high degree of instrumentation to bring the tunnel on-line and for subsequent research operation. Four basic measurement systems are provided which include facility calibration instrumentation, process monitoring instrumentation, research model instrumentation, and data acquisition. The first two are facility related and are required to bring the tunnel into operation and to monitor critical facility functions. Over 1500 individual measurements, as outlined on figures 2 and 3, have been identified for these two categories of instrumentation. A significant feature of this instrumentation is that most of it will be retained in the tunnel for subsequent tunnel calibration checks, with a significant portion to be selected and used in conjunction with research data acquisition.

The number and type of instrumentation channels for research data acquisition is shown on figure 4. Included are the familiar model related and tunnel parameter instrumentation typically required to acquire research data. Of note is the addition of a model deformation measurement system and the use of the newly developed Electronically Scanned Pressure Measurement System (ESP) for pressure model application. This list, although rather complete, can and no doubt will change as requirements change.

Data acquisition is a central function of any complex measurement system. The NTF data system complex, illustrated on figure 5, provides subsystems for research data acquisition, process monitoring, facility control, and data management. The key features of this system include redundancy provided by use of four identical computers and switchable peripherals, transfer of data among subsystems, real-time display, on-site posttest data analysis, a communication link to the Central Data Reduction Center, and national user access for pretest entry for test planning, software development, and debugging.

## Research Instrument Development

To meet the challenges imposed by the cryogenic and high pressure operation in the NTF, a comprehensive development program was required. A good portion of this work, addressing the measurement areas listed on figure 6, began about 4 years ago and is still ongoing. Considerable progress has been made to date in most areas and is reflected in separate papers covering the first five categories listed in figure 6.

Progress also has been made on the remaining items listed. Mach number and $LN_2$ flow measurement presented both stringent accuracy and time response requirements. Fast response digital quartz pressure transducers were selected for the Mach number system which meet control system response requirements and provide the $\pm 0.002$ Mach number uncertainty desired. For $LN_2$ flow measurement, the ultrasonic flowmeter was selected and is still undergoing test and evaluation. This sensor provides the fast response, accuracy, and dynamic range needed in the design of the NTF control system. Work is currently underway aimed at selecting and developing a suitable flow

visualization system for NTF. Facility design dictates that any system considered must be located within the plenum of the tunnel--which is at cryogenic temperature. Both schlieren and shadowgraph approaches are under consideration and problems of alinement, thermal effects on windows, and other system components are currently being investigated. In addition, a schlieren system has been designed for the Langley 0.3-Meter Transonic Cryogenic Tunnel which will provide for direct facility testing and system evaluation. In direct support of the instrument development activities and selection of facility instrumentation, a detailed measurement analysis was initiated. The ultimate, and ambitious, aim of the effort is to analyze the total wind tunnel measurement process--from sensor through final data. To date an analysis of critical tunnel parameter measurements has been made which directly aided in the selection of primary tunnel instrumentation.

The measurements listed in figure 6 certainly do not comprise all the anticipated NTF instrument requirements. Future activities will include development of flow diagnostic instrumentation, dynamic stability, side wall, and flow--through force balances, gust and flutter instrumentation, and fast response model pressure instrumentation. This list is certainly not complete and it is anticipated that additional new measurement requirements will be generated once the facility is operational.

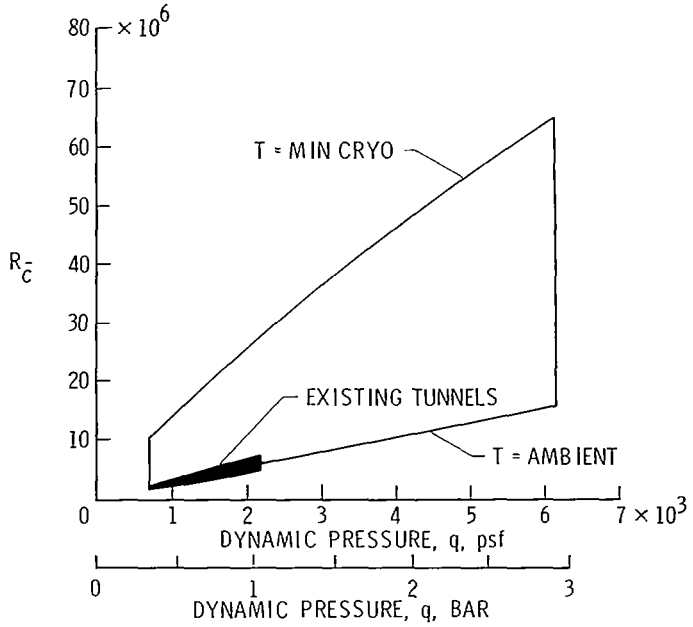


Figure 1.- Typical NTF operating envelope;
M = 0.90, c = 14.32 cm (0.47 ft).

- PRESSURE
  - WALL STATICS
  - CENTERLINE STATICS
  - CONTRACTION CONE RAKE
  - TEST SECTION RAKE
  - BOUNDRY LAYER RAKES
- TEMPERATURE
  - COOLING COIL SURVEY
  - TEST SECTION RAKE
- TURBULENCE & NOISE
- FLOW ANGULARITY

Figure 2.- Tunnel calibration instrumentation (1300 measurements).

- STRUCTURAL TEMPERATURES
- COMPONENT TEMPERATURES
- $LN_2$ FLOW
- PLENUM STATIC PRESSURE
- SCREEN DIFFERENTIAL PRESSURE

Figure 3.- Facility and process monitoring instrumentation (250 measurements).

- MODEL INSTRUMENTATION (CHANNELS)
  - FORCE (18)
  - PRESSURE (1024)
  - TEMPERATURE (80)
  - AOA (5)
  - STRAIN (10)
  - POSITION (12)
  - ACTUATORS (12)
  - FOULING CIRCUITS (2)
  - MODEL DEFORMATION
- TUNNEL PARAMETERS
  - MACH NUMBER
  - REYNOLDS NUMBER
  - DYNAMIC PRESSURE

Figure 4.- Number and type of instrument channels for initial operation.

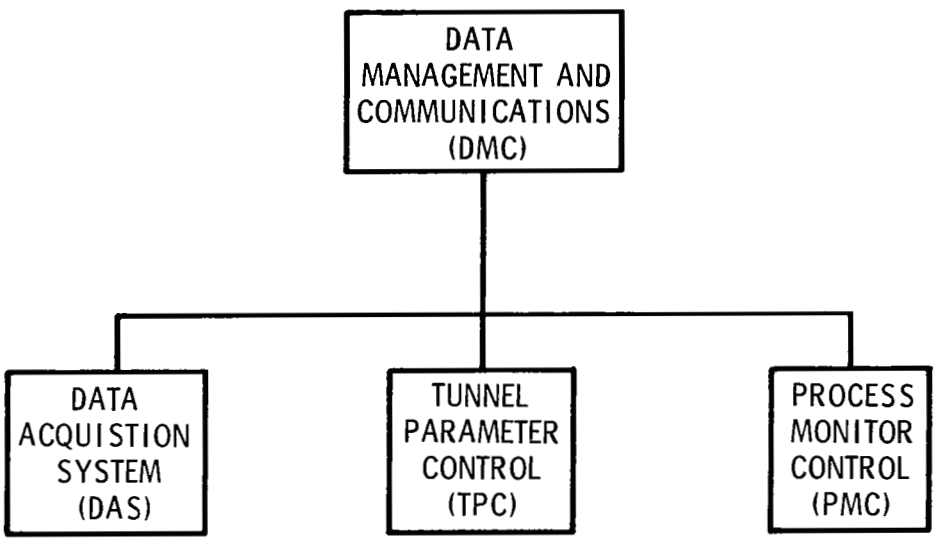


Figure 5.- Data system functional block diagram.

- FORCE BALANCES
- MODEL PRESSURE
- MODEL ATTITUDE
- TEMPERATURE
- MODEL DEFORMATION
- MACH NUMBER
- $LN_2$ FLOW
- FLOW VISUALIZATION
- MEASUREMENT ANALYSIS

Figure 6.- Ongoing research instrument development areas.

# THE NATIONAL TRANSONIC FACILITY DATA SYSTEM COMPLEX

Charles S. Bryant
Langley Research Center

## SUMMARY

The National Transonic Facility Data System Complex will be composed of four central processing units configured in a fully connected, distributed network. Each of the four computer systems in this network and the associated analog and digital data acquisition, recording, control, and display equipment are described and functional capabilities outlined.

## INTRODUCTION

Reliable instrumentation is essential when used in a major wind tunnel such as the National Transonic Facility (NTF). Also, due to operating costs, as high as $32 per second, automation is a prime consideration. Of this cost, over $31 per second is for liquid nitrogen which is injected into the circuit to permit testing at higher Reynolds number. The NTF (ref. 1) will be a 2.5-meter (8.2 feet) cryogenic, high Reynolds number, fan-driven, transonic wind tunnel and is scheduled for initial operation in 1982. It will operate at Mach numbers from 0.1 to 1.2, stagnation pressures from 100,000 to 900,000 $N/m^2$ (14.5 to 130 psia) and stagnation temperatures from 352 degrees down to 80 degrees Kelvin (174 to -316 degrees F). The maximum Reynolds number capability will be 120 million at a Mach number of 1.0 based on a reference length of 0.25 meters (10 inches). A perspective view of the facility is shown in figure 1.

This paper describes a multicomputer configuration which uses a fully connected distributed network to support the NTF data system complex measurement devices. The instrumentation will reach many areas of the facility. A plan view of the control room, test section, and significant transducer locations is shown in figure 2.

Actual implementation of this system will be carried out over a 6-year (1977-1982) period. Minor changes have evolved in the initial design concept and will continue to do so during this period. The conceptual hardware and functional software design is an LaRC effort.

Actual hardware manufacture, integration, and system software implementation have been contracted to several computer equipment vendors and computer related service companies.

## GENERAL DESCRIPTION OF THE DISTRIBUTED NETWORK

The complex will include four MODCOMP classic 7863 computers in a point-to-point, fully connected, distributed network configuration as shown in figure 3. The principle activities to be supported by the NTF instrument complex illustrated in this figure are (1) data base management and communications (DMC), (2) research measurement data acquisition and display (DAS), (3) tunnel parameter control (TPC), and (4) process monitoring (PMC). The distributed network approach was chosen to simplify definition of the functional software into more modular parts to allow implementation by the various groups involved in the design and to permit use of similar hardware configurations to improve availability and maintainability. This design will allow essential processes to continue when major hardware failures occur. This will be achieved by switching peripherals and essential input/output subsystems from faulty equipment to operational equipment and by permitting a degradation in response of non-time critical activities. Research measurement data acquisition and process monitoring are identified as essential functions which must be fully supported at all times.

The six serial I/O links between the four CPU's form the point-to-point communication lines of the network (fig. 3). Direct communication between all CPU's will be possible and indirect communication between one computer and the other two will be possible through the DMC and its links. Each of these high speed serial links can transfer 200K bytes per second.

The DMC and DAS will each contain 256K words (16 bit) of solid state MOS error correcting memory and the TPC and PMC will contain 128K words. Memory cycle time is 150 nanoseconds.

A group of DMC standard peripherals including three magnetic tapes, two line printers, two card readers, three teleprinters, four alphanumeric color CRT's and other graphic output devices will be individually or group switchable to the other computer subsystems through two dual access programable I/O bus switches and three dual access programable peripheral selector switches. The resulting functional hardware block diagram is shown in figure 4. The Research and Model Preparation DAU capability will be switchable through a programable dual access peripheral selector switch to the DMC when problems exist in the DAS CPU. A similar switching function on the PMC will switch the Control DAU to the TPC through a programable dual access I/O bus switch.

The DAS, TPC, and PMC subsystems will use an alphanumeric console CRT for system control and a large capacity disk unit for program and local data storage. Accumulated data will be transferred from the local disk to a magnetic tape unit for permanent storage. Since each local disk unit is of the removable cartridge type, if hardware failures occur the data accumulated at each system could be physically transferred to the data management CPU and recorded directly on magnetic tape after a test.

## DATA BASE MANAGEMENT SUBSYSTEM

The data base management and processing CPU will control access to all standard peripheral equipment, maintain master files of all processors, library routines, user application programs, archival data for comparison, and logical files of information for the other three computers.

Job entry control will be via a standard alphanumeric CRT. Two 1000 cards-per-minute card readers will allow input of logical files to be used by this CPU or passed to the other CPU's.

Listing devices will include two 600 lines-per-minute printers and three 120 character-per-second teleprinters. An interactive 0.569 x 0.432 meter (22.4 x 17 inch) plotter will provide report quality plots. A 48-cm (19 inch) diagonal, 512 x 512 resolution, interactive color graphic CRT will provide online presentation of test progress. Additional hardcopy output will be available on a 79 dots-per-cm (200 dots per inch), 28-cm (11 inch), electrostatic printer/plotter. Data collected during several weeks of a given test can be stored and recalled from the system archival files for comparison with data being obtained during a current tunnel run.

Recording devices will include three independently controlled magnetic tape units. These units are 9-track, dual density, 315/630 bits per cm (800/1600 bits per inch) with recording speeds of 60K or 120K bytes per second. The computer subsystems will all use the same type of system disk unit. This disk is a larger capacity unit with 166 megabytes capacity, 36-millisecond average access and 806K bytes transfer rate. The DMC will support posttest and real-time batch processing for obtaining listed or plotted data for planning follow-on tests.

This system also includes a communication handler to provide access to outside computers such as NASA's Instrument Research Division for program development, test, and debugging, and LaRC central computer complex for transmittal of test data for additional analysis and data reduction. Several other synchronous and asynchronous lines will be available at rates from 110 to 1200 baud to connect to other National computing facilities using line protocols supported by the complex. This access will be beneficial to groups scheduling tests which require customized processing and will permit program development debugging prior to the actual schedule test. It can also be used to return data to outside sources concurrent with the ongoing test.

## DATA ACQUISITION SUBSYSTEM

The DAS system as shown on the left side of figure 5 will be principally concerned with the management of 256 channels of research measurements from the tunnel and 64 channels of setup data from three model preparation areas. Each of these NEFF 620 series 200 amplifier per channel DAU's are separate and can operate independent of each other. Both of the DAU's will be located in the control room. The model preparation areas will each utilize a remotely located patchboard to provide shared access to the 64-channel DAU. Measurement

conversion will occur at rates up to 50,000 samples per second for each DAU. Each low-level differential channel will include programable gain ranges from 4 to 131 mV full scale and high-level ranges will cover the 0.262 to 8.388 volt range. DIP plug-type three pole active antialiasing filters with break frequencies of 1, 10, and 1,000 Hz are available. Automatic calibration for gain and offset will be under software control. Calibration signals are derived from an Electronic Development Corporation model 501 programable voltage standard. Overall inaccuracy of the DAU is estimated to be no more than 0.2 percent of full scale.

Future plans call for an interface to a 28-channel FM tape recorder to accommodate data bandwidths up to 20 kHz. A programable interface will route the FM output to the setup area DAU input to permit postrun digitization and playback current with test section data acquisition.

Discrete function inputs/outputs are available to provide controls to powered or movable models, drive numeric digital indicators with computed coefficients, run numbers, Mach numbers, etc., and accept inputs from user-oriented data acquisition control panels.

Five electronic pressure scanner (ref. 2) DACU's will be interfaced to the DAS via an IEEE 488 interface to accommodate tests requiring up to a thousand pressure measurements. These units scan all pressure ports electronically at a 14 kHz rate with 500 measurements per second throughput. Measurement inaccuracy is no more than 0.25 percent of full scale over a pressure range of 34,475 to 689,502 $N/m^2$ (5 to 100 psia).

## TUNNEL PARAMETER CONTROL SUBSYSTEM

The tunnel parameter control subsystem does not include an independent DAU but receives feedback information from the PMC DAU and its remote measurement units. The subprocess microcomputer controllers will be used for control of (1) Mach number, (2) stagnation temperature, (3) stagnation pressure, (4) drive speed, and (5) test section configuration and model control. Additional digital inputs/outputs with watchdog timer features will be made to insure that hardware interlocks and permissives are in order and that safe operation can be achieved.

## PROCESS MONITORING SUBSYSTEM

The process monitoring CPU, console CRT, and disk will be as previously described for the other CPU's. The DAU is the NEFF 620 series 400 low-level multiplexer and accommodates 256 channels, 16 of which are dedicated to calibrate inputs. Inputs will range from single-ended $\pm 8$ V full scale to low-level differential $\pm 4$ mV full scale. Sampling rate will be up to 10,000 measurements per second. The process variables monitored will include measurements such as tunnel pressure and stress, drive system temperatures and vibration, power consumption, etc. Discrete function input/outputs will drive alarms, bells, and visual displays to indicate out-of-limit conditions.

In addition to the local DAU, the PMC will interface to four Remote Measurement Units (RMU's) and three event sequencers. The RMU's will be located near the tunnel wall in four different locations and accommodate 160 measurements. Analog-to-digital conversion will take place in the RMU and the values digitally transmitted to the control room RMU interface where another RS-232-C link will carry the information to the PMC. The three event sequencers will each have an independent RS-232-C interface to the PMC. A total of 2600 discrete digital inputs and outputs will transmit process status to the sequencers from throughout the tunnel complex. This information will then be analyzed and sent to the PMC for processing and recording.

DAU switching similar to that previously discussed for the DAS will exist between the PMC and TPC.

## CONTROL ROOM FUNCTIONAL ACTIVITIES

The various control room functional activities are shown in figure 6. At position (1) will be the Tunnel Control Operator. He will operate and monitor the tunnel test controls for fan speed and inlet guide vane angle (these two determine Mach) and pressure and temperature. The equipment located in front and to the right will support this activity. A typical tunnel control operator CRT display is shown in figure 7.

The Model Control Operator (2) will operate and monitor controls for the model support system and test section configuration, which is determined by the reentry and wall flaps. His support equipment is in front and to the left of his location.

The Facility Engineer (3) will monitor the overall facility status and be the control room supervisor. He is concerned with such things as liquid nitrogen supply, electric power, overall facility safety, and general test coordination. A typical Facility Engineer CRT display is shown in figure 8. Beside him the Test Engineer (4) has graphic display CRT's to monitor the overall model test progress. He has control of the test from the standpoint of adding or deleting runs.

The Computer Operator (5) is responsible for initial startup of the computer systems, reconfiguration of the equipment if hardware failures occur, mounting tapes and disks, placing paper in plotters and line printers, and monitoring status from the computer operating system software.

The Applications Programer (6) prepares special software for real-time calculations and displays and for the posttest analysis and data formatting.

The Research Engineer (7) may be the model designer or his representative and will be viewing and interpreting the real-time data.

The Model Preparation Area Operator (8) will perform several of the previously discussed functions in the process of pretest model buildup and checkout which will include span test, calibration, leak testing, and other

activities as required by special model designs. A typical CRT display used by the Model Preparation Area Operator, Research Engineer, and Test Engineer is shown in figure 9.

## CONCLUDING REMARKS

The NTF could be an expensive wind tunnel to operate, principally because of the cost of liquid nitrogen. Therefore, reliable automation is essential. The distributed computer network along with hardware interlocks on critical controls should provide acceptable reliability. The shared peripherals approach has minimized hardware costs and will improve system maintainability since fewer peripherals are required. Certainly segmenting the instrumentation complex into subsystems will simplify the software design problems encountered in a single, large system approach. Also, the segmented approach permits more redundancy for enhancing reliability and fewer problems in defining and coordinating the efforts of software development teams. The smaller software structure in each separate CPU will be much more responsive to revision and enhancement.

## REFERENCES

1. Howell, R. H. and McKinney, L. W.: The U. S. 2.5-Meter Cryogenic High Reynolds Number Tunnel. Presented at the 10th Congress of the International Council of the Aeronautical Sciences, Oct. 3-9, 1976.

2. Juanarena, D.: A Distributed Processing High Data Rate Multiport Wind Tunnel Pressure Measurement System, for presentation at the 23rd International Instrumentation Symposium, May 1-5, 1977.

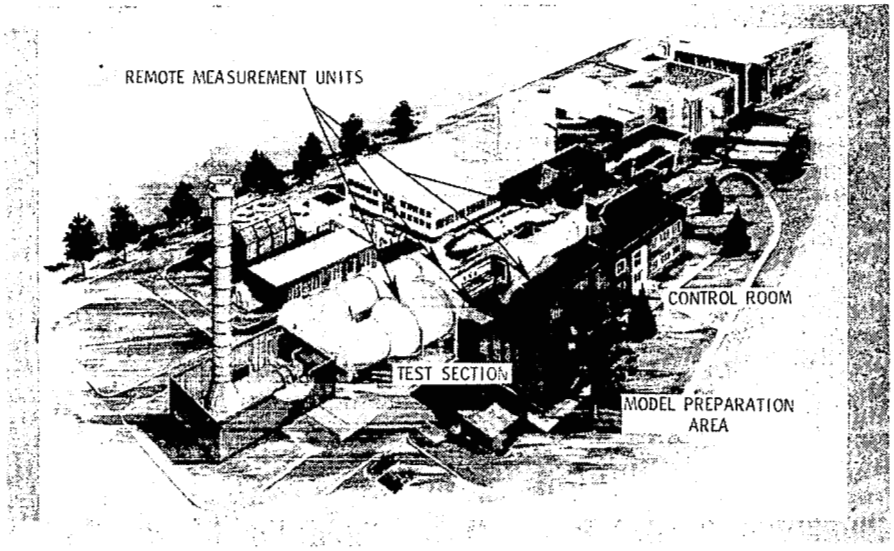


Figure 1.- Perspective view of NTF showing data system complex areas.

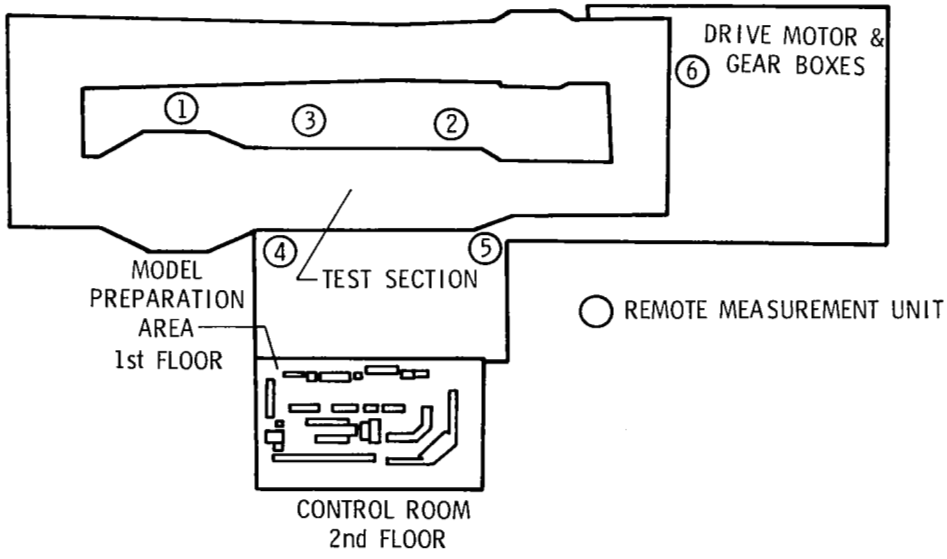


Figure 2.- Control room, test section, and remote measurement units.

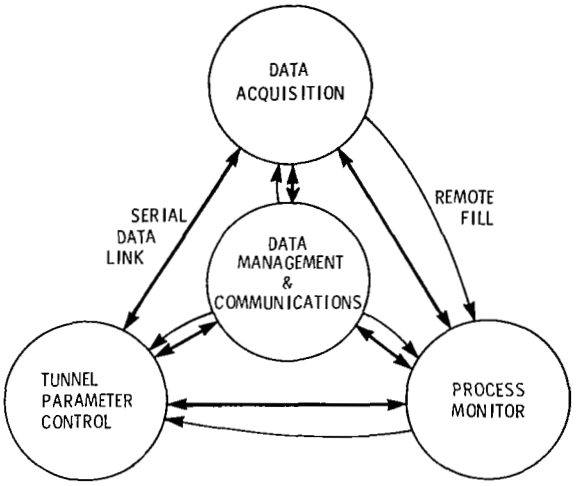


Figure 3.- Data system complex - fully connected distributed computer network.

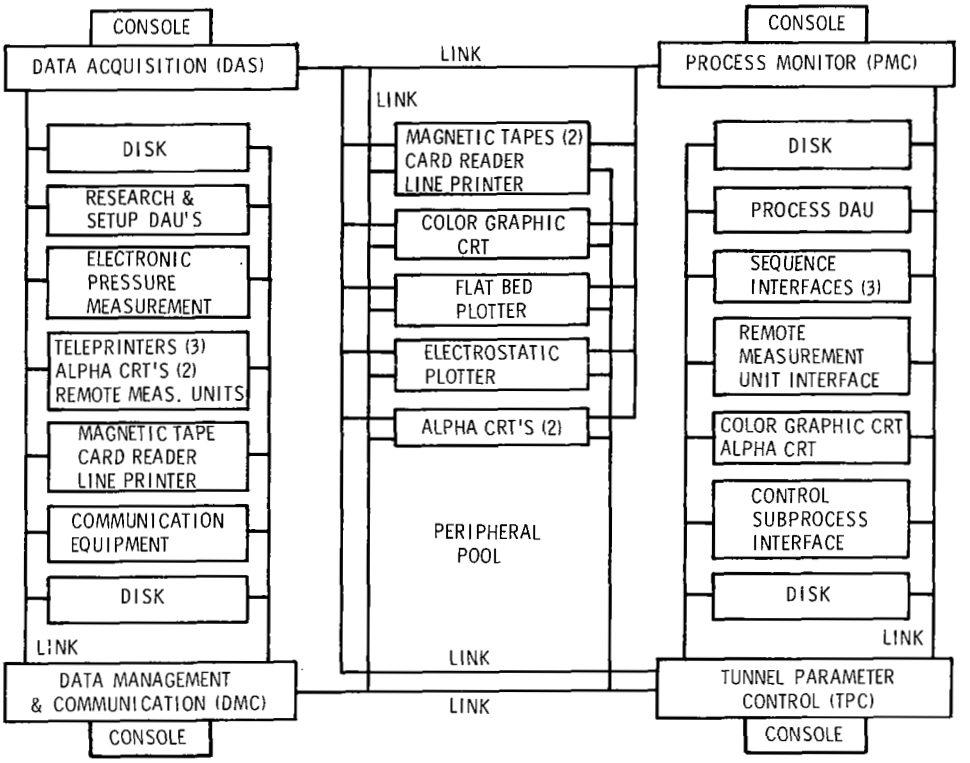


Figure 4.- Data system complex functional equipment connection.

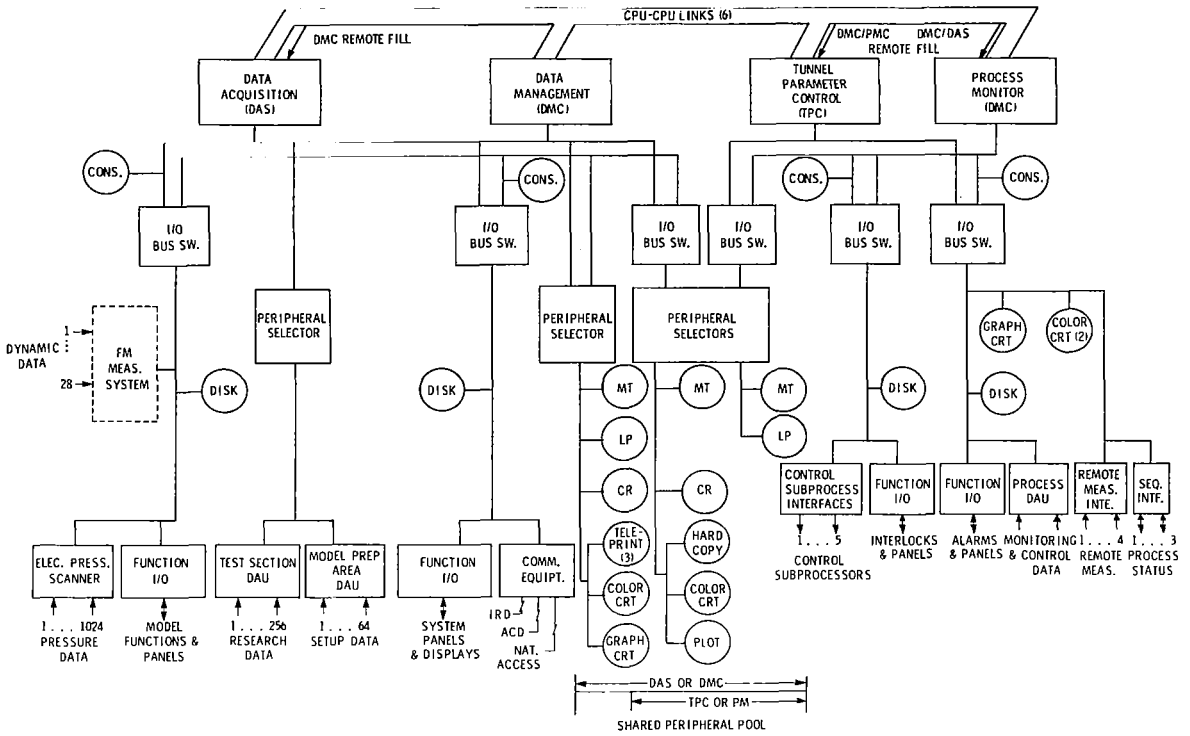


Figure 5.- NTF data system complex block diagram.

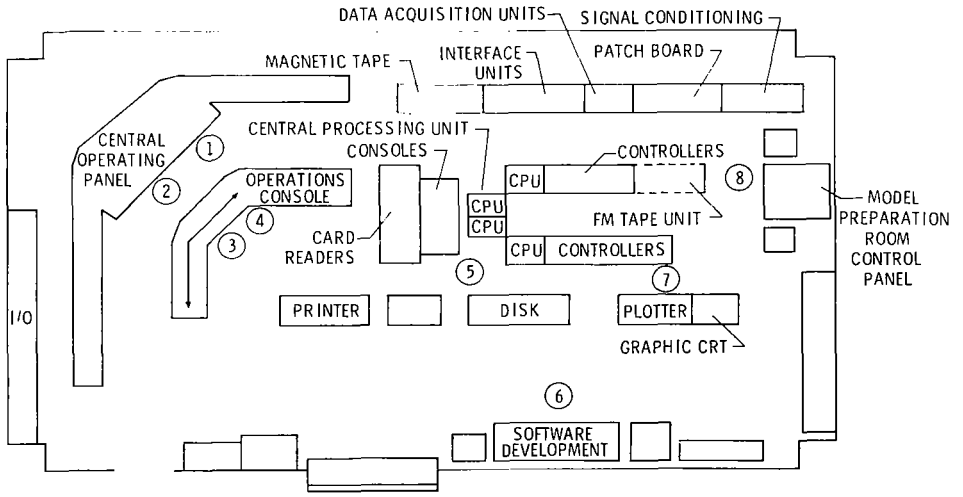


Figure 6.- NTF control room functional activities.

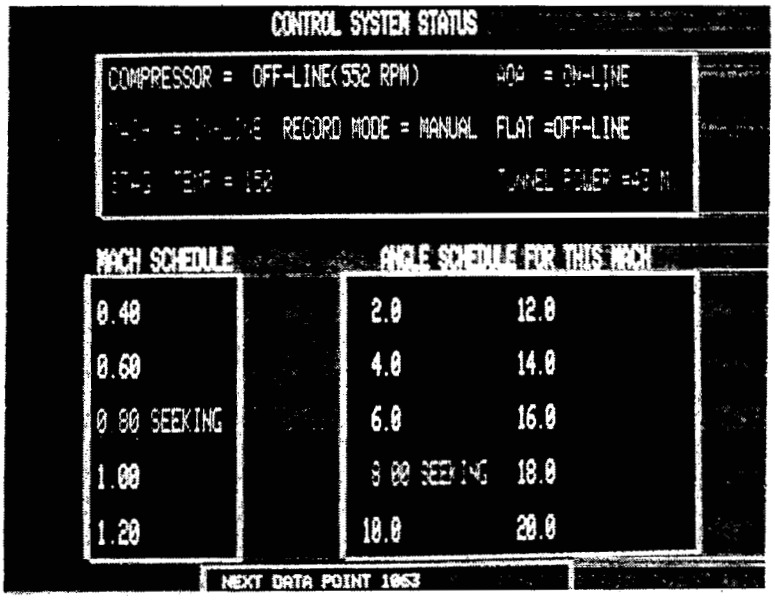


Figure 7.- Control system status CRT display.

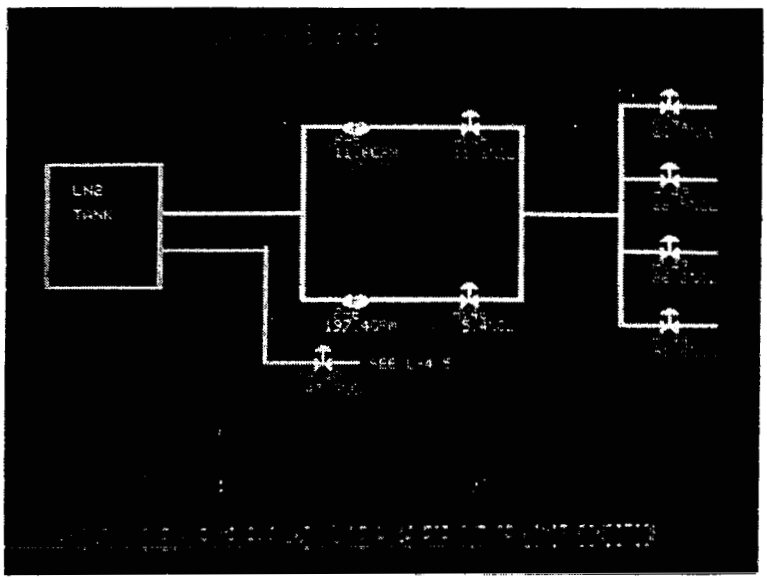


Figure 8.- Facility engineer CRT display.

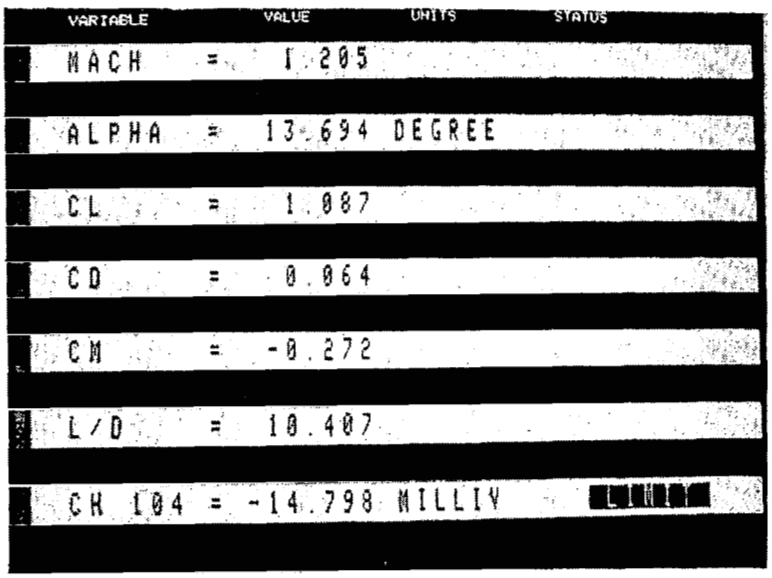


Figure 9.- Test engineer CRT display.

# CRYOGENIC WIND TUNNEL FORCE INSTRUMENTATION

Alice T. Ferris
Langley Research Center

## SUMMARY

NASA LaRC has developed one-piece strain gage force balances for use in cryogenic wind tunnel applications. This was accomplished by studying the effect of the cryogenic environment on materials, strain gages, cements, solders, and moisture-proofing agents and selecting those that minimized strain gage output changes due to temperature. Wind tunnel results obtained from the Langley 0.3-Meter Transonic Cryogenic Tunnel were used to verify laboratory test results.

## INTRODUCTION

The National Transonic Facility will impose rather severe requirements on the measurement of aerodynamic forces and moments. Not only does the cryogenic environment present an unusual surrounding for the force balance, but also, because of the tunnel's high density capability, the magnitude of the load to be measured can be much greater than that of a conventional tunnel of the same size. Although pushing the state of the art, initial studies indicate that one-piece, high-capacity strain-gage balances can be built to satisfy cryogenic requirements.

This paper will outline the work that has been accomplished at Langley Research Center while investigating the effects of the cryogenic environment on one-piece multicomponent strain-gage balances for use in the National Transonic Facility (NTF) at the National Aeronautics and Space Administration (NASA), Langley Research Center (LaRC), Hampton, VA. The NTF is scheduled to begin operation in mid-1982.

## BALANCE LOAD CONSIDERATIONS

Since the aerodynamic forces and moments will be much higher in the NTF as compared to a conventional tunnel of the same size, the balance load carrying capacity for a given size diameter becomes quite important. Design studies and experimental results have indicated to what degree the load carrying capacity can be increased and still meet existing rigid balance performance criteria. Figure 1 indicates the loads that can be carried by balances that range in size from 2 cm (1 inch) to 10 cm (3.5 inches) in diameter. A typical ratio of simultaneous loads on a six-component balance is presented in the table in the upper left of the figure. The lower curve was empirically derived from LaRC's existent balances which fall on or below this curve. It was found that the load-to-diameter ratio could be increased to that of the middle curve without degrading performance. Three balances have been constructed with this increased load capacity with good results. These balances, hereafter called high-capacity balances, are shown as the shaded circles on the middle curve. Three high-

capacity balances are shown on the figure as unshaded circles. The upper circle indicates that a balance will have to have a diameter of approximately 9 cm (3.4 inches) to carry the maximum loads expected in the NTF. A mid-range balance, designated NTF-101, has been fabricated and is currently being calibrated. This balance was designed for use in initial tunnel tests in the "pathfinder" model.

The maximum load carrying capacity for a given diameter can be increased further by using a three-component balance when this is appropriate. The maximum load carrying capacity of three-component high-capacity balances is depicted by the upper curve.

Two immediate consequences of going to high-capacity balances can be increased balance deflections and more critical or demanding calibration procedures. With increasing deflections, second-order interactions become more pronounced making it imperative that crossload combinations be applied in the calibration procedure. Evaluation of all second-order terms have long been an LaRC policy so this presents no new requirement.

The basic design of a balance for LaRC cryogenic applications will not differ significantly from that of LaRC conventional balances. Figure 2 is a drawing of NTF-101. The major design difference is that of minimizing areas of high stress concentrations, such as threads, and finding model and sting attachment methods that will maintain a good fit throughout the cryogenic temperature range and under large temperature gradients. Figure 2 shows the model and sting attachment designs chosen for NTF-101. Additional design work is continuing in this area.

A survey was conducted to find suitable balance materials for cryogenic use. If a balance is allowed to follow the wind tunnel operating temperature, the balance material must meet yield strength, fracture toughness, and impact strength requirements at temperatures down to 77 K ($139^{o}$R). Figure 3 presents information on two materials for LaRC conventional balances and three others being considered for cryogenic use.

The maraging steels, developed by International Nickel Company, are so named from the fact that the alloy is martensitic in the annealed condition and attains its ultra-high strength by a simple aging treatment. The numbers 200, 250, and 300 correspond to the typical yield strengths developed after aging (in English units).

The HP 9-4-25 steel is a member of a family of steels developed by Republic Steel Company to improve impact strength while maintaining high yield strengths.

A chromium-nickel-copper alloy developed by Armco Steel Company, 17-4 PH, achieves its strength and hardness through a combination of a martensitic transformation and precipitation hardening.

In-house testing is currently in progress to confirm these physical characteristics obtained from manufacturer's brochures and to obtain the fracture toughness at 77 K ($139^{o}$R) which is not now available. As anticipated, the change in yield and ultimate strength of balance materials at 77 K ($139^{o}$R) was

not a problem since most materials tend to be stronger at lower temperatures; however, they also tend to become brittle. The significant decrease in impact strength of the conventional balance materials at 77 K (139°R) indicates that these materials become quite brittle at cryogenic temperatures.

A criteria was established for NTF that required materials used at cryogenic temperatures to have impact strengths that meet or exceed the room temperature impact strength of conventional materials for that application. This criteria should insure that impact failures should not be any more of a risk in NTF than in a conventional wind tunnel. However, the number of metals that have both high yield strength and high impact strength at cryogenic temperatures is very limited.

Of the three candidate cryogenic materials, Maraging 200 has been chosen over Maraging 250 because of its higher impact strength at cryogenic temperatures and chosen over the HP 9-4-25 because it has a much simpler heat treatment procedure and is available in the smaller quantities we use. HP 9-4-25 must be bought in quite large lots.

Since the selection of Maraging 200, the shortage of cobalt, one of the constituents of the maraging steels, has seriously impacted the availability of this material. A survey of various steel companies' stock has disclosed a limited supply of Maraging 225 and a steel developed for the B-1 Project, Af1410. Both of these materials are being evaluated as to their suitability for cryogenic balance applications. Evaluation of other materials will continue until a satisfactory "backup" material is found or the maraging steels become more plentiful.

## TEMPERATURE CONSIDERATIONS

Because of the wide operating temperature range of the NTF, it is necessary to have a balance that either has well-behaved, definable, and minimized temperature-induced output over the entire temperature range or has temperature control to hold the surrounding environment of the balance to a known, stable condition. Both approaches are being evaluated. Since the preliminary wind tunnel studies, conducted in 1974, used a "standard" type balance and placed the most emphasis on thermal control; an evaluation program was undertaken in 1975 to see if improved strain gage technology could be used to produce a balance that would operate satisfactorily at cryogenic temperatures.

### Cryogenic Strain Gage Application Development

Comprehensive tests were made using test beams to determine the best combination of strain gages, adhesive, solder, wiring, and moisture-proofing on each of the candidate balance materials. This program was designed to define, and minimize where possible, the effects of the cryogenic environment on strain gage output when compared to its output at room temperature.

A Karma (K-alloy), SK-11, strain gage was made to our specifications for the selected balance material, Maraging 200. This gage with its self-temperature-compensation factor of 11 minimized the apparent strain output (no-load output due to temperature variation) over the entire cryogenic temperature range. Also, the change in gage factor (sensitivity shift) of the SK-11 gage was most nearly equal and opposite to the change in modulus of the Maraging 200, thereby minimizing sensitivity shift vs. temperature (1.1% shift 297 K (540°R) to 77 K (139°R)).

## Adhesive

Various adhesives were subjected to thermal shocks and large strains while the output was checked for evidence of permanent zero shifts or hysteresis under load. The selected epoxy-based adhesive that met these tests was M-610, a product of Micro-Measurements.

## Solder

Solder connections were subjected to a number of thermal cycles from 394 K (710°R) to 77 K (139°R). Three of the tested solders maintained their electrical integrity throughout the tests. However, the two solders containing antimony showed a tendency to become brittle and crystallize after long-term cryogenic exposure. A solder containing 1.8% silver, 570-28R, did not exhibit this tendency. Therefore 570-28R, marketed by Micro-Measurements was selected for cryogenic balance applications. The only undesirable characteristic of this solder is its high melting point 570 K (1030°R) that requires that greater care must be exercised when applying this solder to the small wiring and solder dots of the bridge wiring.

## Wiring

The wiring used for cryogenic applications is silver-plated copper wire with Teflon insulation. It was discovered during tests of connectors for cryogenic applications that a thermocouple effect was evident on one lead. A 15 μV (0.3% F.S.) shift over a temperature change of 180 K (325°R) was generated at the junction of one of the balance wires and one of the lead-in wires. This finding indicates that it may be necessary to check all wiring junctions in cryogenic balances for thermocouple effects that will introduce errors into balance output.

## Moisture Proofing

No moisture-proofing compound has been found that does not have some effect on apparent strain when applied over the strain-gage grid, although some were found that were much better than the standard ones previously used.

While research is continuing in this area, a rubber-based moisture-proofing compound, Micro-Measurements M-coat B, is being applied only to exposed terminals and wiring.

## BALANCE HRC-2

A balance designed specifically for evaluation was fabricated and gaged in accordance with the information obtained from the aforementioned testing and evaluation program. This balance, designated HRC-2, is shown in figure 4. It is a three-component balance (normal, axial, pitch) that is 2.54 cm (1.0 inch) in diameter and 21 cm (8.352 inches) long and is suitable for use in the Langley 0.3-Meter Transonic Cryogenic Tunnel. It is made of Maraging 200 steel and has SK-11 Karma gages that are installed using M-610 adhesive and 570-28R solder. M-coat B is applied to all exposed wires and terminals. In addition, HRC-2 has Minco thermofoil resistance heaters for thermal control and type T (copper-constantan) thermocouples for temperature readout.

The balance is wired as a "moment" balance. The sum of the outputs of the forward and aft bridges is proportional to the total moment applied to the balance while the difference of the two outputs is proportional to the applied normal force. Existing LaRC balances are wired to produce outputs that are directly proportional to normal force and pitching moment by having half of each bridge located in both the forward and aft cages. Since temperature gradients are most likely to occur along the length of the balance, a "moment" balance will more nearly result in having all four gages of a specific bridge at the same temperature, thus minimizing gradient effects and simplifying temperature compensation and data reduction.

## CALIBRATION

As previously mentioned, the high-capacity balances require extra precautions during calibration because of increased deflections. A second calibration requirement is that of calibrating at cryogenic temperatures. The test beam studies indicated that the output of a bridge designed for cryogenic use gives predictable and repeatable output at cryogenic temperatures. However, until a large number of balances have been calibrated at cryogenic temperatures to verify that the change in output due to temperature can be mathematically determined and expressed, it will be necessary to calibrate cryogenic balances over the entire temperature range.

As a preliminary attempt to obtain calibration data on HRC-2, the balance was mounted inside a cryogenic chamber and loads were applied to weight-pans that extended outside the chamber. While this method did not permit a full simultaneous loading of all components, it did provide enough data to show that the sensitivity change with temperature was within 0.05% of that predicted by the test beams. The interaction coefficients showed less than 0.1% full scale change with temperature in all but two coefficients (these differed by 0.4% F.S.). The apparent strain output of the balance

was nonlinear with temperature and appears to be a function of how well the four gages are matched. In addition, the forward and aft gage apparent strain output was very repeatable under steady state conditions while axial apparent strain showed more variation from test to test. Further testing is planned with both balances and test beams to determine the factors affecting apparent strain output. These calibration curves are presented in figures 5 and 6.

The selected approach for calibration makes use of a cryogenic calibration fixture that will replace the normal loading fixture, as shown in figure 7, is being readied for checkout. Liquid nitrogen passages and electric resistance heaters built into the fixture will allow normal calibration procedures and equipment to be used over the entire calibration load and temperature range.

## THERMAL CONTROL

Thermal control of a force balance is difficult since the insulators or heaters must not interfere with the transmission of the forces and moments across the measuring beams and, in addition, since the balance is constructed of a poor thermal conductor it is difficult to distribute heat evenly or contrive an effective heater control feedback circuit. At present, a cantilever convection shield extends forward over the balance acting as a baffle to reduce heat losses due to convection, resistance heaters are attached directly to the balance at several locations, and bakelite insulator inserts can be installed at the forward and aft attachment points.

Research is continuing in this area to reduce conduction and convection losses, to improve heat distribution, and to optimize the heater control feedback circuit.

## LANGLEY 0.3-METER TRANSONIC CRYOGENIC TUNNEL TESTS

### Test Setup

To verify and pull together the data and information developed in the laboratory, tests were conducted in the Langley 0.3-Meter Transonic Cryogenic Tunnel in July 1979 using balance HRC-2. The model and balance are shown in figure 8. The test conditions were chosen to give the same Reynolds number and thus the same aerodynamic input at two different temperatures, 300 K ($540^{\circ}$R) and 110 K ($198^{\circ}$R). The tests were made at Mach numbers of 0.3 and 0.5. Aerodynamic data were taken only after the tunnel and balance temperatures had stabilized. However, transient data were obtained while tunnel conditions were being changed from one test condition to another to get a feel for stabilization times for a balance of this size. It must be noted that stabilization time is dependent not only on the absolute temperature change but also on the tunnel conditions that alter convection cooling (i.e., pressure, Mach no., etc.). As shown in figure 8, a model-balance interface and a convection shield made of bakelite could be used to reduce heat loss

when the balance was heated. They would, however, also affect stabilization time when the heaters are off. Therefore, the transient data obtained represents only a small portion of the entire spectrum of possibilities generated by combinations of tunnel and model conditions.

In addition to the original test conditions, runs were made at an intermediate temperature, 200 K ($360^{\circ}$R), and at 300 K ($540^{\circ}$R) and 110 K ($198^{\circ}$R) at a constant dynamic pressure instead of Reynolds number. See figure 9. (The delta wing model configuration chosen is relatively insensitive to Reynolds number effects.)

## Test Results

On-line data were obtained using a programmable desk-top calculator interfaced to a 10-channel scanner, voltmeter, clock, and plotter. The 10 channels of data were: Tunnel temperature, four balance temperatures, two angle-of-attack transducers, and three balance components (pitch forward, axial, pitch aft). Nominal tunnel conditions were keyed in manually. Limited corrections were applied to the data including temperature corrections, interactions, tare loads, and sting bending. Figures 10 and 11 show examples of the preliminary data obtained using this system. The agreement shown at the three different test conditions for $C_n$ and $C_m$ is very good. The axial loads of this test were quite low compared to the design full-scale load of the axial component. Even so, the $C_A$-$\alpha$ data shown in figure 11 are still within the quoted $\pm$0.5% full-scale accuracy of the axial component. Several runs made using a blunt body that deliberately loaded the axial component to its design load capacity shows agreement much like that shown in figure 10.

It was hoped that the balance output could be corrected to account for both the sensitivity change and the zero load output change with temperature based on the laboratory tests. It was apparent quite early in the wind tunnel test series, however, that axial zero-load output variation with temperature was not following the predicted curve even though pitch forward and pitch aft were. Therefore, all data were reduced using a wind-off zero taken after stable tunnel conditions were reached. Sensitivity corrections were applied as determined from the laboratory tests.

The heater control instrumentation had no difficulty heating the balance bridges to 300 K ($540^{\circ}$R) at any tunnel condition or model insulator configuration. It was quite apparent, however, that the convection shield improved the stability of the output signal and reduced the power required to heat the balance. The front insulator had a much smaller effect as indicated by the following data:

Tunnel Conditions
M = 0.5 P = 1.2 bar T = 110 K (198°R)

| Convection shield and front insulator | Convection shield only | No insulators |
|---|---|---|
| 130 watts | 138 watts | 195 watts |

The heater feedback control circuit was not satisfactory. As mentioned previously, because the balance material is a poor conductor, the feedback sensor must be located near the resistance heater to minimize lag time in the control circuit. However, this arrangement means that the temperature control set point had to be set above the desired 300 K (540°R) in order to maintain a 300 K (540°R) reading at the bridge location. At each tunnel condition the heater control set point had to be manually adjusted until the required gage temperature was reached. Also, because of the rapid change in convection cooling, getting a heated-balance wind-off zero was very difficult since the balance temperature rose rapidly if the heater control set point was not adjusted manually to compensate for decreased thermal losses.

Transient data was taken on strip chart recorders. From these records it was determined that it took the tunnel approximately 40 minutes to go from the 300 K (540°R) operating conditions to the 110 K (198°R) operating conditions. The balance temperature tended to lag behind the tunnel temperature by about 10 minutes (see fig. 12). When the tunnel and balance temperatures are changing, as in the previous example, the stabilization time is a function of both the tunnel and balance heat transfer characteristics. In an effort to isolate only the balance heat transfer characteristics, the tunnel conditions were held at a constant 110 K (198°R), $P_t$ = 1.2 bar, M = 0.5 and the balance heaters that had been holding the balance temperature at 300 K (540°R) were turned off. In this test it took the balance 15 minutes to stabilize to tunnel temperature as shown in figure 13. To obtain another data point, the tunnel operating temperature was changed 30 K (50°R) (120 K (220°R) to 90 K (170°R)) as rapidly as allowed by operation specifications to check how the balance reacted to relatively small temperature changes. The tunnel took 3 minutes to stabilize at the new conditions and it took the balance 10 minutes to stabilize (fig. 14). These stabilization times are too large to meet NTF requirements. The effect of temperature transients results in undesirable and currently uncorrectable time dependent no-load zero shifts (or drift). This indicates that while balance temperature is changing it is not possible at this time to get accurate force data. Basic strain gage research utilizing test beams and small balances is currently underway to pinpoint the cause of these time dependent output shifts so they may be minimized or eliminated if possible. This effect will be investigated further with the cryogenic calibration fixture which allows independent control of the front and rear temperature inputs. This will allow us to deliberately introduce transients in order to determine the correction factors that must be applied to data obtained during transient temperature conditions. If this approach fails and test procedures cannot be modified to allow adequate stabilization time, thermal control will be a necessity.

## CONCLUDING REMARKS

One-piece multicomponent strain-gage balances have been designed to meet the requirements imposed by the NTF cryogenic environment. These balances are a result of extensive studies in the areas of design, balance materials, strain gages (including application techniques), and cryogenic calibration.

The laboratory and wind tunnel results indicate that these balances will yield reliable, repeatable, and predictable data from 300 K (540°R) to 110 K (198°R) under steady-state conditions.

Work is continuing in a number of areas to reduce the effect of the cryogenic environment even further where possible and to study the problems associated with transients and thermal gradients.

In addition, new and improved methods of thermal control are being studied to improve heat distribution, heater control, and insulators.

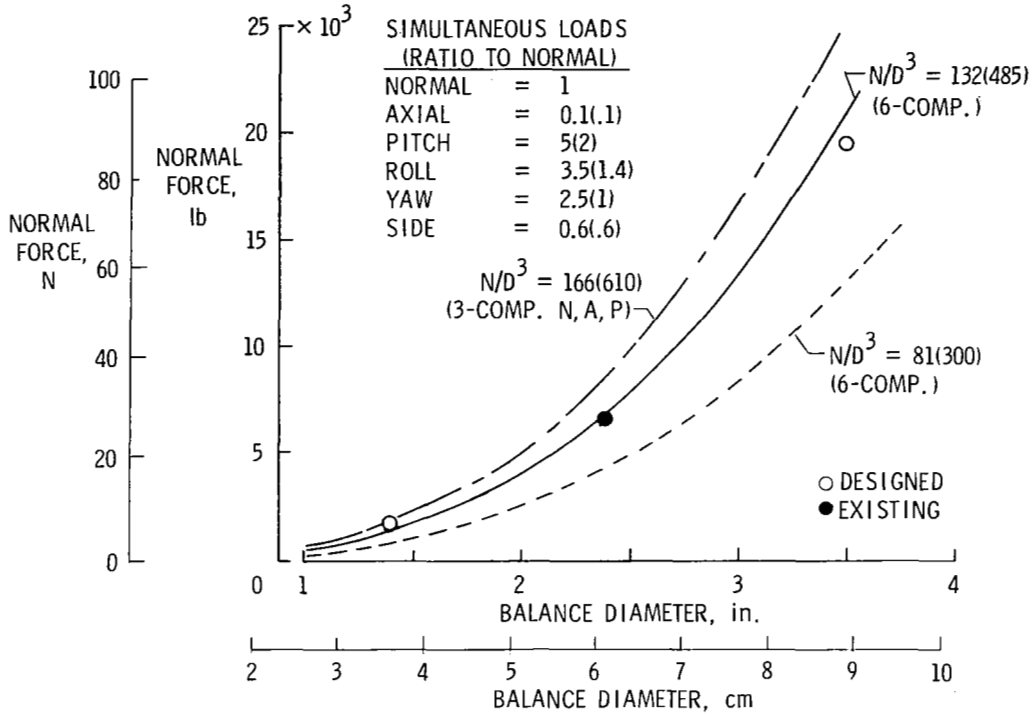


Figure 1.- Relationship between load carrying capacity (N) and diameter (D).

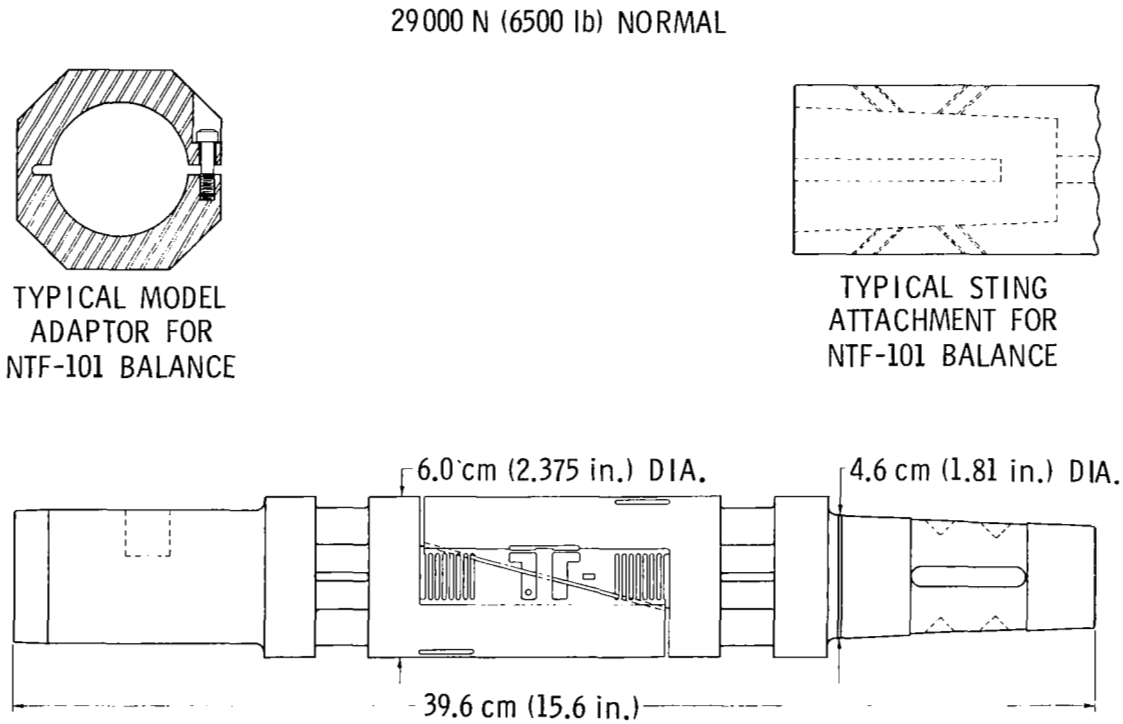


Figure 2.- Drawing of prototype balance NTF101.

## CRYOGENIC MATERIALS

| MATERIAL | TENSILE STRENGTH GPa (ksi) YIELD ROOM TEMP | TENSILE STRENGTH GPa (ksi) ULTIMATE ROOM TEMP. | IMPACT STRENGTH CHARPY-V J (ft-lb) ROOM TEMP. | IMPACT STRENGTH CHARPY-V J (ft-lb) $139^{0}R$ |
|---|---|---|---|---|
| MARAGING 200 | 1.46 (212) | 1.49 (216) | 49 (36) | 38 (28) |
| MARAGING 250 | 1.79 (260) | 1.86 (270) | 27 (20) | 18 (13) |
| HP 9-4-25 | 1.28 (185) | 1.38 (200) | 57 (42) | 34 (25) |

## CONVENTIONAL MATERIALS

| | | | | |
|---|---|---|---|---|
| 17-4 PH | 1.21 (175) | 1.31 (190) | 27 (20) | 4 (3) |
| MARAGING 300 | 2.00 (291) | 2.06 (299) | 34 (17) | 15 (11) |

Figure 3.- Strength and impact characteristics of balance materials.

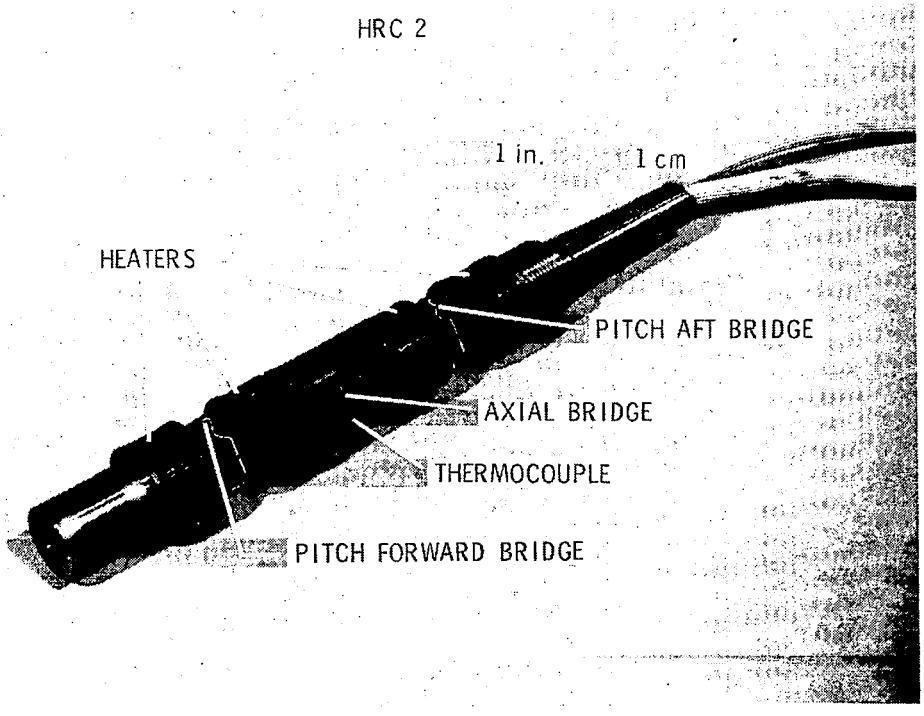


Figure 4.- Evaluation balance HRC-2.

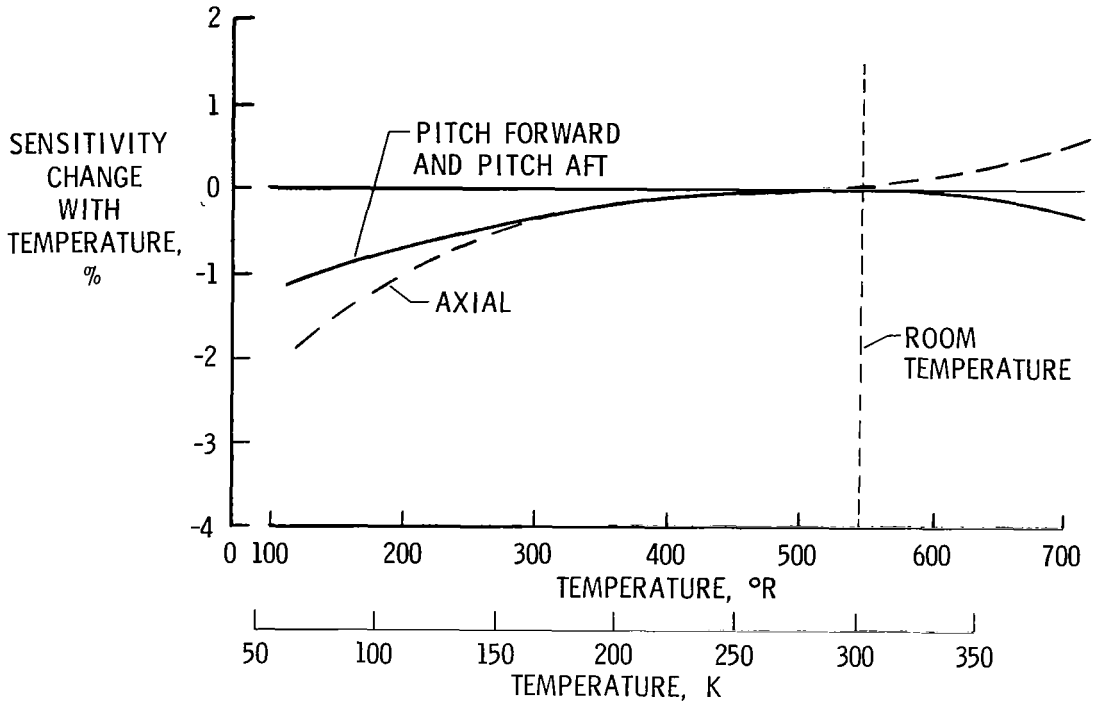


Figure 5.- Sensitivity change with temperature of evaluation balance.

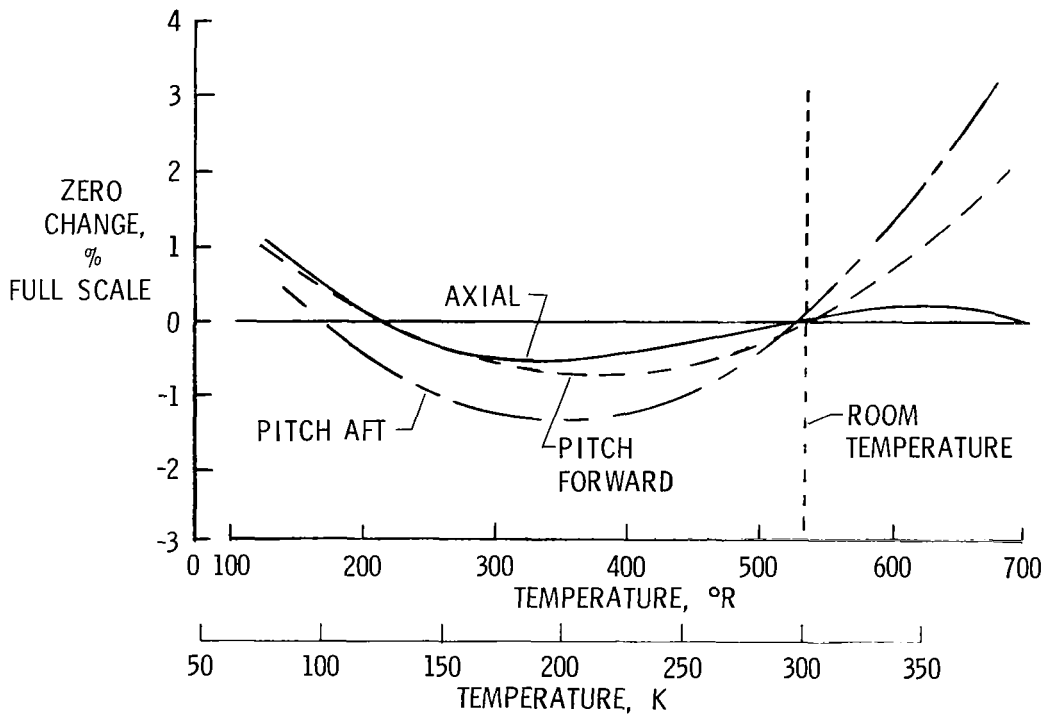


Figure 6.- Zero change with temperature of evaluation balance.

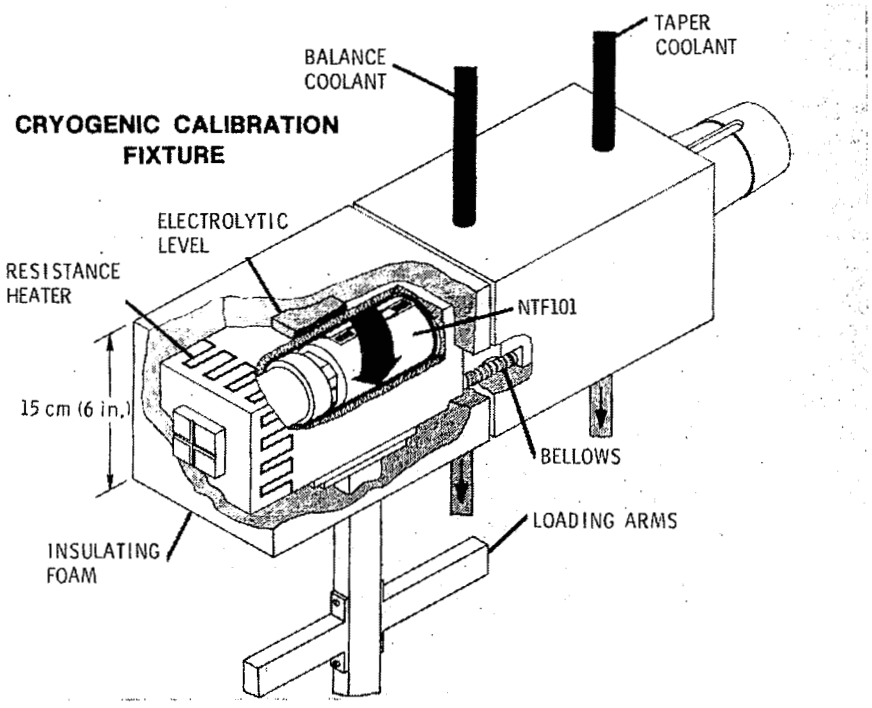


Figure 7.- Drawing of cryogenic calibration loading fixture.

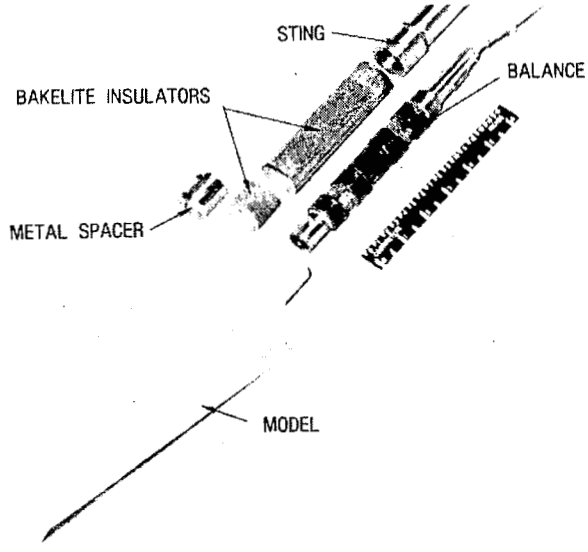


Figure 8.- Evaluation balance with model.

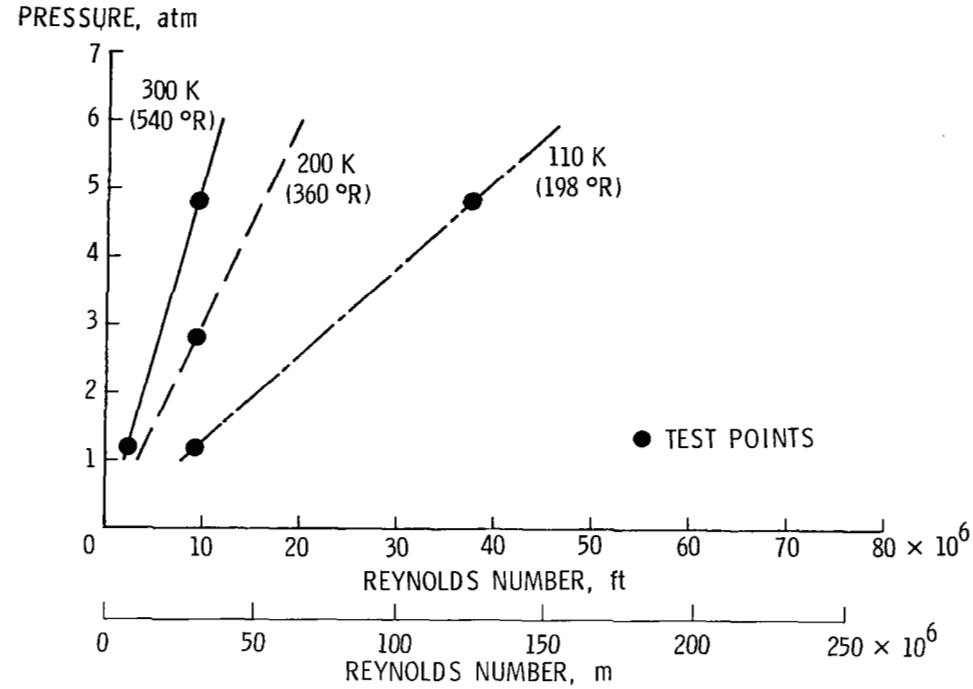


(a) M = 0.3.

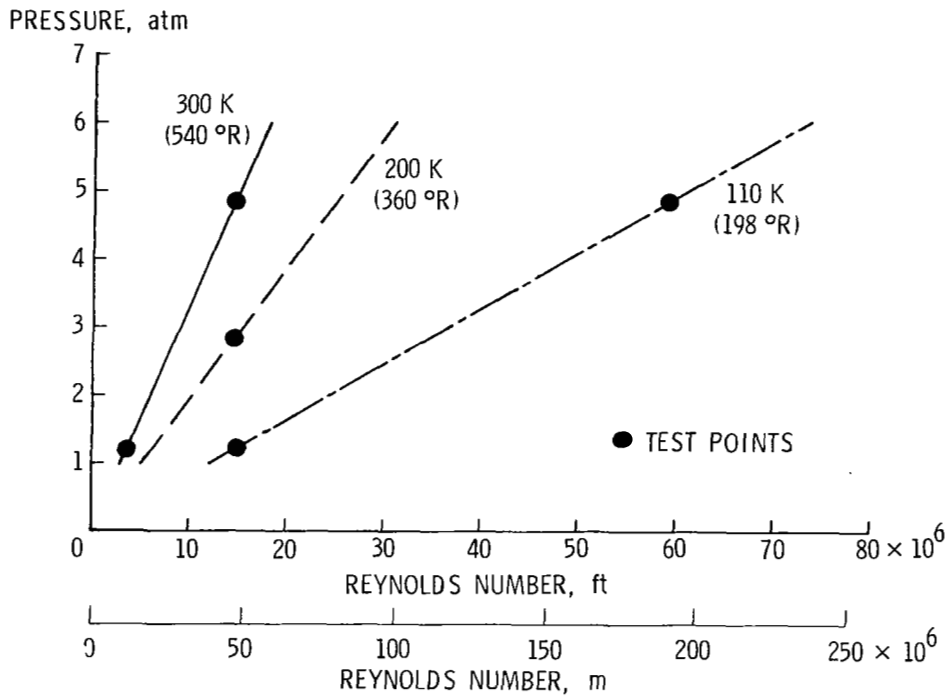


(b) M = 0.5.

*Figure 9.- Tunnel conditions for balance evaluation tests.*

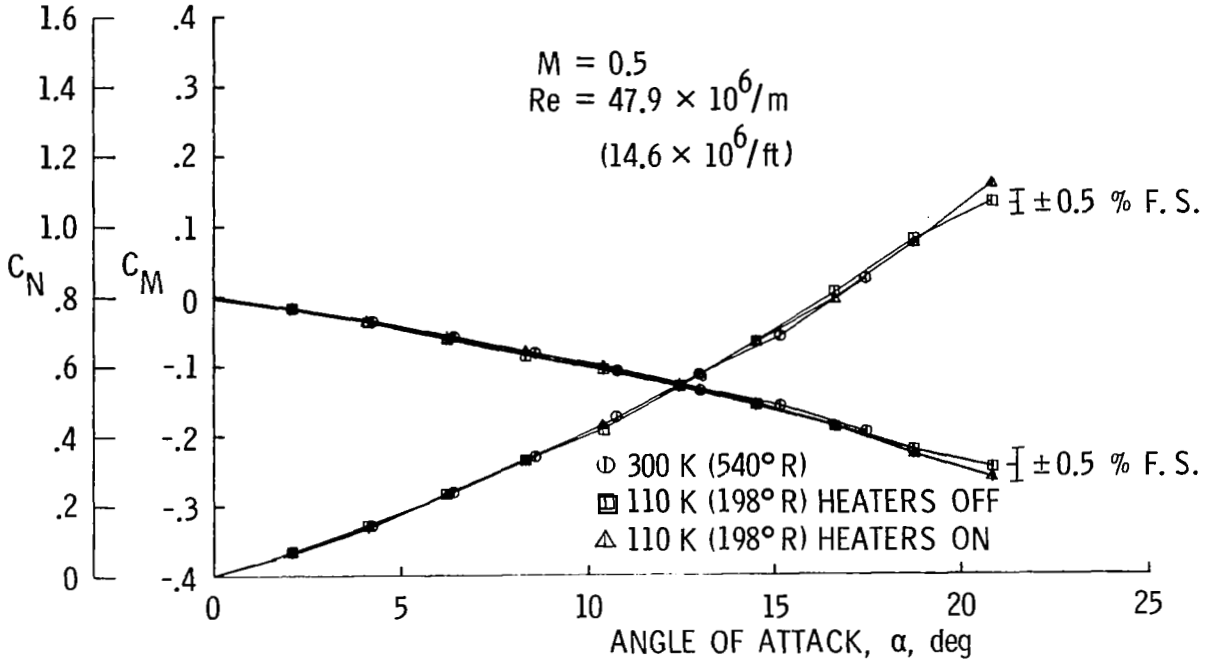


Figure 10.- Force balance data from tests in Langley 0.3-Meter Transonic Cryogenic Tunnel.

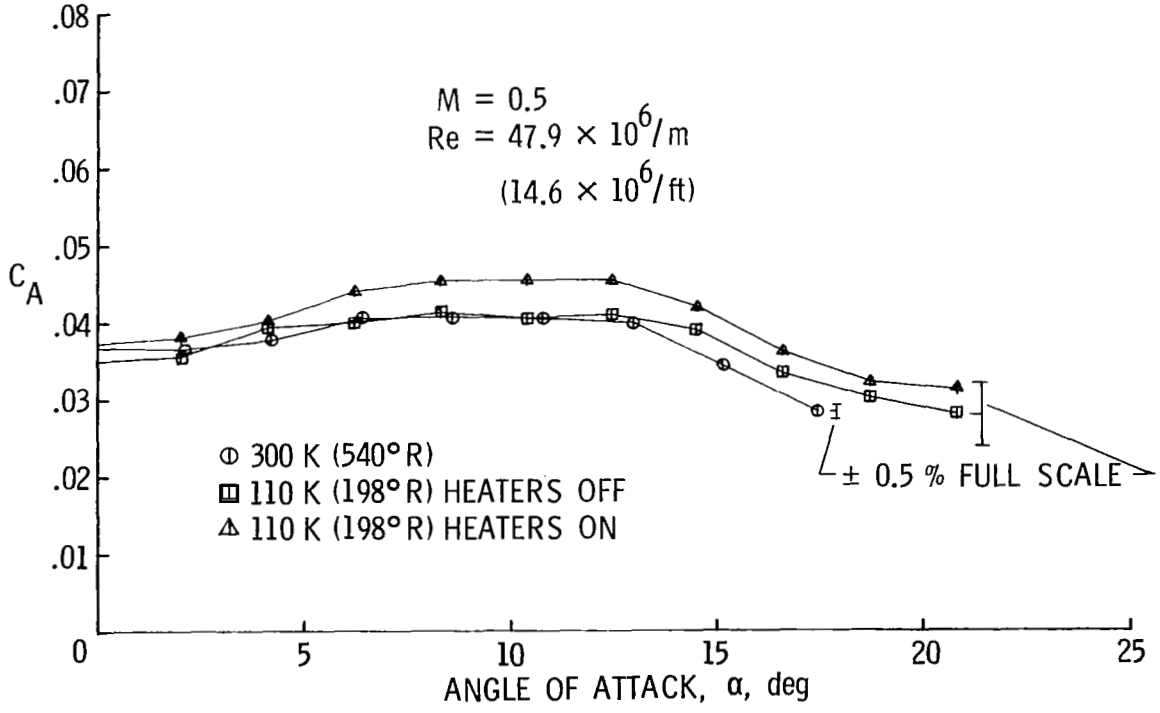


Figure 11.- Force balance data from tests in Langley 0.3-Meter Transonic Cryogenic Tunnel.

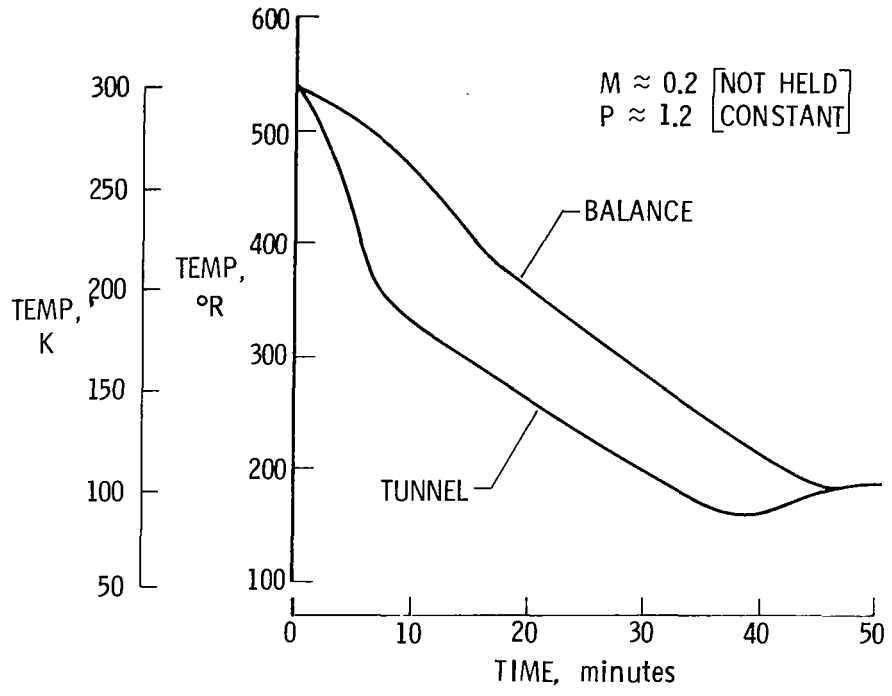


Figure 12.- Temperature response of balance and tunnel.

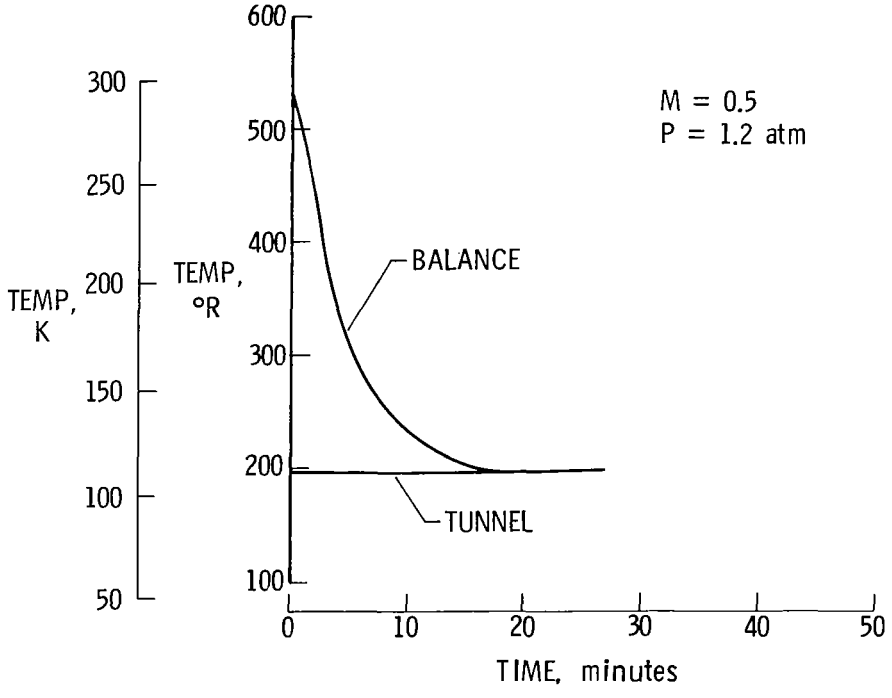


Figure 13.- Balance temperature response.

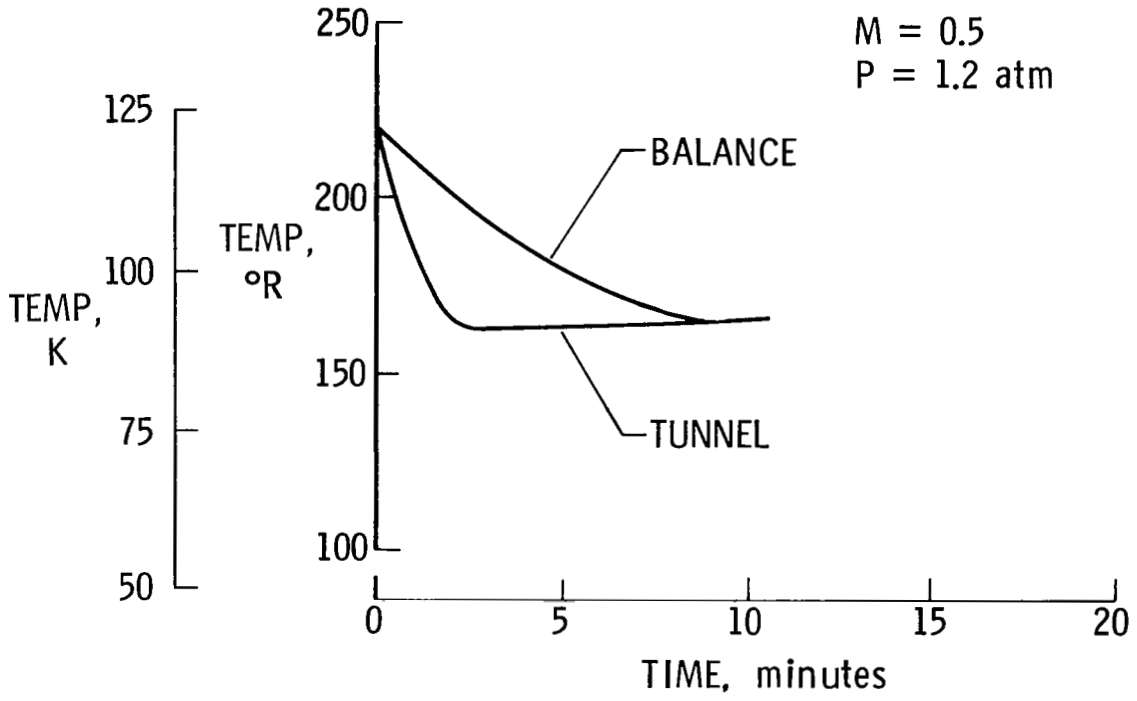


Figure 14.- Temperature response of balance and tunnel to small changes.

# PRESSURE MEASUREMENT SYSTEM FOR THE NATIONAL TRANSONIC FACILITY

Michael Mitchell
Langley Research Center

## SUMMARY

Over the last 4 years the Electronically Scanned Pressure (ESP) Measurement System has been developed at LaRC with the primary objective being to satisfy the pressure measurement requirements of the National Transonic Facility. The unique features of the ESP system are: High data rate (500 measurements per second); small size of sensor module (2.5 cm W x 5.6 cm L x 3.0 cm H); one sensor per port; and ability to perform in situ calibration. The system is capable of making a large number of pressure measurements simultaneously. The ESP system has undergone an extensive field evaluation and the overall results show that the ESP system can make measurements within 0.25 percent of full scale in a liquid nitrogen environment provided the module is contained in a temperature controlled enclosure (currently under development), maintained at a constant temperature, and the system is calibrated immediately before each measurement. The system is also compatible with the distributed processing concept.

## INTRODUCTION

With the advent of the National Transonic Facility (NTF), a more advanced and demanding level of measurement instrumentation is required. One of the more important parameters to be measured in NTF is the model pressure distributions and the facility flow quality. Until very recently, the commercially available pressure measurement systems did not satisfy the NTF pressure measurement requirements. Because of the high operational costs of this facility, the system must maintain a high data rate of at least 500 measurements per second (mps), which includes acquiring the research data, processing this data into predetermined engineering units and outputting the data to the data acquisition computer. The pressure measurement system must be capable of making a large number of measurements simultaneously. For instance, during the tunnel calibration, the system must make approximately 1100 measurements simultaneously. During the research studies, the system must provide the capability of making up to 1024 model pressure measurements. The sensing element of the system must be small in size so it can be placed in the models. This eliminates using long tubing lengths thereby improving the response time. The NTF requirements also dictate that the system maintain a measurement uncertainty of 0.5% of full scale or better and be compatible with the distributed processing concept. These requirements are listed in figure 1. Over the past 4 years an Electronically Scanned Pressure (ESP) Measurement System (fig. 2) has been under development at LaRC to satisfy these requirements.

## ESP System

The unique features of the ESP system are the one sensor per port concept and the capability to perform in situ calibration. The system is comprised basically of three components: the 32-channel Electronically Scanned Pressure Sensor Module, the Data Acquisition and Control Unit (DACU), and the Pressure Calibration Unit (PCU). A brief description of each of these components (refs. 1, 2, and 3) is as follows.

ESP sensor module.- A schematic representation of the ESP sensor module is shown in figure 3. The module consists of 32 solid state piezoresistive pressure sensors, a 32-channel analog multiplexer, an instrumentation amplifier, and a two-position pneumatic switch. This configuration allows each sensor to be addressed digitally to provide an amplified analog output as well as the capability of switching the pressure inputs from the measurement ports, $P_X$, to the calibrate port, $P_{cal}$, to provide in situ calibration. A photograph of a 32-channel ESP sensor module is shown in figure 4. The electronics package contains the instrumentation amplifier, a digital decoder, and the electrical inputs through spring loaded contacts to the sensor substrate. The sensor substrate contains 32 pressure sensors and four 8-channel differential multiplexers bonded to an aluminum substrate. The two-position pressure switch is a pneumatically activated slide plate with drilled holes that allow the calibration pressures to be routed to each of the pressure sensors through a common manifold in one position or to allow the $P_X$ pressures that are connected to the pressure port plate to be applied directly to the pressure sensors. The 32-channel ESP sensor module is a rectangular package 2.54 cm x 5.6 cm x 3.0 cm not including the pressure tubing. This module can be electronically addressed at over 100,000 times per second.

Data acquisition and control unit.- The DACU (fig. 5) is a microprocessor based instrument contained in a rack mountable enclosure that provides the following functions: (1) Data acquisition and storage, (2) sensor addressing, (3) control of PCU and reading of quartz gage pressure standard, (4) data reduction, (5) display of any pressure channel measurement in engineering units, (6) formatting and outputting of data to wind tunnel computer, and (7) interfacing to a host computer over interface bus.

The DACU under control of either the host computer or from the front panel key pad can perform in situ calibration, acquire pressure data, and reduce this data to engineering units for up to 512 channels of pressure measurements. The general purpose interface bus allows up to 14 DACU's to be paralleled to provide additional pressure measurement capability if a larger number of channels are required. Input parameters allow software selection of: (1) Calibration, data acquisition, data reduction, and data output subprograms, (2) number of channels of pressure inputs, (3) number of measurements to be averaged, (4) time delay between reading, and (5) number of frames of data to be acquired.

The raw data acquisition rate of the DACU is approximately 20,000 measurements per second (mps) for single point readings and approximately 10,000 mps

for time averaged readings. The overall data throughput rate for single point raw pressure readings is approximately 5,000 mps and 500 mps for single point measurement output in engineering units.

Pressure control unit.- The PCU (fig. 2) under control of the DACU provides the following functions: (1) Applies control pressures for pneumatically switching the ESP sensor modules to either the measurement or calibrate position and (2) applies three calibrate pressures sequentially to each of the ESP sensor modules.

The PCU contains three compound pressure regulators that allow each calibration pressure to be set manually in a range from $3.447 \times 10^3$ N/m$^2$ (0.5 psia) to $6.895 \times 10^5$ N/m$^2$ (100 psia), and a high accuracy (0.03% FS) quartz pressure gage for remote measurement of these calibration pressures by the DACU. The PCU can be operated up to 76.2 m (250 ft) from the DACU so that it can be located as close as possible to the ESP sensor modules to minimize calibration time.

## ESP Facility Tests

Over the past year, an extensive field evaluation of the ESP system has been undertaken to determine the reliability and capabilities of the ESP system and to determine its performance relative to conventional mechanically scanned pressure measurement systems. The evaluations covered a large spectrum of facilities and test conditions (see fig. 6), with full scale pressure ranging from $3.477 \times 10^2$ N/m$^2$ absolute (0.05 psia) to $2.068 \times 10^5$ N/m$^2$ absolute (30 psia). The test requirements ranged from using one 32-channel ESP sensor module outside the plenum chamber to using 21 32-channel sensor modules inside the test model.

Throughout the field evaluation, the ESP system did not experience any performance failures. The overall results of the various tests show that the ESP system can make the required pressure measurements with measurement accuracy comparable to the existing scanning type pressure measurement techniques, and can make the measurements at least 48 times faster.

## Cryogenic Environment Test

Tests were made in the laboratory to determine the ability of the ESP system to perform in a temperature controlled enclosure with a cryogenic external environment. The ESP sensor module was placed in a temperature controlled enclosure which consisted of a 28-ohm heater box covered with 2.54-cm-(1-in.) thick styrofoam. All the electrical leads and pneumatic tubes were fed through the styrofoam to the module. The enclosure was placed in the cryogenic environmental chamber at 297 K. The pressure sensors in the ESP module were calibrated and a set of measurements was taken.

The average zero differential pressure output was computer to be approximately 0.06 percent of full scale for the 32 sensors. The chamber was

- HIGH DATA RATE
  - 500 mps
- LARGE NO. OF PRESSURE MEASUREMENTS
  - 1103 TUNNEL CALIBRATION PRESSURES
  - 1024 MODEL PRESSURES
- SMALL SIZE
  - FOR THOSE PRESSURE SENSORS LOCATED IN MODEL
- HIGH ACCURACY
  - 0.5% F. S.
- COMPATIBLE WITH DISTRIBUTED PROCESSING CONCEPT

Figure 1.- General requirements for NTF pressure measurement system.

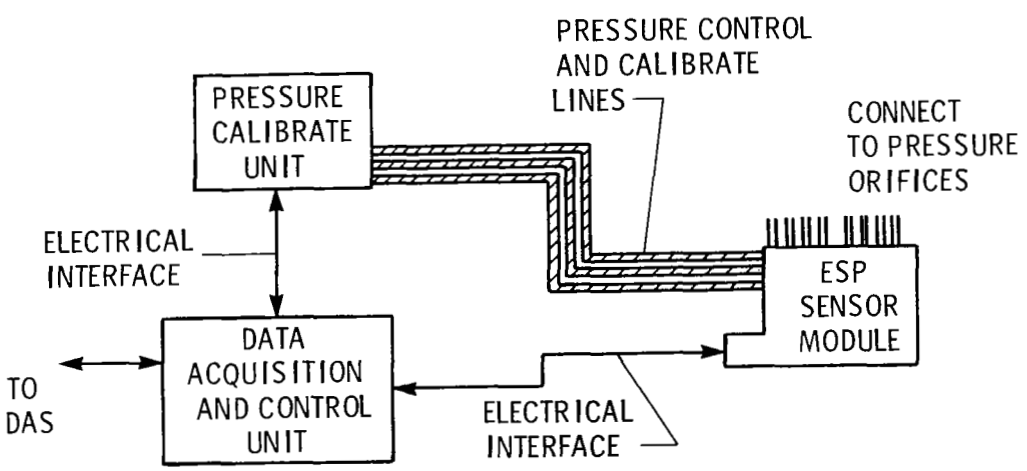


Figure 2.- Electronically scanned pressure measurement system.

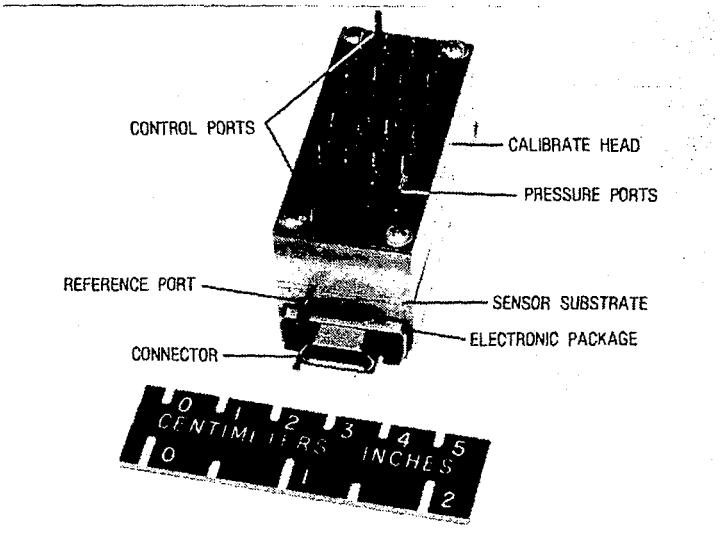


Figure 3.- 32-channel electronically scanned pressure sensor module.

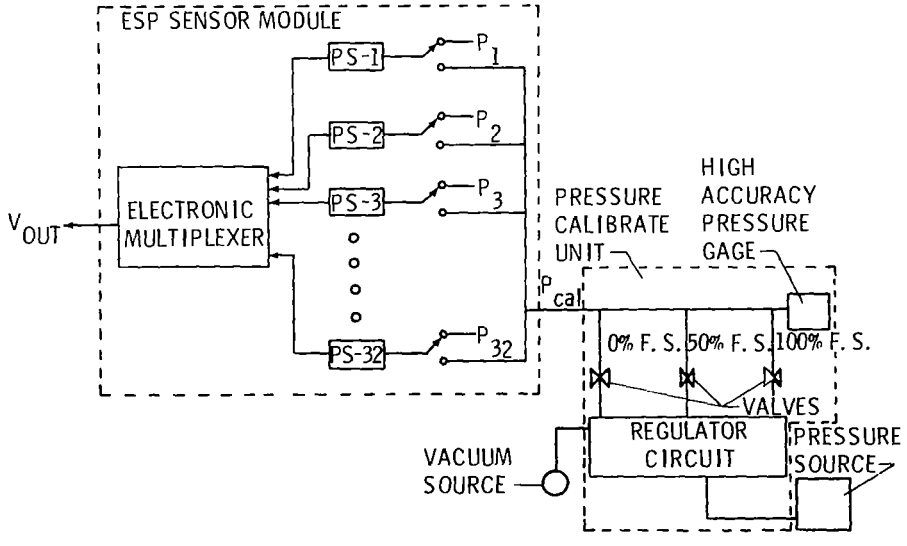


Figure 4.- Schematic representation of ESP sensor module.

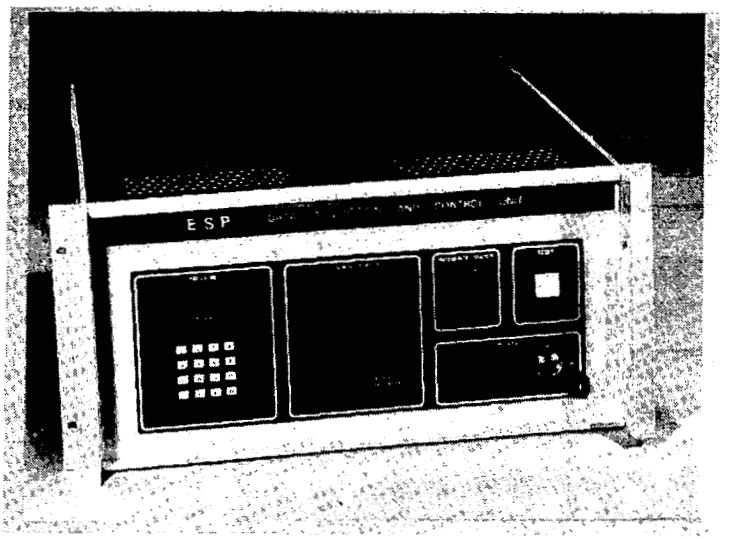


Figure 5.- 512-channel data acquisition and control unit.

| FACILITY | TYPE | NO. PRESSURE MEASUREMENT | FULL SCALE PRESSURE kPa (psi) | MEASUREMENT UNCERTAINTY %F. S. |
|---|---|---|---|---|
| $CF_4$ | BLOW DOWN | 32 | 0.345 (0.05) | 1.00 |
| $CF_4$ | BLOW DOWN | 64 | 34.5 (5) | 0.25 |
| UNITARY | CONT. FLOW | 32 | 34.5 (5) | 0.20 |
| V/STOL | CONT. FLOW | 630 * | 34.5 (5) | 0.25 |
| 8' TPT | CONT. FLOW | 32 * | 34.5 (5) | 0.50 |
| SCRAMJET | COMBUSTION | 128 | 206.8 (30) | 0.50 |

* ESP SENSOR MOUNTED IN MODEL

Figure 6.- Field evaluation of ESP sensor system.

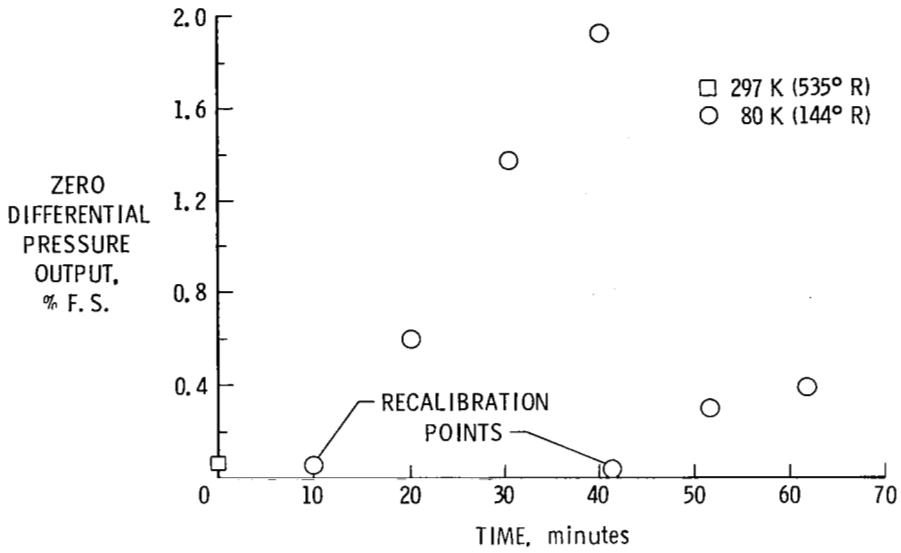


Figure 7.- Zero differential pressure output versus time.

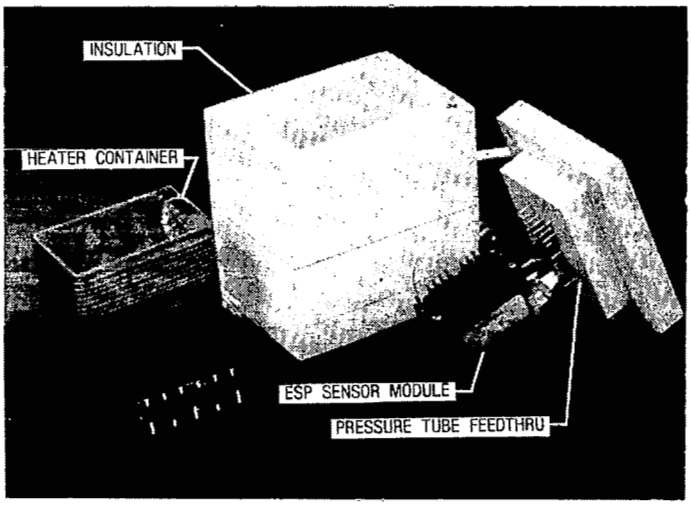


Figure 8.- 0.3-meter ESP temperature controlled enclosure.

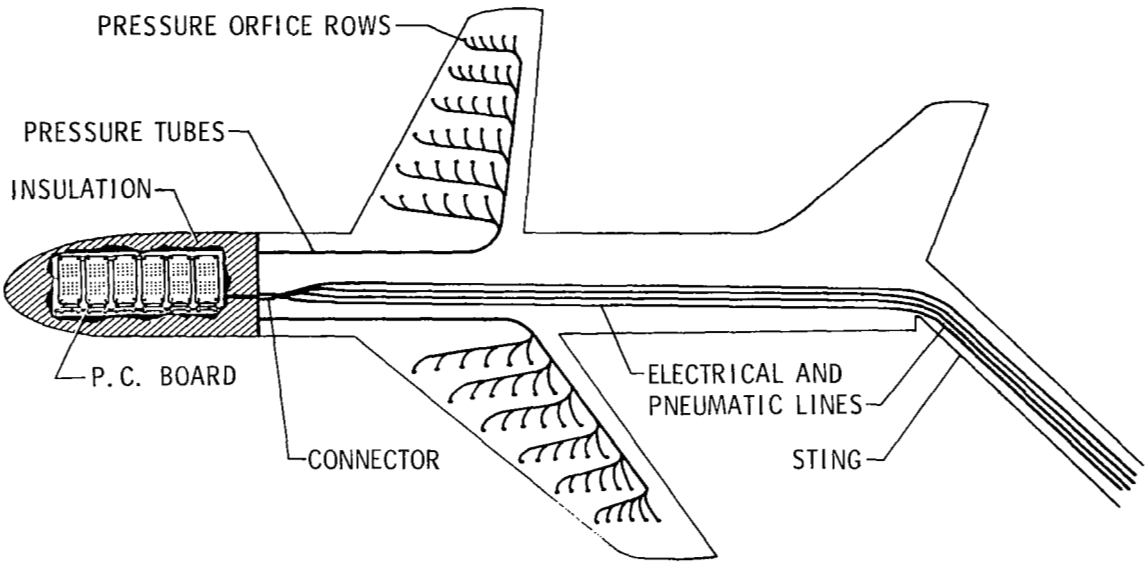


Figure 9.- Typical ESP installation.

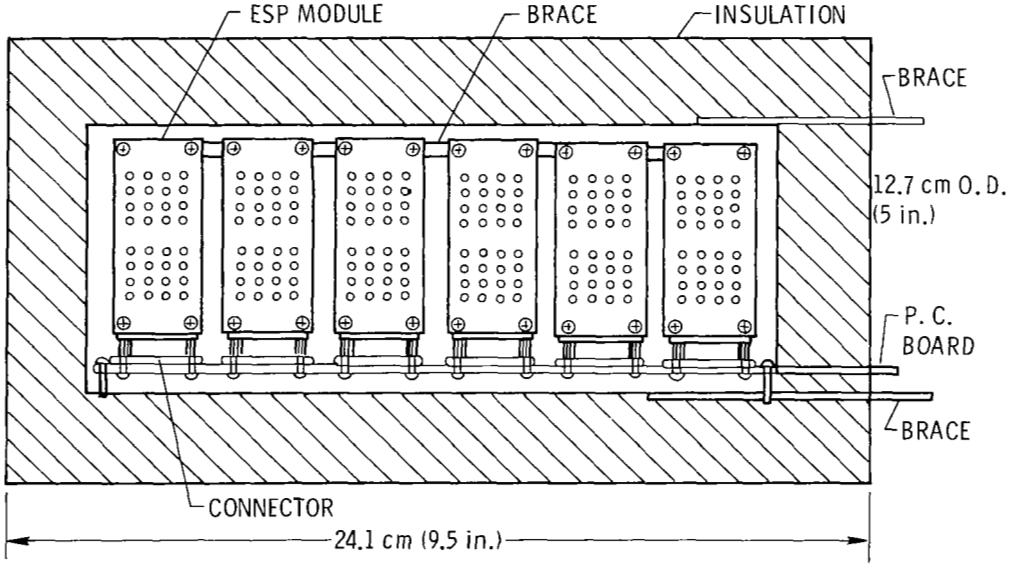


Figure 10.- ESP temperature controlled enclosure for pathfinder.

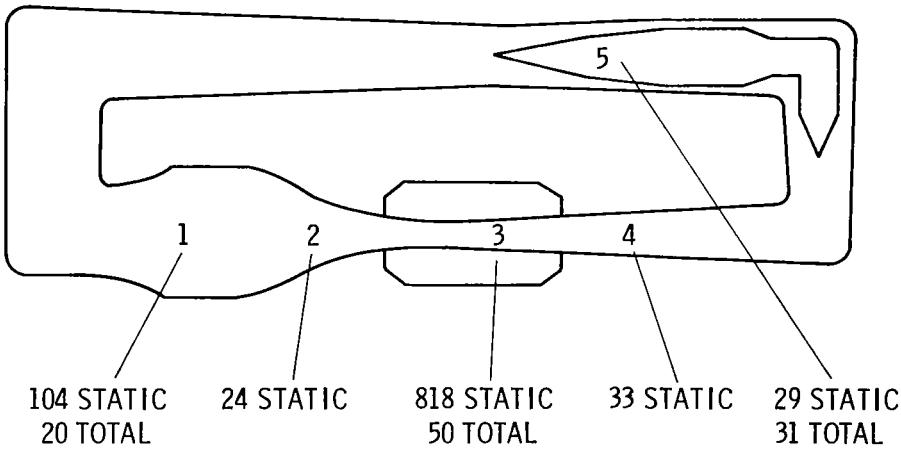


Figure 11.- Distribution of tunnel calibration measurements using ESP system.

# MODEL ATTITUDE MEASUREMENTS IN THE NATIONAL TRANSONIC FACILITY

Tom D. Finley
Langley Research Center

## SUMMARY

The National Transonic Facility has established a requirement for the precise measurement of model pitch and roll. Two approaches to this problem are being explored. The conventional approach to model attitude measurements at Langley Research Center involves the use of precision accelerometers to detect the attitude of the model with respect to the local vertical. Testing has indicated that this technique can be used in the NTF with only a slight degradation in accuracy. A problem which persists when using accelerometers is that of response. The slow response of this type of measurement system has forced us to consider the use of an optical measurement system. A contract presently in effect calls for the study of the problems associated with using an interferometric angle measurement system in the NTF environment. This paper describes the work done to date on both these approaches.

## INTRODUCTION

This paper describes the work done toward making measurement of the model's pitch and roll attitude in the National Transonic Facility. The effort is divided between two approaches: An inertial measurement which is an extrapolation of existing technology into a cryogenic environment; and an optical technique developed by Boeing Aerospace Company who is presently under contract to NASA to investigate the possibility of adapting this system to the NTF environment. This paper describes the approaches, their promise and limitations, and the work done in each area up to the present, including a summary of their status and plans for further work.

## SYMBOLS

| | |
|---|---|
| $\alpha$ | pitch attitude, degrees |
| $\phi$ | offset angle, degrees |
| E | output voltage, volts |
| B | electrical bias, volts |
| S | sensitivity, volts/g |
| $\theta_o$ | pitch misalinement, degrees |
| $\theta$ | roll attitude, degrees |
| $\alpha_o$ | roll misalinement, degrees |

# INERTIAL MEASUREMENT OF MODEL ATTITUDE

A critical measurement in any wind tunnel model testing is that of angle of attack. This can be derived from pitch attitude measured with respect to an arbitrary vector (such as the earth's gravity vector). The wind angularity can be inferred from an upright and inverted run of a given model configuration. This wind angularity is simply added to the pitch attitude to produce angle of attack.

An existing technique used extensively in wind tunnels at Langley for making pitch attitude measurements involves the use of precision servo accelerometers to sense the attitude of the model with respect to the local vertical. See figure 1. The following equation is generally used to reduce pitch attitude data

$$\alpha = \sin^{-1}\left(\frac{E-B}{S}\right) - \phi$$

where $E$ is the accelerometer output in volts, $B$ is the electrical bias in volts, $S$ is the sensitivity in volts per $g$, and $\phi$ is the offset angle (angle between the model zero and the sensitive axis of the accelerometer).

To use these transducers in conventional wind tunnels at Langley has required considerable effort. It has been necessary: To work closely with manufacturers to produce units qualified for this application; to exhaustively test every unit to provide a basis for selection; to compensate, control, or isolate the units from the environments; to develop application technique to handle and install these units; to educate users as to how to extract maximum accuracy from these systems; and to optimize data acquisition and reduction techniques to minimize errors. Some of this effort will be detailed below.

Even the best small servo accelerometers available commercially have several sources of error that must be dealt with in order to approach a pitch attitude measurement with an uncertainty approaching the $0.01^{o}$ required for precise wind tunnel testing. Characteristics which must be considered include hysteresis, stability, temperature coefficients, long-term repeatability, resolution, linearity, range, bias, scale factor, frequency response, damping, effect of vacuum, supply voltage effects, alinement, noise, output impedance, and rectification errors. Many of these sources of error have been minimized by the manufacturers of modern precision servo accelerometers. The areas that remain critical are stability, temperature effects, and rectification.

The stability of a unit is determined in the design and the manufacturing process. Our testing is to select only the units with suitable stability for this application. The problem is that $0.01^{o}$ corresponds to 175 micro-g's which is less than 0.002% of full scale range. Special tests have been developed to determine the long and short term stability under a given environment. The data from acceptance tests are plotted and repeat calibrations are added to this history sheet for the life of the unit. This provides a

means of selecting the best units initially and shows problems which might develop during the use of the unit in the tunnel.

The temperature effects have been handled in two ways. Some of the accelerometers purchased have very good temperature characteristics for both zero shift and sensitivity change. These units are then temperature compensated over a range from 293 K (528°R) to 343 K (618°R) using special resistors and thermistors. These can be used in many of the conventional tunnels at Langley. The other technique is to provide heaters and temperature sensors for the accelerometers so that they remain at a constant 343 K (618°R). This is obviously required for a cryogenic environment.

The rectification characteristics of an accelerometer, i.e., its generation of a dc output voltage when subjected to vibration, has proved to be the hardest problem to solve. We have worked with manufacturers who have gone so far as to redesign the mechanical element of the accelerometer just to improve this one characteristic. These efforts have not been particularly successful and at present we use two methods to minimize the source of error selection and isolation. The procurement specifications are very strict so that the manufacturers must select their best units. This reduces the problem and generally limits the critical area to higher frequencies where structural resonances cause rectification in all three axes. The solution to this problem has been to mount the accelerometer on vibration-isolation pads inside a special housing. The pads are a commercially available poly-acrylic material that has internal damping. The size of the pads is adjusted to provide a resonance at about 300 Hz. This reduces the vibration level at the accelerometer by 20 to 1 at 2 kHz which reduced the rectification by 400 to 1 since this type of error is proportional to the square of the g level.

Another inertial device used at Langley is an electrolytic bubble which is manufactured commercially and detects the angle between its base and the local horizontal. The unit is similar to a carpenter's bubble except electrodes are placed in the liquid (a special electrolyte) so that the output can be sensed remotely. This provides a means of leveling the model remotely before and after each test to establish "wind-off zeroes" for balance and pitch attitude accelerometer equation updates. These devices can also detect wind-on zeroes under smooth conditions.

## Cryogenic Chamber Tests

One approach to model attitude measurements in the NTF involves the use of heated accelerometers similar to the units used in conventional tunnels. To investigate problems associated with this approach we ran tests in a cryogenic test chamber. The tests were to determine the effect of the environment on sensitivity and bias. A pair of bubbles in a heated package were used to set the accelerometer at two pitch angles, $0^{\circ}$ and $5^{\circ}$. The output at $0^{\circ}$ at various temperatures indicates bias shift with temperature while the difference in the outputs at the two angles is a measure of sensitivity.

The first configuration tested involved placing a standard heated accelerometer package inside an outer case to increase the insulation. Tests showed this to be erratic. This was partly because of the rings used to suspend the smaller case inside the larger case and partly because of the bracket assembly. To avoid the bracket problems the remainder of the tests were conducted with the package mounted directly to the bottom of the plate holding the bubble assembly. The ring assembly holding the inner case could not be adjusted to eliminate changes in attitude so the standard package was tried without additional insulation. This proved to be the most repeatable of all the data taken even though the heater was running at its full capacity of 35 watts at 83 K (150°R). The bias shift was less than 0.02° and the sensitivity shift was repeatable. (See fig. 2 and fig. 3.) This shift was apparently caused by the gradient on the accelerometer. The top of the accelerometer was 65 K (117°R) cooler than the control temperature of 343 K (618°R) when the chamber went to 83 K (150°R). Sensitivity shift is apparently a function of heater power. The sensitivity increased by 1% with the heater power at 35 watts.

This data indicated that to minimize temperature effects on accelerometers for NTF it will be necessary to redesign the heater-insulator package. The differentials in the old package are caused by having the heater wrapped around the sides of the accelerometer only, so that no heat is provided to the ends. This design will be modified for future cryogenic applications.

## Tests in the 0.3-Meter Transonic Cryogenic Tunnel

In July 1979 this accelerometer package was tested in the 0.3-meter cryo tunnel. It was mounted on a turntable used to control the pitch attitude of the model for the 2D test. Heated bubble assemblies were mounted on this and the opposing turntable to determine their performance in the cryogenic environment and to provide additional data for comparison. The primary readout of pitch attitude for this tunnel is a heated shaft encoder geared to one of the turntables.

Figure 4 shows the room temperature calibration of the accelerometer and the shaft encoder using a precision inclinometer as a reference. The performance of the accelerometer at room temperature is very good and approaches the laboratory accuracy. The error in the shaft encoder was well within the limits expected for a device with a resolution of 0.01° especially considering that mechanical gearing is being used.

Data was taken over a wide angle range at various temperatures, pressures, and Mach numbers. There were no detectable effects from changes in pressure or Mach number but the sensitivity of the accelerometer changes with temperature. (See fig. 5.) These data are in reasonable agreement with the results determined in the chamber and underline the need for an improved design of the heater-insulator system.

## Design of a 3-Axis Package

The preliminary design of a system capable of measuring pitch and roll is shown in figure 6. The bubble will be used as a means of zeroing the model. The longitudinally mounted accelerometer will measure pitch and the other two accelerometers will be used to measure roll. The use of two units to measure roll is based on the NTF requirement of $\pm 180^{o}$ roll. The unit closer to horizontal at any given roll setting will be used to measure roll.

The equations used to reduce the data are more complex since there are interactions between the pitch and roll axes. The pitch equation is identical to the normal equation except that the offset angle is a function of the roll attitude.

$$\alpha = \sin^{-1} \left(\frac{E-B}{S}\right) - \phi \sin (\theta - \theta_o)$$

The roll measurement is more complicated in that the effective sensitivity as well as the offset angle are a function of pitch attitude.

$$\theta = \sin^{-1} \left(\frac{E-B}{S \cos 2}\right) - \phi \sin (\alpha - \alpha_o)$$

This is further complicated by the fact that this equation provides only the principle value of the trigonometric function and the third accelerometer's output must be monitored to determine the quadrant.

Since the pitch equation involves the roll attitude and vice versa, it will be necessary either to solve the equations simultaneously or use an iterative technique. Three iterations will reduce the uncertainties in either measurement to insignificant levels; therefore, this method is recommended. The use of simultaneous equations becomes very involved and may prove to be slower than the iterative solution.

## Limitations of Inertial Devices

There are certain limitations associated with using inertial devices to measure model attitude. This is particularly true in the case of the NTF. The following considerations have forced us to consider alternate approaches.

The accelerometers must be specially built or selected based on manufacturers' tests. This makes the units expensive. On receipt the accelerometers are subjected to extensive testing to assure conformance to specifications and provide a data base for unit selection and for comparison to subsequent calibration data. The units must be temperature compensated and retested or wrapped with a custom heater. The vibration isolation pads are installed and the system is retested. Often the pad arrangement must be modified and again tested. All of the above are expensive and time consuming.

Since the model vibrates considerably and the accelerometer measures this, the dynamics on the output signal are large. Often the accelerometer is subjected to dynamics of 5 to 10 g's. Obviously, to measure the output to an accuracy of 175 micro-g's ($0.01^{o}$) it is necessary to drastically filter the signal. This causes lag in the measurement which is particularly disadvantageous in the NTF because of the high operation cost.

Another problem in the use of inertial devices to measure model attitude is their sensitivity to "sting whip." This is centrifugal acceleration caused by a dynamic pitching or yawing motion of the sting model assembly. This causes an error that is very difficult to correct for or even detect without the use of several other sensors. This type of error is especially problematical since it is not an error in the accelerometer and therefore cannot be reduced by any laboratory testing or selection.

Further considerations include the fact that: The servo accelerometers are fragile, require special handling, and must be repaired or replaced periodically; the measurement of roll and pitch require the use of multiple accelerometers; and the space and wiring requirements of the package.

## OPTICAL TECHNIQUE FOR MEASURING MODEL ATTITUDE

### Theory and Background

The Boeing Aerospace Company has developed an optical system designed specifically for measuring model attitude in wind tunnels. One such system has been operational in the Boeing Transonic Tunnel since late 1978. A similar system was designed and built for Langley Research Center in 1978. Assuming a system of this type can be used in the NTF, many of the problems associated with the inertial measurement will be avoided.

In 1971 Boeing designed a laser interferometer for the measurement of model attitude in wind tunnels. It used two corner cubes on top of the model to provide two return beams that allow the differential height of the corner cubes to be measured to 1/4 wavelength. Boeing offered to bring this system to Langley and in late 1971 it was tested at Langley's 8-foot TPT. The unit was very precise and provided excellent data except under certain conditions. In the transonic Mach number range the unit was erratic and the designer decided after several attempts at modifying the conditions that the erratic behavior was caused by variations in the medium along the two return light paths. This is caused by turbulence which is present in certain degrees in all wind tunnels.

Boeing worked to modify this system and in 1975 devised a new approach to the problem using a hologram over a single corner cube. (See fig. 7.) The designer has applied for a patent on this system which trades off resolution for sensitivity to turbulence. The spacing on the lines in the hologram determines the separation of the two return beams. Decreasing this spacing obviously reduced the resolution in angular displacement but this also

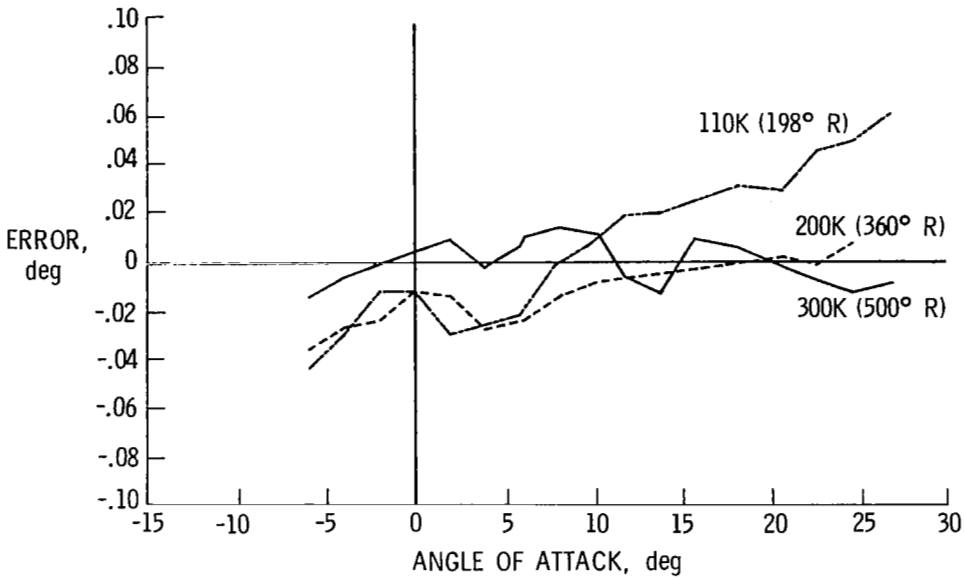


Figure 5.- Accelerometer error in 0.3-m Tunnel test.

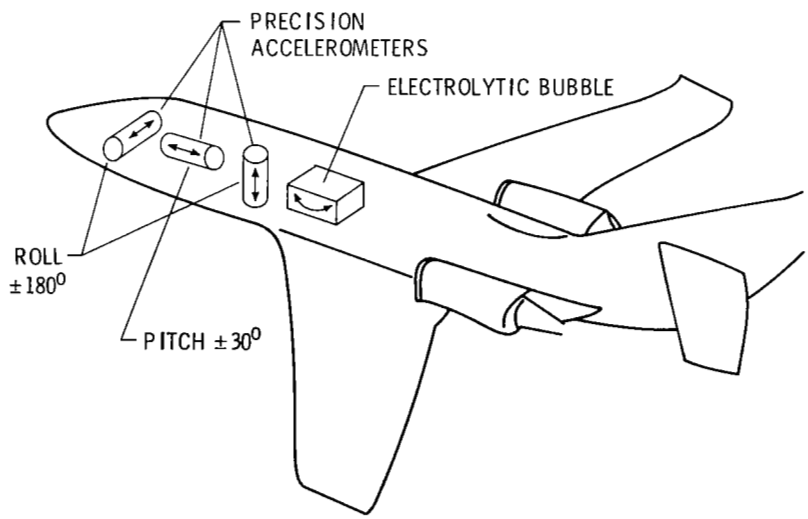


Figure 6.- Use of inertial devices in an NTF model.

# TEMPERATURE INSTRUMENT DEVELOPMENT

# FOR A CRYO WIND TUNNEL

Edward F. Germain
Langley Research Center

## SUMMARY

The development work which extended conventional wind tunnel thermometry into the cryogenic wind tunnel range is reviewed. The emphasis is on stagnation temperature measurements where a mix of platinum resistance thermometers and thermocouples is necessary to satisfy all the requirements. Calibration and thermocouple homogeneity test equipment are described. Test results and experience support the use of copper-Constantan thermocouples.

## INTRODUCTION

Work over the past few years has shown that conventional wind tunnel thermometry can be extended to satisfy cryo tunnel requirements. Note however that more than one sensor type may be necessary and certain details take on new significance.

The National Transonic Facility (NTF) temperature measurement requirements run the gamut from gas to model temperature and include structural and component temperatures not often a concern in a conventional tunnel. In-house work in temperature instrumentation was concerned with upgrading support capabilities, investigating options, verifying decisions, and refining application techniques. This report is focused on the most difficult requirement, stagnation temperature measurement where these three items should be noted:

1. Reynolds number calculation requires stagnation temperature be determined within $\pm$0.3 K over the range of 77 K to 340 K.

2. There is a tunnel control requirement for a sensor with a 1-second time response.

3. Tunnel calibration requires that temperature distribution be determined with a $\pm$0.5 K uncertainty comparing one point to another.

Various sensors were considered to fill these requirements. Initially thermistors and temperature sensitive diodes showed potential. In the Langley 0.3-Meter Transonic Cryogenic Tunnel type T (copper-Constantan) thermocouples satisfied most requirements. For accuracy in measuring stagnation temperature, an inexpensive industrial type platinum resistance thermometer (PRT) proved superior to thermocouples.

Thermistors were tested but ruled out for NTF use because of poor stability over the full operating range. The more stable thermistors tested were heavily encapsulated with glass such that their slower time response became a negative factor. Add to this poor interchangeability and grossly nonlinear thermal response and it appears thermistors will be used in cryo tunnels only in narrow range tests which require high sensitivity. Diodes, on the other hand, may have more future applications than thermistors, but there were no probes available commercially to suit the particulars of NTF. Diodes were then ruled out because of probe development cost.

Clearly the most direct and least costly way to satisfy NTF requirements was to build upon the successful 0.3-meter cryo tunnel experience and use thermocouples and PRT's. In particular,

1. It had been shown that a PRT can determine stagnation temperature with an uncertainty of less than 0.3 K. The sensor used in the 0.3-meter tunnel had a time constant of 2 or 3 minutes. For operating economy the need was for a sensor with a time response of seconds while retaining long term high accuracy.

2. The 1-second time response controls requirement is easily met with a thermocouple. The goal was to improve on the 1% accuracy usually associated with thermocouples in order to more nearly match test conditions from one run to the next.

3. Experience in the 0.3-meter tunnel showed that a thermocouple network is an economical system for measuring spacial variations in temperature within $\pm 0.5$ K. The question then is what is required to accomplish this in a larger facility.

## PLATINUM RESISTANCE THERMOMETER

The International Practical Temperature Scale of 1968 (the IPTS-68) is based in part on a formulated relationship between temperature and the resistance of a strain-free, high purity platinum wire. A properly designed PRT can be expected to be very accurate over a cryogenic tunnel temperature range with only a few fixed calibration points. The resistor, of course, needs to be insulated and protected from the environment. As a result, it responds more slowly than a bare-wire thermocouple.

The decision was made to search for a commercially available probe which most nearly satisfied the NTF needs and thereby avoid the expense of a special design. Seven manufacturers had a total of 14 probe types which appeared to potentially suit the NTF application. A complete program was set up to test 2 of each of the 14 types. X-ray shadowgraphs were made of each unit to determine the location and geometry of the temperature sensing element and the details of the four-wire lead attachment. Tests were performed to look for accurate match to the IPTS-68, self-heating and immersion details, errors due to thermal voltages, and for electrical insulation. Calibration stability was checked through 100 cycles to $LN_2$ temperature.

Two probes appear to be superior for the NTF application. One is now installed in the 0.3-meter cryo tunnel for life tests under operating conditions. Its time constant may be as short as 10 seconds, but this remains to be determined in use. Incidentally, the complications of a bridge, transmitter, or other signal conditioning are avoided by using a potentiometric method to measure resistance, with the sensor powered by a constant (usually 1 μA) current.

## THERMOCOUPLES

Thermocouples have always been the workhorse temperature sensor for wind tunnels. They are reliable, easy to apply, and can be made small for fast response and minimum thermal perturbation. Thermocouples are passive with essentially no self-heating. It is reasonable to expect that previous wind tunnel experience can be extended into a lower temperature range.

The often quoted disadvantage of thermocouples, especially at cold temperatures, is low thermoelectric power, dE/dT, typically 16 μV/K at 80 K. This in itself is not a problem considering modern readout electronics. The problem arises as a consequence of parasitic e.m.f.'s which may develop because of inhomogeneous sections of wire located in temperature gradients. Sharp temperature gradients typical around cryogenic equipment magnify the parasitic e.m.f.'s. Couple this with the low thermoelectric power and the error in terms of temperature may become significant.

A final disadvantage concerns the complicated temperature-voltage relationship. If individual calibrations are to be avoided, some degree of standardization for interchangeability is required. This turns out to be a significant problem at cold temperatures, since thermocouple wires are generally not available with close limits of error below 220 K.

### Selection of Wire for NTF

Type T (copper-Constantan) thermocouple wire was chosen for NTF use for several reasons. Experience with this wire in the 0.3-meter cryo tunnel was satisfactory. It proved superior to type E (Chromel-Constantan) and type K (Chromel-Alumel) in homogeneity and calibration match to standard tables. Type T wire is the only thermocouple pair available with a recognized ASTM accuracy specification in the low temperature range. Special limits of error wire are quoted as ±1% from -300°F (89 K) to -75°F (214 K). And finally, type T wire has the advantage of simple polarity recognition because of the color of copper. Polyimid film insulators suitable for cryo tunnel applications are not always available with color codes. In a facility the size of NTF with hundreds of thermocouple circuits each with several connection points, simple polarity recognition is very important.

The disadvantages of type T wire concern the high conductivity and malleability of copper. There are ways to minimize these physical disadvantages such that type T wire becomes the obvious choice for NTF. For

example, the conductivity can be handled by thermally conditioning the leads to minimize conduction to an active junction.

Type T wire is a poor selection for a sheathed, hard packed ceramic insulator thermocouple wire assembly. This material configuration has been avoided by using polyimide film insulated wire in a small bore tube conduit in an application where sheathed wire might otherwise have been used.

## Homogeneity

The thermoelectric homogeneity previously mentioned can be described by looking at a basic thermocouple of materials A and B joined at points 1 and 2 (fig. 1). The observed phenomena as it applied to thermometry is stated simply as the net voltage generated.

$$E_n = \int_{T_1}^{T_2} S_{AB}\, dT$$

where $T$ is absolute temperature and $S_{AB}$ is the "relative Seebeck coefficient." If this thermocouple is to be a thermometer, then $S_{AB}$ cannot vary with distance $X$ along the wire. Thermoelectric homogeneity is just a statement of the fact that $S_{AB} = f(T)$ only.

The apparatus used to check the homogeneity of thermocouple wire is shown in figure 2. Wire is pulled into then out of a vat of $LN_2$ as it is wound from one spool to another. A nonsymmetric temperature gradient is established in the wire, steep where it enters the $LN_2$ and more shallow as it recovers to room temperature. An electric circuit is completed from the ends of the wire through slip rings to a potentiometer recorder. Thus, as the wire is pulled through the $LN_2$, a nonsymmetric temperature gradient travels along the wire such that if an inhomogeneous portion of wire enters the $LN_2$, a parasitic voltage is generated and recorded.

Strip chart traces typical of some poor sections of type E, K, and T wires are shown in figure 3. The larger vertical deflections are the undesirable spurious voltage totally unrelated to thermocouple junction temperatures. The background voltage from slip ring noise is only about 2 microvolts. Of all the wires tested, the type T wires always proved to be the more homogeneous. In fact, the spike on the lower trace, figure 3, was the only spurious e.m.f. from a 50-foot length of type T wire. Examination of this wire showed a physical defect in the Constantan wire at that point.

## Calibration

Detailed calibration of thermocouples for the 0.3-meter cryo tunnel was made by comparison with a standard PRT in a liquid bath from room temperature down to 175 K. The next lowest point available was the $LN_2$ boiling point (about 77 K). Efforts to bridge the gap between 77 K and 175 K with an inexpensive apparatus were not satisfactory and the shape of the calibration curves remained questionable. Today these calibrations are accomplished with the equipment shown in figure 4. The main features of the apparatus are internal to the cryostat as shown schematically in figure 5. In essence, a copper equalizer block looks at an $LN_2$ environment. The block would normally seek the temperature of the liquid except that it can be electrically heated to a higher desired temperature. Heat leakage from the equalizer block is controlled by varying the pressure of the transfer gas which for these purposes has been dry nitrogen at a low pressure. The calibration is a comparison one with the block temperature determined with a standard PRT.

The first data taken with this calibration equipment is shown in figure 6. Thermocouple "error" is plotted over a range from 77 K to about 300 K. As used here "error" is the deviation of the thermocouple output from the standard NBS tables. Calibration points on four wire samples from one spool all fall in the shaded area. The wires tested well within the ASTM special limits of error as shown in the figure. A linear correction factor brings all the points to within $\pm 0.2$ K.

As a further justification of the use of type T wires, of the dozens of samples of thermocouples tested for cryo tunnel use, all the type T wires tested within the $\pm 1\%$ limits of error. All type K and E wires tested exceeded this limit.

## Comments on Applications

Thermocouples for NTF high accuracy requirements will get special handling. Contiguous lengths of a thermocouple circuit from the active junction to the tunnel wall, through a penetration then on to a reference junction will be cut from a continuous length of wire. Each piece will be identified as to channel and location. All wire will be checked for homogeneity. Sections showing parasitic e.m.f.'s in the $LN_2$ test will not be used inside the tunnel in order to minimize "short range" inhomogeneity errors. Long range inhomogeneity (i.e., calibration differences from one end of a length of wire to another) will be picked up by a calibration schedule. The schedule will be developed as calibration data is gathered.

Wall penetration and other connections in a thermocouple channel can be an error source. Spurious e.m.f.'s depend upon the temperature gradients, the thermoelectric quality of the conductors and whether foreign conductive materials were introduced in manufacturing the connector. Tests on a popular quick disconnect multichannel connector/wall penetration showed errors as high as 3 K for crimp connection of wire to pin and 30 K when solder was used.

Clearly this type of error decreases as the gradient is decreased so that it is important to minimize temperature differences across even so-called thermocouple connectors. High accuracy thermocouple circuits in NTF will use calibrated wire penetrating the tunnel wall directly through a compression fitting in order to avoid this problem.

## CONCLUDING REMARKS

All indications are that the NTF goals will be met although the results are not all in. A commercial PRT is proving to have long term accuracy in excess of the requirement. Its time constant remains in question. There is under development a method to measure PRT time constants in situ.

The goal of spacial uncertainty of $\pm 0.5$ K on a thermocouple network is within reason through suitable preinstallation tests, special handling, and attention to other details. Ultimately this evaluation will be made during the calibration of NTF by comparison with other instruments including a PRT.

The 1-second time response appears to be no problem. Published data came into question as applied to a cryo tunnel. For that reason, time constants on a test thermocouple are being made in the 0.3-meter cryo tunnel at a matrix of conditions. The setup involves heating the thermocouples a few degrees with an alternating current, then observing the temperature-time history on a digital oscilloscope after the heating current is switched off.

The 0.3-meter cryo tunnel continues as a test bed to broaden the base of experience for NTF temperature instrumentation.

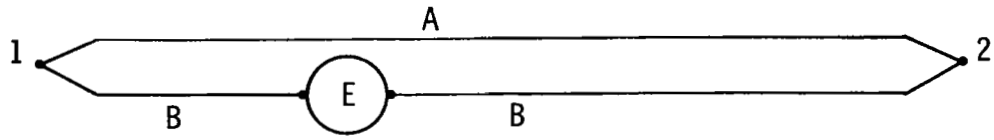


$$E_n = \int_{T_1}^{T_2} S_{AB}\, dT$$

Figure 1.- Thermoelectric thermometer.

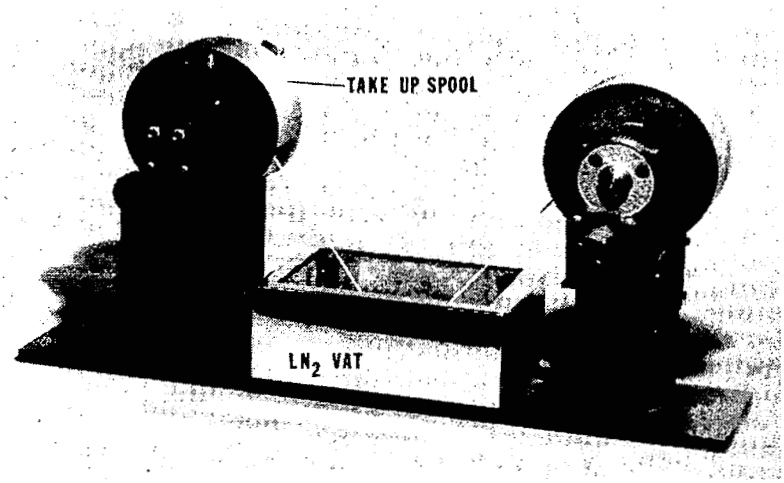


Figure 2.- Thermocouple wire homogeneity test apparatus.

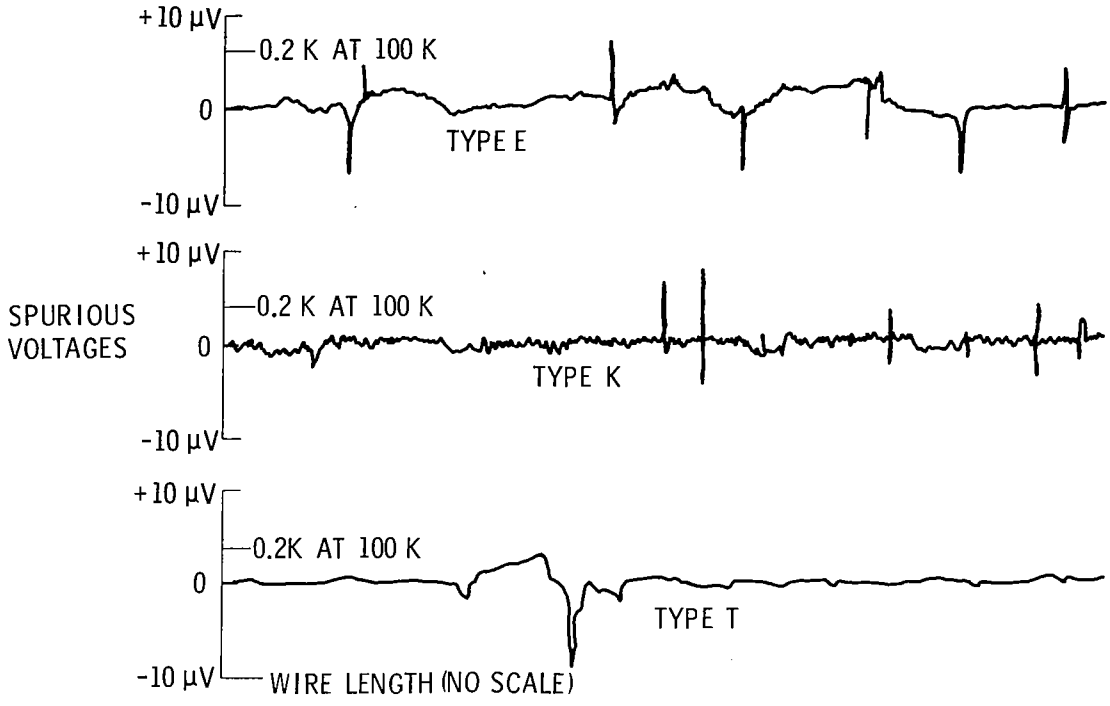


Figure 3.- Typical homogeneity test results.

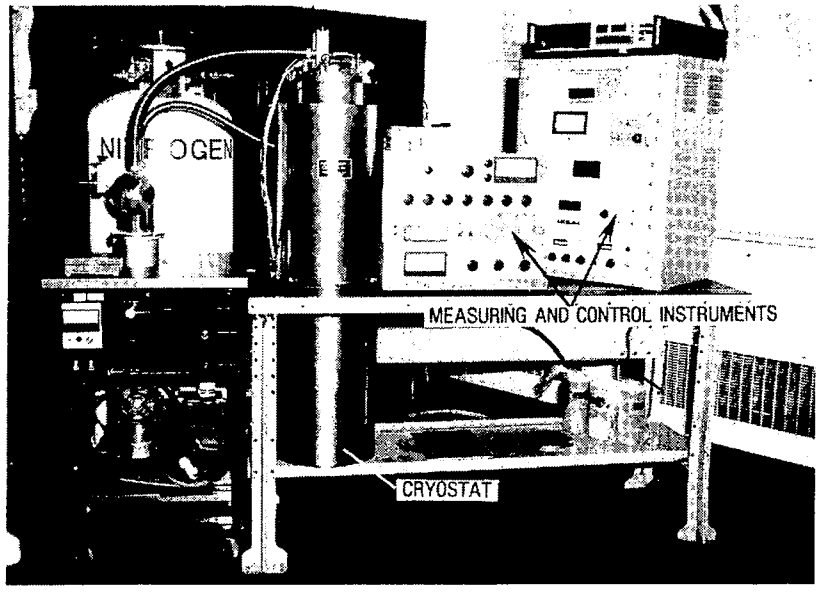


Figure 4.- Low temperature calibration apparatus.

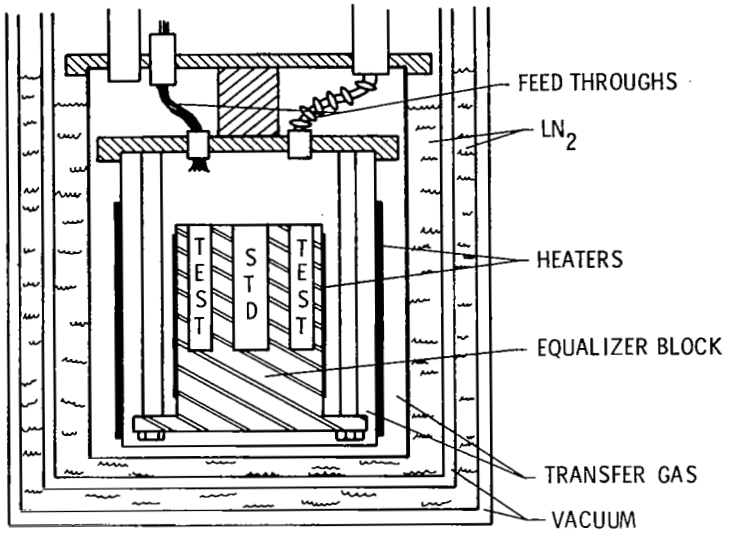


Figure 5.- Schematic of components internal to cryostat.

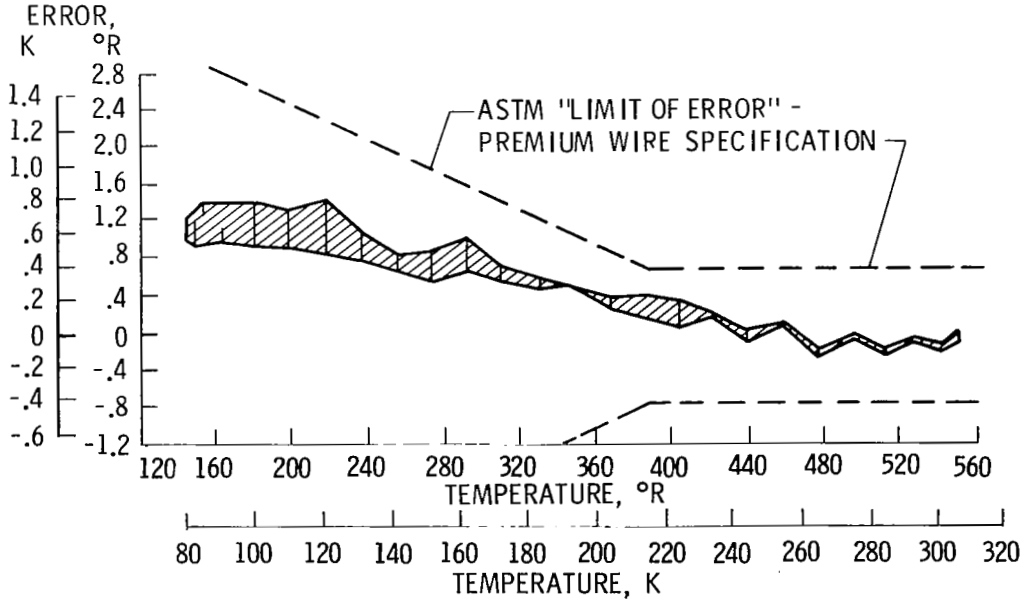


Figure 6.- Results of the calibration of 4 type T thermocouples.

## SYSTEM SPECIFICATIONS AND CONSTRAINTS

The desired characteristics for the deformation measurement system are that it be nonintrusive, "real time," and provide area mapping or a multipoint scan of the model surface specifically to measure a maximum deformation of 7.62 cm (3 inches) with an accuracy of ±0.064 mm (±0.0025 inch). Measurement parameters affecting these requirements are shown in Table I.

TABLE I.- MEASUREMENT PARAMETERS

| | |
|---|---|
| Viewing area | 0.9 meter square |
| Model pitch angle | -11 to +19 degrees |
| Number of points | 50-100 |
| Measurement time | <2 seconds |
| Frequency response | 1 Hz to 100 Hz |
| Operating environment: | |
| Temperature | 78 to 344 K |
| Pressure | 896 kPa max |
| Noise | ≈150 dB SPL |

Other constraints of a physical nature are as follows:

1. Camera mounting--presently, the only mounting positions for the camera(s) having a direct view of the model are in the tunnel floor or ceiling. Access to the 5-inch-diameter windows is between deep structural beams, approximately 56 cm (22 inches) deep and 13 centimeters (5 inches) apart. On the tunnel centerline, these dimensions cannot be exceeded because other components exist over these locations.

2. Vibration environment--the actual vibration levels and frequency spectrum are unknown; however, it is assumed that significant vibration levels will be encountered within the frequency range of interest and vibration isolation or subsequent compensation will be required.

3. Dimensional stability--it is known that the model support and the sensor mounting structures will move with respect to each other as temperature varies during a run. Some form of automatic registration and the techniques to implement it will be required.

## DISCUSSION OF CONCEPTS

### Stereo Photogrammetry

In this technique, two (or more) cameras view the object from different positions and angles. Given a number of fixed reference points, three-dimensional motions can be extracted by noting the change in the position of points on the object with respect to the reference points. Of significance is the fact that this is a non-real-time approach and requires extensive data reduction procedures after the fact. High resolution is possible if one can define reference points within the viewing area and that these points maintain their position relative to the model. Because this technique has been implemented in other LaRC facilities and the data reduction algorithms and procedures exist, this approach is presently planned as a "backup" approach for the NTF facility. Present reduction procedures are labor intensive requiring manual spot location sensing from frame to frame. Once located, lens and window distortion corrections must be applied and finally, coordinate transformation from camera coordinates to model coordinates must be accomplished. A continuing effort is being exerted to improve this procedure in order to reduce the time required to obtain the finished data.

### Scanning Photogrammetry

This technique is geometrically similar to the above approach but is electronic from the beginning and thus provides the real-time or almost real-time capability desired. Shown schematically in figure 1, the system is programed to rapidly scan a preselected array of points on the model. On succeeding scans, if the points have moved, their new location is determined and become the initial locations examined on the next scan, etc. The system consists of two (or more) cameras which employ image dissector tubes as their sensors. By electronically scanning an aperture over the image plane, using pre-programed deflection potentials, the system can move rapidly from spot to spot. Once at a position, a miniscan of the neighborhood quickly centers a displaced spot in the aperture, determines the displacement coordinates, and stores them in memory as the initial position for the next scan.

Preliminary results from a contract effort investigating this technique have allowed some conclusions to be drawn. Active light source targets will be necessary. Passive targets, in order to appear as a fixed pattern and to minimize focusing variations accompanying large model excursions, would have to be small and would then require intense illumination levels to achieve a satisfactory signal-to-noise ratio at the detector. By directing the X-Y scanning system, in contrast to a raster scanning technique, discrete points can be addressed and tracked with sufficient speed to allow low frequency dynamic data to be obtained. A laboratory model suggests that 50 to 100 measurement points can be resolved to a resolution of $\pm 0.076$ mm ($\pm 0.003$ inch) at frequencies to 200 Hz. Additionally, there is a trade-off to be made among (1) the number of targets tracked per second, (2) the vibration amplitude, and (3) the target contrast and brightness.

All of the approaches discussed require extensive processing of data. Most of the approaches are stereo in nature, some of them in real time and some after the fact, however, all of the approaches discussed are remote measurement concepts and will require extensive coordinate transformations to arrive in a body axis environment. Lens, window, medium, and sensor motion corrections will have to be determined and applied to the data. Dynamic measurements in real or almost real time will require elaborate, high-speed computational equipment and algorithms to accomplish these tasks. Figure 5 schematically illustrates the systems being studied and reveals many common aspects.

The addressing of these problems is proceeding with both in-house and contract efforts. A system which emulates the scanning photogrammetry approach, though inadequate for the NTF requirements, has been purchased to investigate the sensor mounting geometry, sensor vibration environmental effects, model illumination and stereo coordinate transformation, and distortion correction computations. Observing a complete system will place problem areas in perspective for further definition. It is anticipated that currently available image processing equipment will be procured to investigate the real-time computational aspects. The mounting and installation problems associated with active sources on the model will be pursued by in-house personnel. The problem of determining how many targets and their spatial locations on the model will be addressed in cooperation with aerodynamic research personnel.

## CONCLUDING REMARKS

The measurement of model deformation, complicated significantly by the constraints and operational environment of the NTF, is a difficult task with many identifiable problems to overcome. Previous development efforts and computational procedures developed have made the stereo photogrammetry approach the prime candidate for this measurement. Extensive work will be required to provide faster and more efficient processing of the data. Current developments in the area of scanning photogrammetry suggest that real-time acquisition of multipoint (50-100) dynamic data (10-30 Hz) may be possible. Significant problems exist in the areas of sensor motion compensation (or illumination); optical path anomalies, their identification and compensation; and target location and mounting.

## REFERENCE

1. Idesawa, Masanori; Yatagai, Toyohiko; and Soma, Takashi: Scanning Moiré Method and Automatic Measurement of 3-D Shapes. Applied Optics, Vol. 16, No. 8, August 1977, pp. 2152-2162.

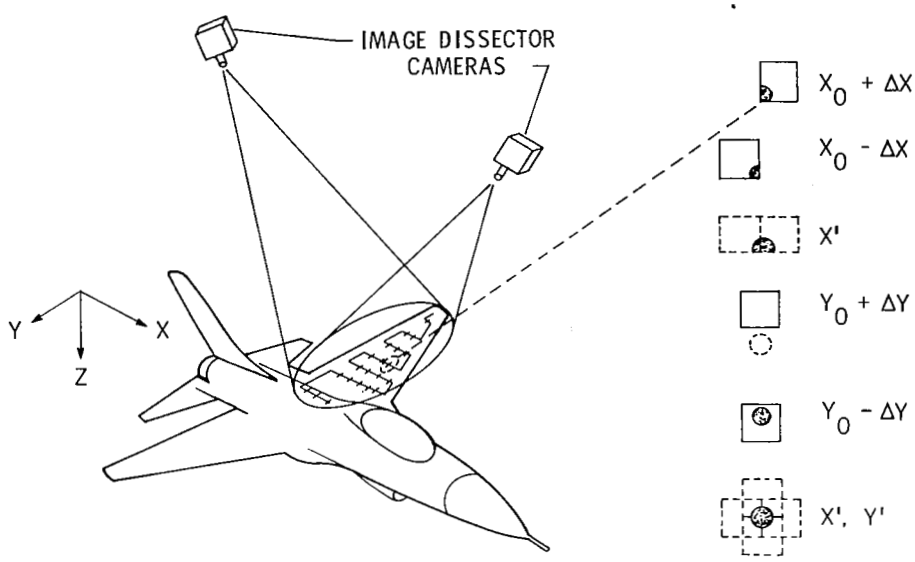


Figure 1.- Scanning stereo photogrammetry.

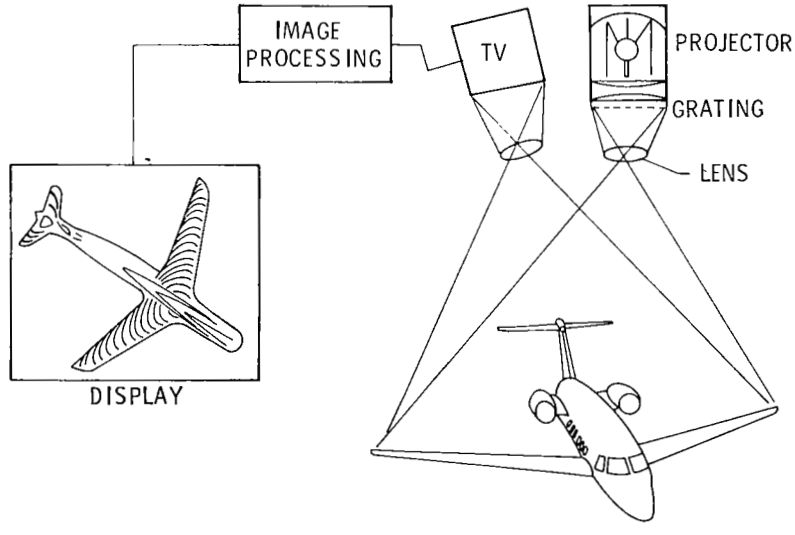


Figure 2.- Moiré topography.

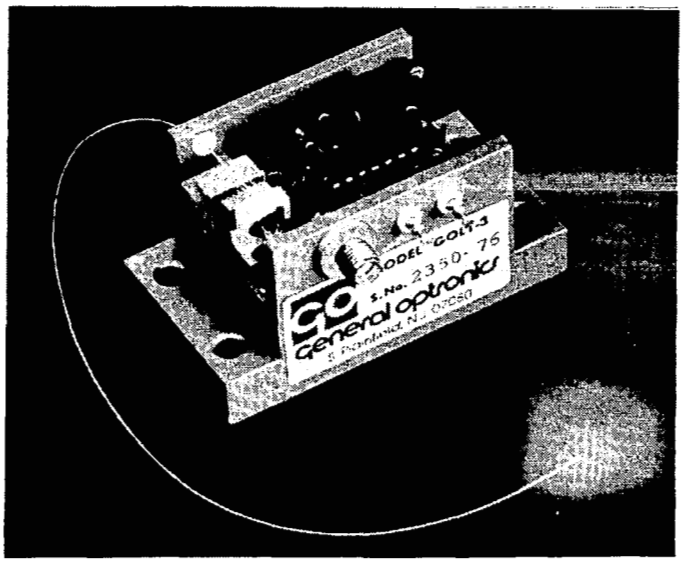


Figure 3.- Microwave modulated laser transmitter with fiber optic transmission line.

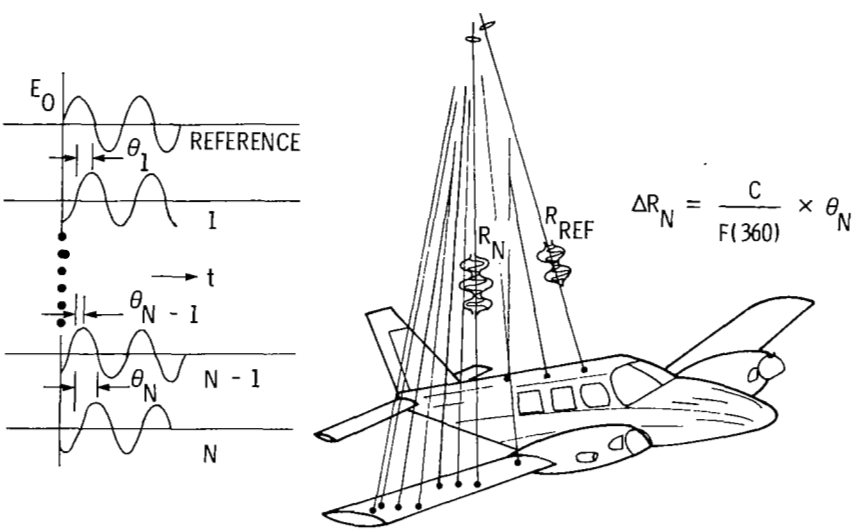


Figure 4.- Microwave modulated light beam.

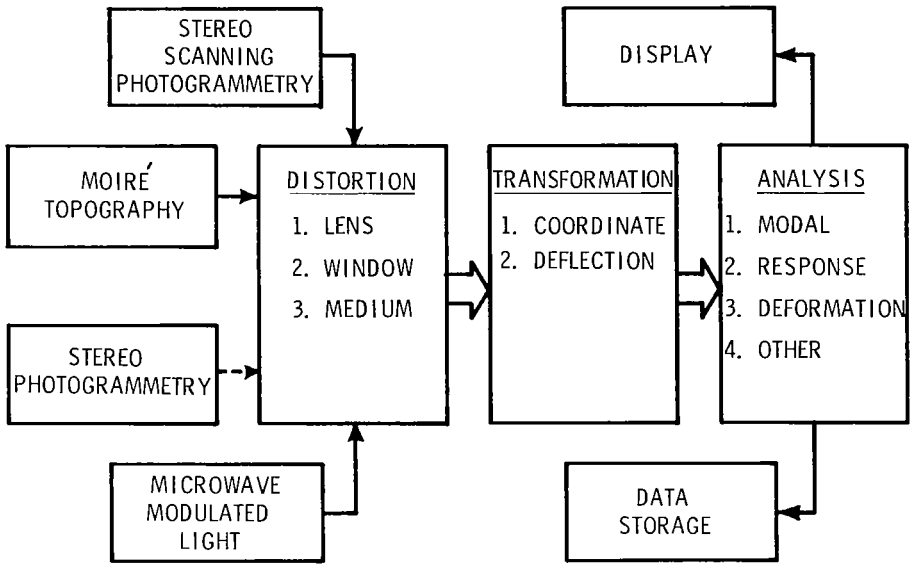


Figure 5.- Model deformation measurement.

# SESSION V - MODEL/STING TECHNOLOGY

# CRYOGENIC MODELS/STING

## TECHNOLOGY SESSION

Clarence P. Young, Jr.
Langley Research Center

## OVERVIEW

The advent of high Reynolds number ($R_e$), high dynamic pressure testing in a cryogenic environment offers exciting and difficult challenges for the researcher and model/sting systems design engineers. Although much experience has been obtained in the use of the Langley 0.3-Meter Transonic Cryogenic Tunnel, new technology is required for the design and fabrication of models/stings for testing at high Reynolds numbers and high pressures in the new National Transonic Facility (NTF).

The technology activities reported in this overview are just getting underway at Langley Research Center and are expected to be a continuing effort until the NTF is operational. The papers selected for publication in this session of the proceedings represent the experience obtained to date and reflect the areas of work that are believed to be of primary interest to potential users of the National Transonic Facility.

The 0.3 meter cryogenic tunnel at Langley Research Center became operational in 1973. Many models ranging from two dimensional airfoils to three dimensional simply supported models such as the Shuttle Orbiter have been tested in this facility. Typical test model configurations which have been run in this facility are shown in figure 1. Test temperatures have ranged from 78°K to 283°K which is essentially the same temperature range that models will be exposed to during testing in the NTF. Also tests have been conducted up to total pressures of 6 atmospheres on two dimensional airfoil models. This compares with a peak total pressure operation of 9 atmospheres at high $R_e$ in the NTF. Hence the 0.3 meter tunnel has provided the cryogenic experience but some models in the NTF will be loaded much higher due to higher operating pressures at high Reynolds number and more complex, 3-D models being supported on long flexible stings as compared to the more rigid and simply supported models tested in the 0.3 meter tunnel.

With regard to fabrication, various methods of model construction have been used. These include conventional, casting, welding, and plating techniques. All methods have presented some difficulties as might be expected, but no insurmountable ones. Example problems include the attainment of close model tolerances and surface finish necessitated by higher Reynolds number testing. Also, where screws join dissimilar materials, thermal and/or vibration cycling can cause the screws to back out. The use of good engineering

design practice such as positive locking devices can eliminate this problem. In addition some difficulties were encountered in cases where orifice tubes were soldered into the model. A solder interface left on the surface cracked under thermal cycling. This experience pointed to the need for the orifice hole to be integral with the model surface, if possible, to avoid such problems.

In general the experience with testing in the 0.3 meter tunnel has been good with no model structural failures and no major temperature problems, but with some fabrication problems (which were overcome). It is concluded from this cryogenic test experience that exotic designs are not needed for a cryogenic environment and in general specific model requirements can be met by applying good engineering design practice.

In support of the activation plan for the NTF a major R & D effort is underway to develop the technology needed for the design and fabrication of cryogenic models and sting systems for the National Transonic Facility. The principal elements or tasks associated with this activity include the in-house design and fabrication of two (2) research models and sting systems. The first model, Pathfinder I, is a force and pressure model representative of a transport configuration. The second model, Pathfinder II, is a force model and representative of a fighter configuration. These models are described in references 1 and 2. A general Users Criteria document will be developed around the Pathfinder models experience and published by Langley Research Center approximately one year before the NTF becomes operational. To date, the major experience has been with the design of the Pathfinder I model and this is reflected in the material presented in references 2 through 4. The R & D program objectives and major elements (tasks) are summarized in figure 2.

The major technology activities being carried out in support of the R & D program is depicted in figure 3. The technology work is an interactive, closed loop iterative process beginning with the Research Requirements (model definition) and ending with Model Fabrication. The technology development activities are being carried out at Langley Research Center in a structured programmatic manner. The major goal of the support activities is to accomplish those tasks or elements associated with the aforementioned R & D program.

The Design and Analysis activities depicted in figure 3 are closely related and result in an iterative approach (see discussion on Design by Analysis in reference 3). It should be noted that in the Design area, a Computer Aided Design/Computer Aided Machining (CAD/CAM) capability is being developed at Langley Research Center for application to model design and fabrication. The AD-2000 program which was obtained under the Integrated Program for Aircraft Design Contract (IPAD) with the Boeing Company is being used as the pilot program.

The Analyses activities to date are reported in reference 3. It is anticipated that an integrated program for the analysis of models and support systems will result from this effort and include the necessary static, dynamic, aeroelastic, and fracture mechanics analysis capability.

Materials technology becomes a very important aspect of testing in a cryogenic environment and is discussed in reference 4 with emphasis on Fracture Mechanics aspects and the Material Selection Process. Although the activities in this area have concentrated on metals to date it is anticipated that other materials (e.g. advanced composites) may be selectively used for models and support systems. Reference 5 is a survey paper which presents information on virtually all classes of cryogenic materials ranging from primary structural material to adhesives. The Testing activities include such things as math model verification, materials properties characterization at cryogenic temperatures and testing in the 0.3 meter tunnel to verify design concepts. The 0.3 meter tunnel offers an excellent test bed for structural design verification, study of surface roughness effects, study of sting geometry aerodynamic interference effects, and other types of technology-oriented research activities.

Fabrication is an area where much work is needed to advance the technology. In particular a number of different techniques for building 2-D airfoil models are being studied. One method which offers excellent promise is that of diffusion bonding. Tubes inside the model can possibly be eliminated by diffusing layered material sections together to form pressure passages and then drilling holes into these passages. The problem of obtaining smoother surfaces and closer tolerances (see reference 6) certainly poses fabrication concerns, particularly for the tough materials that will be required for cryogenic testing. Also, the types of equipment needed for accurate measurement of surface finish and validating model tolerances are being investigated.

The conventional design approach for models and stings tested in NTF would require safety factors of three on yield or four on ultimate (whichever is greater). The use of similar safety factors for NTF models would be highly desirable of course for protecting the fan and avoiding damage to the tunnel. However, because of the potentially high aerodynamic loading in the NTF, use of these conventional safety factors would place operating constraints on the NTF test envelope. For example, design working stresses are projected to be $6.9 \times 10^9$ newtons/$m^2$ (100 ksi) or greater for high $R_e$, high dynamic pressure testing. To apply a safety factor of 3 would disqualify most commercially available alloys. Therefore safety factors must be reduced.

A summary of the relaxed primary design criteria selected for the developmental models is given in figure 4. The criteria in figure 4 relaxes safety factors on strength and fatigue, introduces a new requirement in terms of fracture toughness and maintains current practice on aeroelastic safety factors. The basis for relaxing design criteria is as follows: much more attention will be given to design; more in-depth and state-of-the-art analyses will be required; variability on knowledge of loads will be minimized to the extent possible; extensive verification and proof testing will be required; better quality control and inspection during procurement and fabrication will be required; and highly critical model tests will require on-line monitoring of loads and dynamic response. Emphasis will also be placed on fracture control and selection of materials with high fracture toughness.

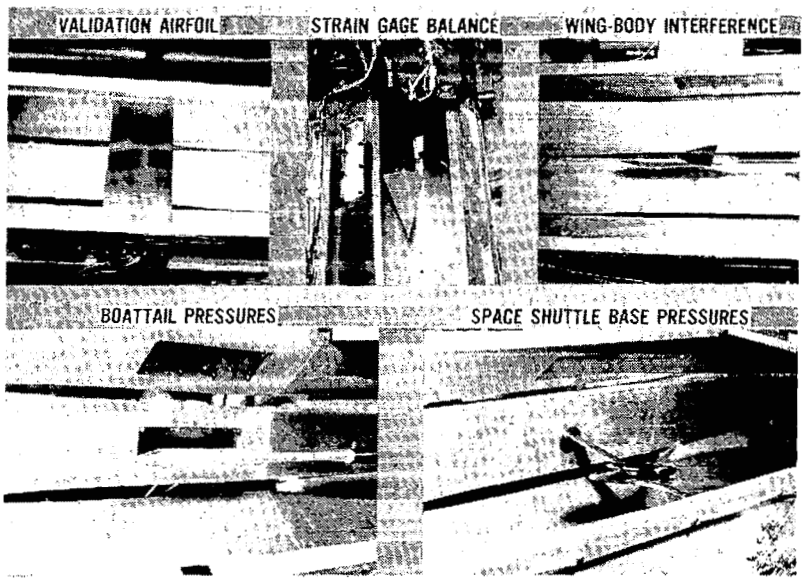


Figure 1.- 0.3-Meter Transonic Cryogenic Tunnel tests in original octagonal test section.

- OBJECTIVES
  - DEVELOP TECHNOLOGY FOR DESIGN AND FABRICATION OF MODELS/ STINGS FOR NTF
  - DOCUMENT REQUIREMENTS
- ELEMENTS
  - PATHFINDER I MODEL (TRANSPORT)
  - PATHFINDER II MODEL (FIGHTER)
  - SUPPORT STINGS
  - USERS CRITERIA DOCUMENT

Figure 2.- Cryogenic models/stings research and development program.

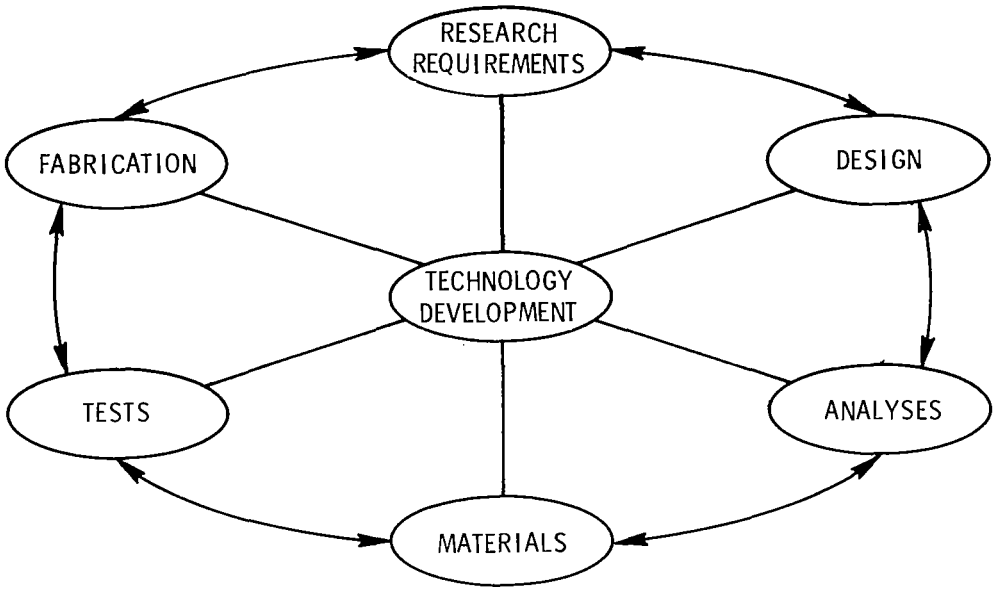


Figure 3.- Major technology development activities.

- STRENGTH - PEAK ALLOWABLE STRESS $\leq$ 2/ 3 YIELD AT TEST TEMPERATURES
- FATIGUE - SAFE-LIFE DESIGN PER MODIFIED GOODMAN DIAGRAM WITH APPLIED SAFETY FACTOR OF TWO (2)
- FRACTURE - MATERIAL SHALL HAVE CHARPY V-NOTCH IMPACT STRENGTH $\geq$ 33.7 m-N (25 ft-lb) AT TEST TEMPERATURES
- AEROELASTIC - SAFETY FACTOR OF TWO (2) AGAINST DIVERGENCE AND FLUTTER (BASED ON TEST DYNAMIC PRESSURE)

Figure 4.- Selected design criteria for Pathfinder I and II models/stings.

the configurations are suitable for generalized aerodynamic research models and to the extent practical are being designed to allow ease of modification, such as replacing the fuselage forebody, aft fuselage and wings.

## SYMBOLS

| | |
|---|---|
| A | aspect ratio |
| A/C | aircraft |
| b | model span |
| c | wing chord |
| $\bar{c}$ | wing mean aerodynamic chord |
| $C_L$ | lift coefficient |
| g | gravity force |
| M | Mach number |
| $M_L$ | local Mach number |
| q | dynamic pressure |
| $R_{\bar{c}}$ | Reynolds number based on mean aerodynamic chord |
| T | temperature |
| t | wing thickness |
| W | wind tunnel width |
| $\alpha$ | angle of attack |

## DISCUSSION

Model Sizing Size has a strong impact on the model design and fabrication problems with the larger models generally being easier to fabricate. However, larger models result in increased tunnel wall interference effects and it is this wall interference effect that determines the maximum acceptable model size for aerodynamic testing. For these models, the size criteria utilized in the analysis by the

subpanel to the Aeronautics and Astronautics Coordinating Board which resulted in the performance specifications for the NTF was used. This criteria was based on an AGARD study. It places constraints on maximum allowable wing span, blockage and planform area. For the two models of interest here, the application of these three constraints result in model sizes expressed in terms of wing span as indicated on figure 1. A transport model designed for low to moderate angles of attack (near cruise condition), is limited to a wing span of equal to or less than 0.6 of the tunnel width. A typical high angle of attack maneuvering fighter is limited to a wing span of equal to or less than 0.2 of the tunnel width, or about 0.45 meters.

Fighter Model Since there are broader considerations in the selection of a model design point for a maneuvering fighter configuration than a transport, the Pathfinder II model is discussed first. The basic geometric characteristics are listed on the left of figure 2. The design loading conditions were selected to be representative of a 7 g maneuver condition at a mach number of 0.9 and 3 thousand meters altitude. This resulted in a wing loading ($C_L q$) of $2.7 \times 10^5$ newtons per square meter and corresponds to a Reynolds number based on chord of 55 million.

Figure 3 presents an operating envelope for the NTF at a Mach number of 0.9 as a function of Reynolds number based on a chord of 14.2 cm and wind tunnel dynamic pressure, q. The lower boundary represents operation at near ambient temperature and the upper boundary is determined by the coldest temperature at which the NTF can operate without condensation at some point on the model. In this case, the local conditions are static temperature at a local Mach number of 1.4. The left and right vertical boundaries are determined by the minimum and maximum operating total pressure of the NTF respectively. The shaded area is representative of the Reynolds number and q range of existing 2 to 2.5 meter tunnels with this size model. The upper end represents Calspan operating with ejectors for short runs. For further reference, the Langley 8 foot TPT maximum "q" is on the order of 48000 newtons per square meter. The region above the shaded band represents the increase in Reynolds number range that can be provided in the NTF with model loads comparable to those obtained in existing tunnels. The Reynolds number for a typical maneuvering aircraft at altitudes from 3 to 12 thousand meters is shown for reference. The Pathfinder II design point is also indicated.

In a Cryogenic Wind Tunnel, the temperature variation as a function of pressure corresponding to condensation at a local mach number of 1.4 results in a variation of Reynolds number with q, between 3 and 12 thousand meters, that is essentially proportional to that of the airplane in the atmosphere. This says of course, that for a constant load factor simulated over the altitude range at full scale Reynolds number in the NTF, the model load will be constant just as it is on the airplane. This is illustrated in figure 4. As Reynolds number is increased at the minimum

NTF temperature, the tunnel q will increase. If a constant airplane g or loadfactor condition is simulated, however, the model angle of attack and thus lift coefficient will be reduced and the resulting $C_Lq$, or lift, will be constant with Reynolds number. If for model design considerations, changes in wing span loading with changes in angle of attack are ignored, this constant lift load will result in a constant wing stress. Therefore, the stress limit will correspond to the maximum $C_Lq$ which will impose a limit on maximum airplane g's or loadfactor that can be simulated at full scale Reynolds number. This limit is independent of the magnitude of Reynolds number. The dynamics of the model/sting/balance configuration which is a function of dynamic pressure, or q, will govern the maximum Reynolds number at which full scale conditions can be simulated. The effect of the $C_Lq$ limit is summarized on figure 5 which is basically an overlay to figure 3 with some of the legend omitted for clarity. The open symbols represent flight conditions, where for a constant simulated load factor condition the model load is constant. It is interesting to note that the strength requirements for a model tested in an existing tunnel (solid symbol) at a q of approximately 72,000 newtons per square meter and a lift coefficient corresponding to a given load factor at 12000 meters are identical to what they will be in the NTF at any of the full scale conditions indicated by the open symbols for the same simulated load factor. This results from the fact that the increase in Reynolds number between the solid symbol and open circle corresponding to 12,000 meters altitude is due entirely to the benefit of cryogenic temperature operation.

The bottom line of this discussion is that both model strength and model/balance/sting system dynamics will play an important role in determining maximum usable NTF test capability for a given configuration. The design conditions chosen for Pathfinder II are ambitious and should explore the limitations of both model strength and dynamics on the testing envelope for this class of configuration.

Transport Model The Pathfinder I model (figure 6) is an advanced transport configuration. The geometric characteristics, which are typical of this class of airplane, are shown on the left of figure 6 and are discussed in some detail in reference 1. The primary design point is for a 1 "g" cruise. However, to insure capability of testing at off-design conditions, the model strength design point is 1.8 "g" at 0.8 Mach number and 10700 meters altitude. The resulting wing loading ($C_Lq$) is $1.34 \times 10^5$ newtons per square meter and the Reynolds number based on chord is 38 million.

The design of this model will focus on those problems associated with the design of high aspect configurations. Since for a given airplane size, the higher the aspect ratio, the higher the tunnel q required for full scale simulation; thus the higher the design load. This is illustrated in figure 7. For a given wing area, an increase in wing aspect ratio is the result of increased wing span as illustrated in the sketch on the right. When a wind tunnel model is sized on an absolute value of the wing span, as the aspect ratio is increased, the scale of the model must be reduced. Therefore, to maintain full scale Reynolds number, the model

must be tested in the tunnel at a higher q. The main part of the figure illustrates this effect for three airplane sizes. The symbols indicate the model design or wind tunnel test q required to achieve full scale RN for three typical aircraft sizes. The slope of the lines shows the increase in wind tunnel "q" required to maintain full scale RN if the aspect ratio is increased on these configurations. The Pathfinder I was assumed to be an intermediate size transport of the L-1011/DC-10 class with an aspect ratio of 9.8.

Figure 8 shows the design point, for this size model, relative to the NTF operating envelope. Again, the lower bound corresponds to the ambient temperature condition and the upper bound is determined by the minimum temperature. Test conditions for existing tunnels and Reynolds numbers achievable with current model loads are indicated. Note that the test conditions for the Pathfinder I model are about a factor of 10 increase in Reynolds number with only a factor 2 increase in test q over current test conditions.

## CONCLUDING REMARKS

An advanced transport and a highly maneuvering fighter configuration have been selected as initial models for the cryogenic high dynamic pressure model technology development program. These models will provide a basis for establishing practical achievable Reynolds number boundaries based on model stresses and model balance sting system dynamics. The model loads, thus the stresses, will be constant in the NTF when matching full scale airplane Reynolds number over the altitude range at a constant load factor. The maximum Reynolds number obtainable under these conditions will be limited by the influence of dynamic pressure on model/balance/sting system dynamics. Reynolds numbers to 25 million, based on chord, can be obtained on the Pathfinder models in the NTF with no increase in loads over those encountered in existing tunnels. These models represent advanced technology configurations and will be used for parametric research studies.

## REFERENCE

1. Bradshaw, James F.; and Lietzke, Donald A.: Pathfinder I Model. Cryogenic Technology, NASA CP-2122, 1980. (Paper 27 of this compilation.)

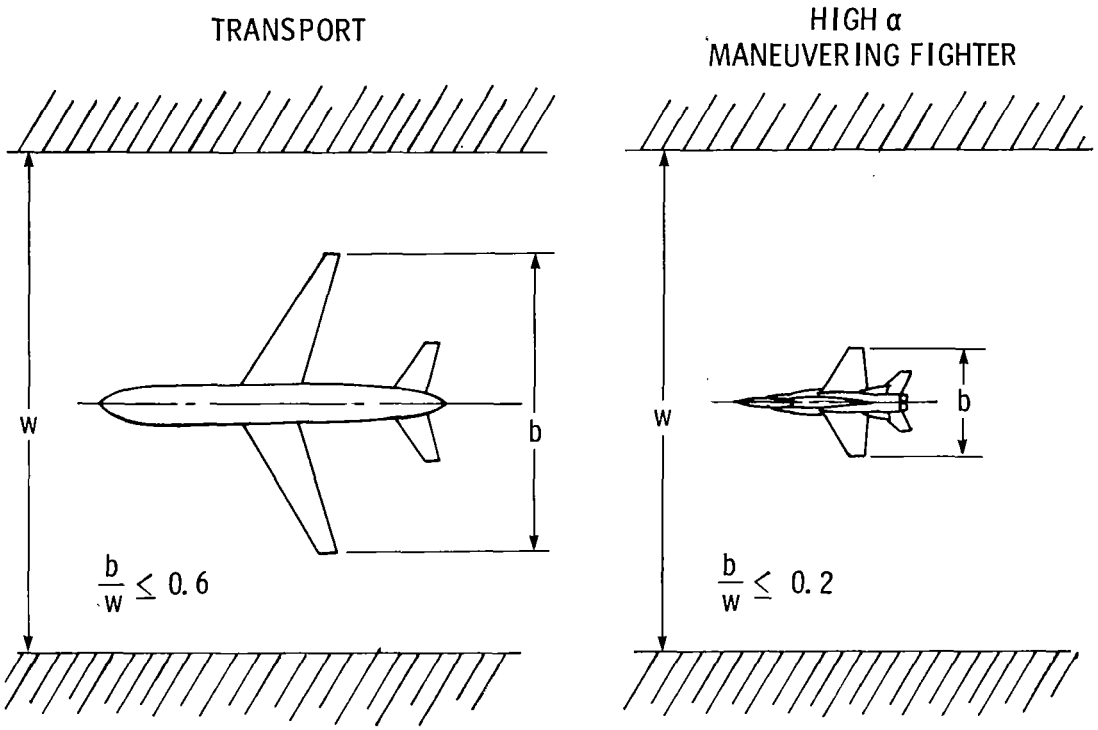


Figure 1.- Model sizing considerations.

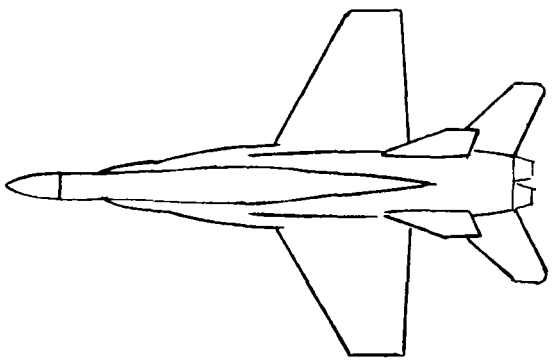

GEOMETRIC CHARACTERISTICS

- ASPECT RATIO = 3.5
- t/c = 0.05 (ROOT); 0.035 (TIP)
- SPAN = 45.7 cm
- $\bar{c}$ = 14.2 cm

DESIGN CONDITIONS

- 7.0 g's AT M = 0.90; ALT. = 3000 m
- $C_L q = 2.7 \times 10^5$ N/m$^2$
- $R_{\bar{c}} = 55 \times 10^6$

Figure 2.- NTF Pathfinder II: high performance maneuvering fighter.

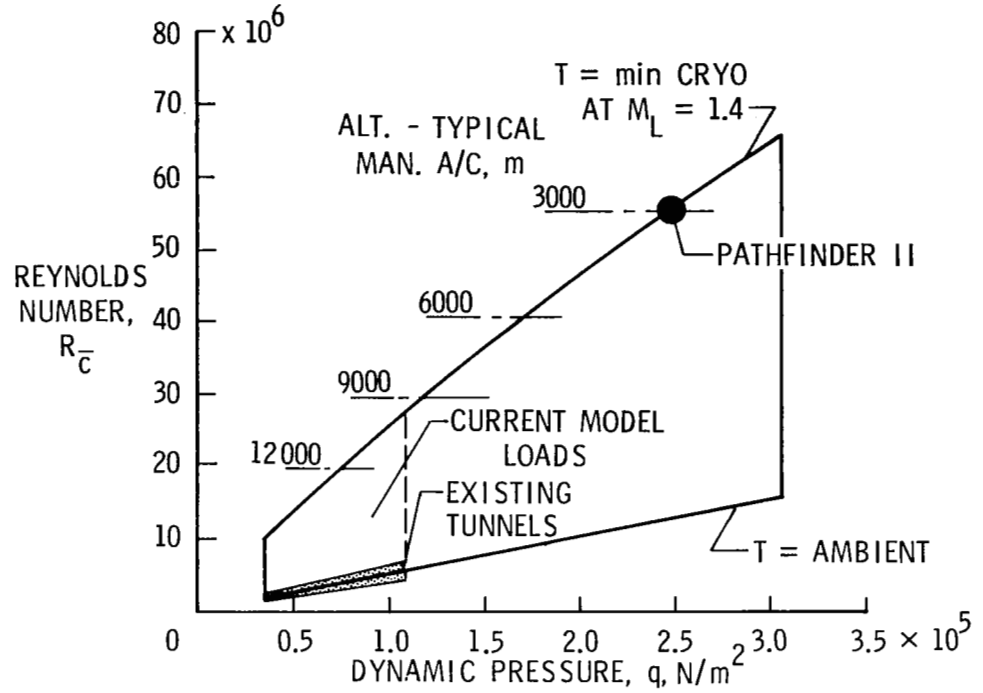


Figure 3.- NTF operating envelope at M = 0.90 for Pathfinder II. $\bar{c}$ = 14.2 cm.

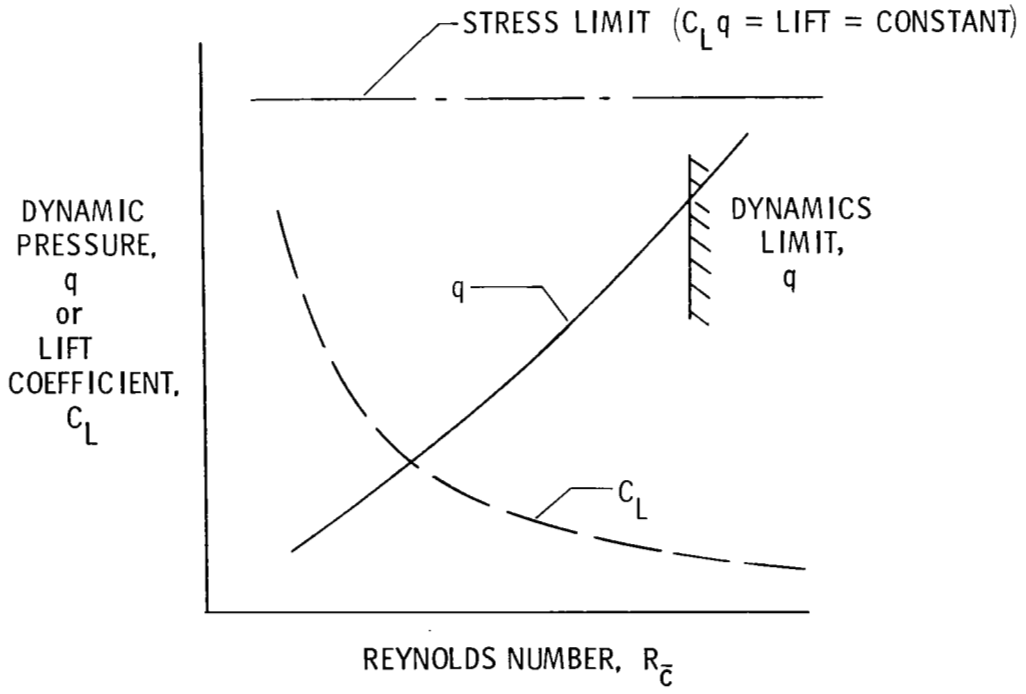


Figure 4.- Model imposed limits on matching aircraft flight conditions.

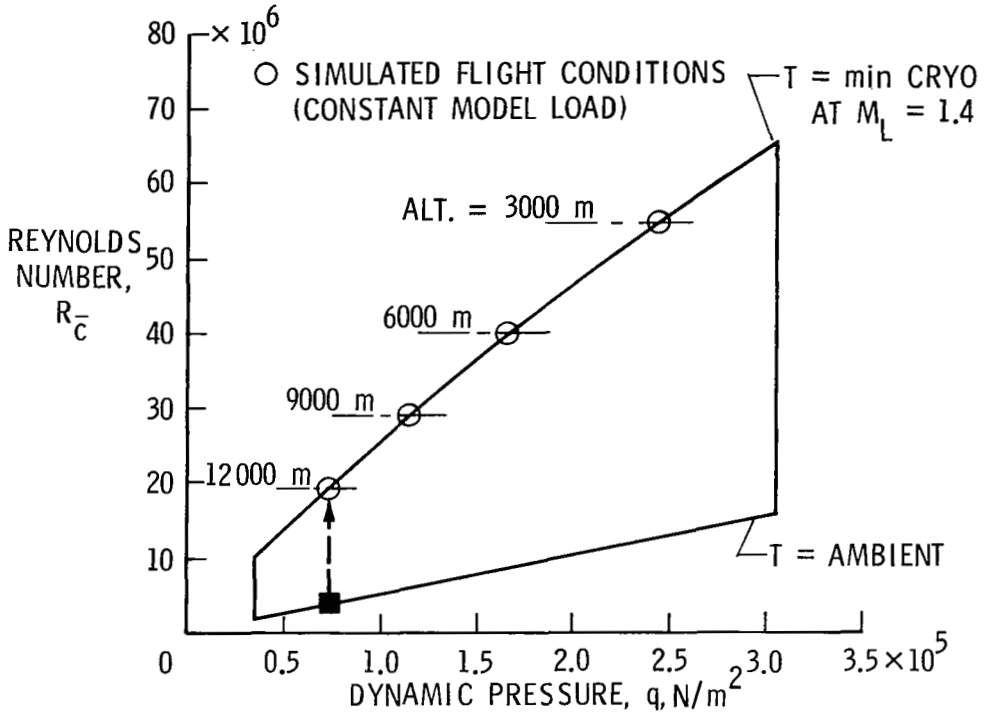


Figure 5.- NTF operating envelope at M = 0.90 for Pathfinder II. $\bar{c}$ = 14.2 cm.

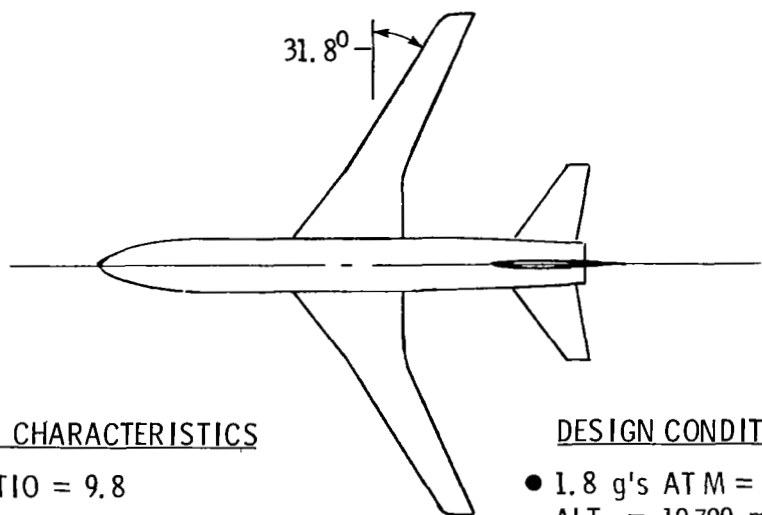


GEOMETRIC CHARACTERISTICS

- ASPECT RATIO = 9.8
- ADV SUPERCRITICAL WING
- t/c = 0.145 (ROOT); 0.106 (TIP)
- SPAN = 187.62 cm
- $\bar{c}$ = 13.7 cm

DESIGN CONDITIONS

- 1.8 g's AT M = 0.80; ALT. = 10700 m
- $C_L q = 1.34 \times 10^5$ N/m$^2$
- $R_{\bar{c}} = 38 \times 10^6$

Figure 6.- NTF Pathfinder I: advanced subsonic transport configuration.

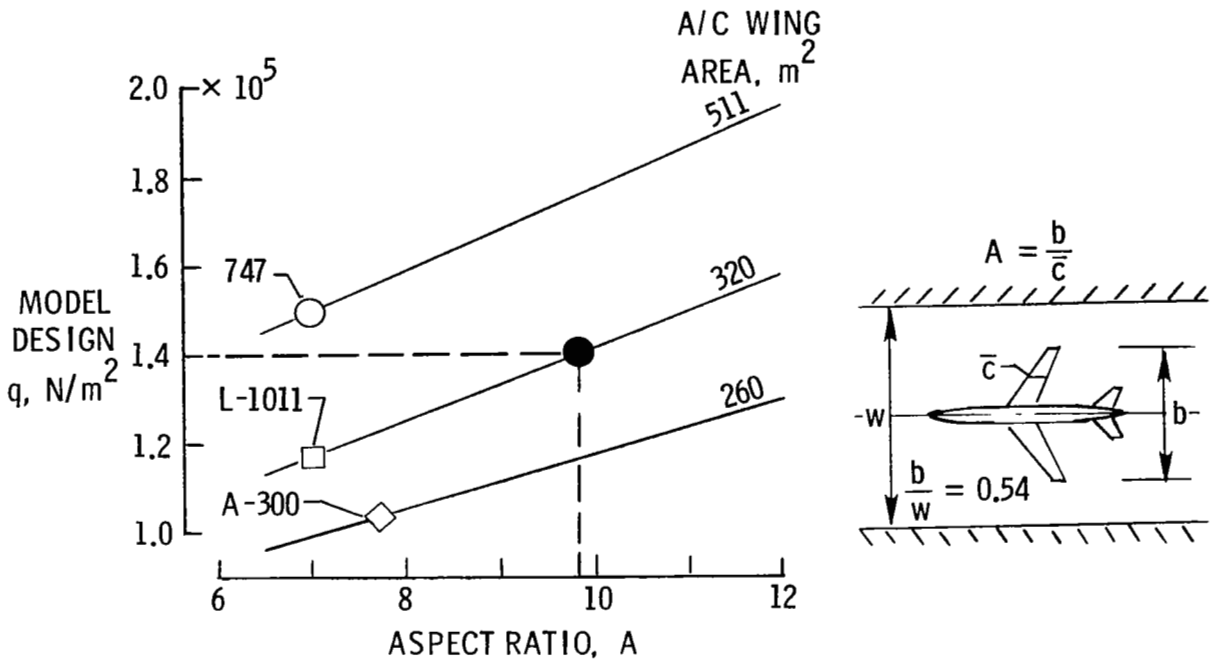


Figure 7.- Effect of aspect ratio and airplane size on model design q. $R_{\bar{c}}$ = full scale at M = 0.8; Alt. = 10 700 m; T = min cryo.

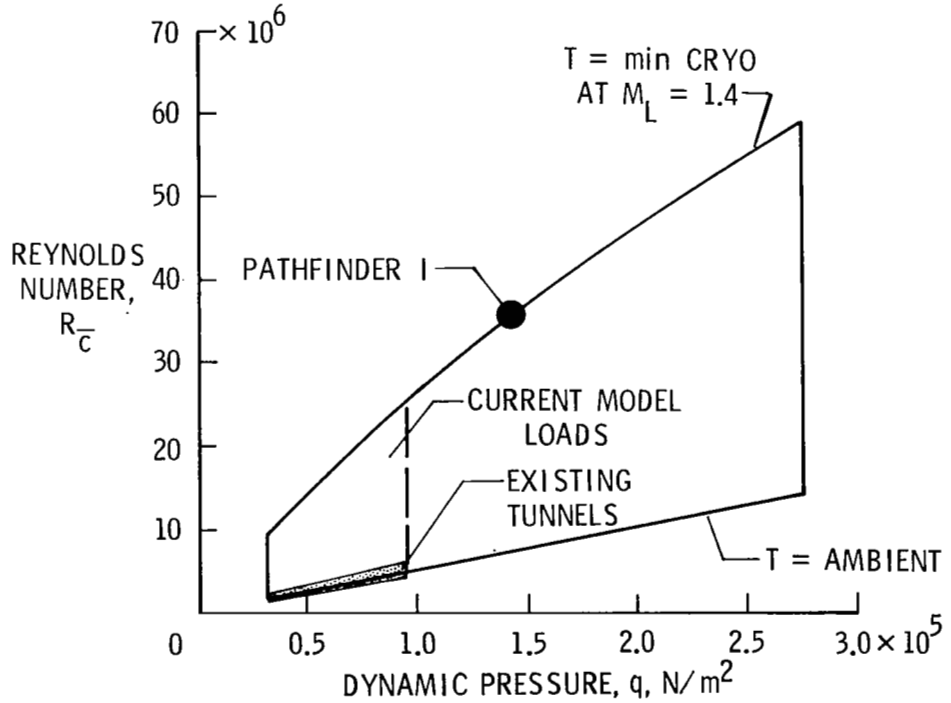


Figure 8.- NTF operating envelope at M = 0.8. $\bar{c}$ = 13.7 cm.

# SOME AERODYNAMIC CONSIDERATIONS RELATED TO SURFACE DEFINITION

Blair B. Gloss
Langley Research Center

## SUMMARY

The requirement for high quality National Transonic Facility test data and the high Reynolds number capability of the NTF have caused NASA to re-examine the areas of model fabrication tolerances, model surface finish and orifice induced pressure error. The results of this re-examination and planned research programs to extend the data base are summarized below.

Better techniques for defining transonic model tolerances are needed even though model tolerance requirements should not be significantly dependent on Reynolds number.

Current specified model surface finishes appear to be compatible with a significant part of the NTF Reynolds number range. It is planned for the National Bureau of Standards to validate the accuracy of the stylus profilometer for surfaces typical of NTF models and develop a light scattering system to measure surface finishes on curved surfaces (wing leading edge regions). NASA tests are planned to determine the acceptability of using existing data on sand roughened surfaces for predicting NTF model surface requirements.

Available data on orifice induced pressure errors cover a part of the NTF Reynolds number range and cover only a small part of the range of the ratio of orifice diameter to boundary layer thickness needed. A research program has been initiated by NASA to extend this data base to higher Reynolds number conditions. Techniques for avoiding orifice edge distortions must be strictly adhered to.

## INTRODUCTION

Because of the high Reynolds number capability of the NTF (see reference 1) with the attendant thin boundary layers and the requirement for high quality test data, NASA is re-examining the aerodynamic considerations related to model surface definition, particularly in the areas of fabrication tolerances, model surface finish and orifice induced pressure errors. Model fabrication tolerance requirements are very difficult to determine because of the accuracies needed in experimental and analytical studies for defining these tolerances at transonic speeds;

The instrumentation which is almost universally used to measure model surface roughness in model shops is the stylus profilometer type equipment. However, there are at least two potential problems associated with the stylus profilometer. Figure 3 depicts these two potential problem areas, roughness slope too steep and roughness frequency too high; it should be noted that the stylus radius is typically 2.5 microns (100 μin.). Since there are no published data which verifies that the stylus profilometer accurately determines surface topography data on surfaces typical of NTF models, it is planned that the National Bureau of Standards (NBS) will compare the topography of a surface typical of NTF models as measured by a stylus profilometer and stereo scanning electron microscope. In addition, the stylus profilometer has great difficulty measuring surface finishes on curved surfaces similar to the leading edge region of wings. The leading edge region of the wing is the region, of course, where the boundary layer is thinnest and thus is the region where the local skin friction is most sensitive to surface roughness. Thus, it is highly desirable to have the capability of measuring surface finish over the leading edge. Towards this end the NBS will develop a light scattering system to measure the surface finish accurately on surfaces with high curvature.

Orifice induced pressure error.- When the static pressure in a flow field is measured by a pressure orifice, the streamline curvature can change in the vicinity of the orifice and eddies can be set up inside the orifice resulting in the static pressure measurement being higher than the true value, references 5 through 9. If the boundary layer thickness is large compared to the orifice diameter, the orifice induced pressure error is small and usually neglected. However, as the Reynolds number increases and the boundary layer becomes thinner, the boundary layer thickness can become small compared to the orifice diameter. Under these conditions the orifice induced pressure error may not be negligible. An additional orifice error, that may be sizable in magnitude, can result from orifice imperfections. Although there are several types of orifice imperfection, experimental data (reference 6) exists only for a burr around the orifice. A burr can produce flow separation in the orifice causing additional streamline deflection. Some other types of hole imperfection which can produce pressure error are out-of-round orifices, particles in the orifice and the longitudinal axis of the orifice not normal to the model surface to mention a few.

Figure 4 presents a compilation of experimental results for orifice induced pressure error of "perfect" (absence of imperfection) orifices from references 5 through 7 (only the subsonic data from reference 5 is included in figure 4). It is shown in reference 6 from local dynamical similarity considerations, that

$$\frac{\Delta c_p}{c_f} = f\left(R_a\sqrt{\frac{c_f}{2}}\right);$$

therefore, orifice induced pressure error is generally presented as $\Delta c_p/c_f$ versus $R_d\sqrt{\frac{c_f}{2}}$. The largest values of $d/\delta^*$ (orifice diameter/boundary layer thickness) for which test results are shown in figure 4 is 4.0. Using the data of reference 7, shown in figure 4, the variation of pressure error, $\Delta c_p$, with Reynolds number, $R_{\bar{c}}$, for three orifice diameters, 0.51 mm (0.02 in), 0.25 mm (0.01 in) and 0.13 mm (0.005 in) are shown in figure 5 where the local skin friction coefficient is taken as 0.0022 and the mean chord, $\bar{c}$, is taken as 0.20 m (0.65 ft). For reference the maximum NTF Reynolds number, Boeing 747 cruise Reynolds number and the maximum Reynolds number available in current tunnels are shown on figure 5. From the data in figure 5, it may appear that a 0.13 mm (0.005 in) diameter orifice is satisfactory for the complete range of NTF Reynolds numbers since the maximum error is only 0.008; however, all the data in figure 5 are for $d/\delta^* < 4.0$, and since $d/\delta^*$ for the high Reynolds number conditions can be of the order of 100, erroneous conclusions may be drawn regarding the level of the orifice induced pressure error if only this data is applied. Further, just extrapolating the curves for the 0.51 mm (0.02 in) and 0.25 mm (0.01 in) diameter orifices to the high Reynolds number region can lead to erroneous conclusions. Therefore, a test program is underway to extend the data shown in figure 5 to higher $d/\delta^*$ values and higher Reynolds numbers. Figure 6 shows a picture of the flat plate model to be used in this test program; the interchangeable orifices have diameters of 3.30 mm (0.13 in), 6.60 mm (0.26 in) and 13.21 mm (0.52 in). The reference orifice diameter is 0.51 mm (0.02 in). Only one of the interchangeable orifices will be in the plate at a time and the untested orifices will be replaced with plugs. Since this plate will be tested in the Langley 7- x 10-foot wind tunnel at low Reynolds numbers, the orifices were scaled up in size so that the proper $d/\delta^*$ could be attained; the complete orifice including plumbing was scaled up for these tests. Local skin friction and boundary layer thickness ($\delta^*$) will be obtained from a boundary layer survey. Figure 7 shows the envelope of $d/\delta^*$ variation with Reynolds number, $R_{\bar{c}}$, for a 0.51 mm (0.02 in) diameter orifice attainable with the present hardware. Although the maximum $d/\delta^*$ encountered in the leading edge region of an NTF wing may be in excess of 100, these data will extend the data base far enough to allow judgement on whether the data may be extrapolated safely to the desired $d/\delta^*$ values. The $d/\delta^*$ range covered in this test will be adequate to directly assess the orifice induced pressure error for a large majority of the orifices on NTF models.

The hole imperfection data of reference 6 only extend to values of $R_d\sqrt{\frac{c_f}{2}}$ of 300. Burr heights of 1/42 the orifice diameter can increase the hole error by a factor of approximately five, figure 8, thus, it is desirable to fabricate orifices that have the hole imperfections minimized. Reference 9 outlines a routine for fabricating orifices with the final step calling for close visual and stylus profilometer inspection of each orifice.

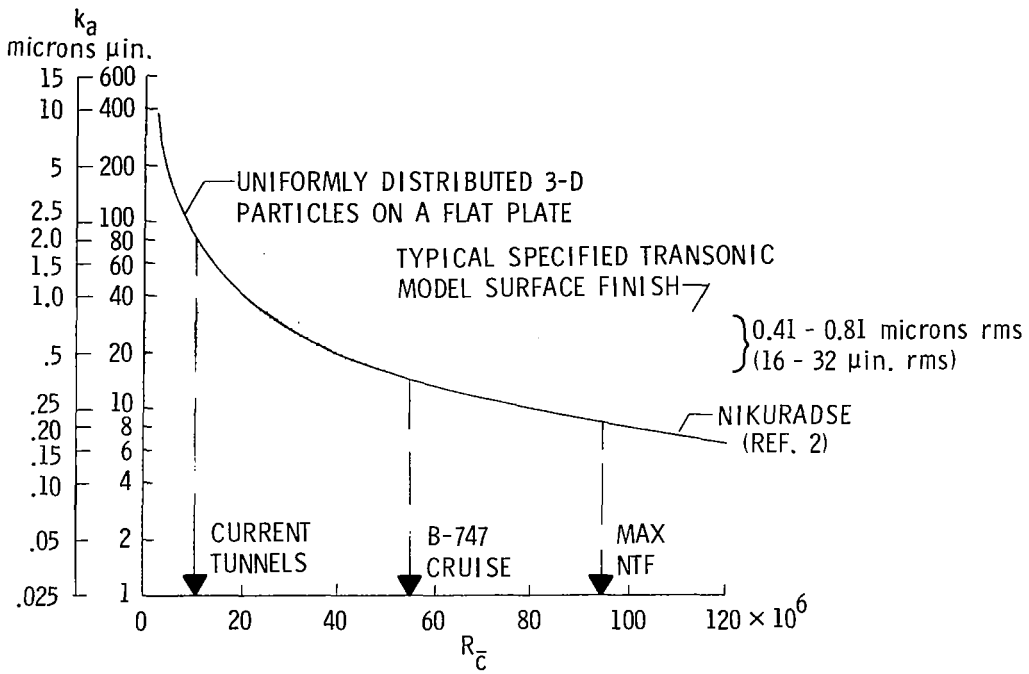


Figure 1.- Admissible roughness ($k_a$) for typical NTF sized models, $\bar{c}$ = 0.20 m (0.65 ft).

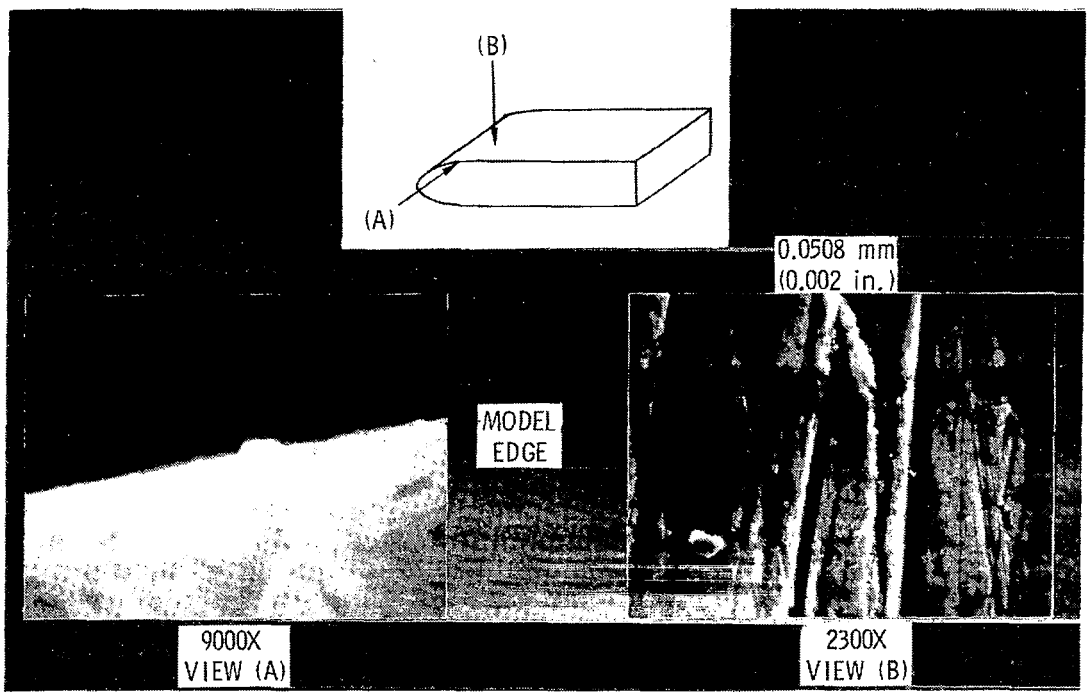


Figure 2.- Electron micrographs of typical NTF model surface. Model surface finish, 0.2-0.3 microns (8-12 μ in.) rms (stylus measured).

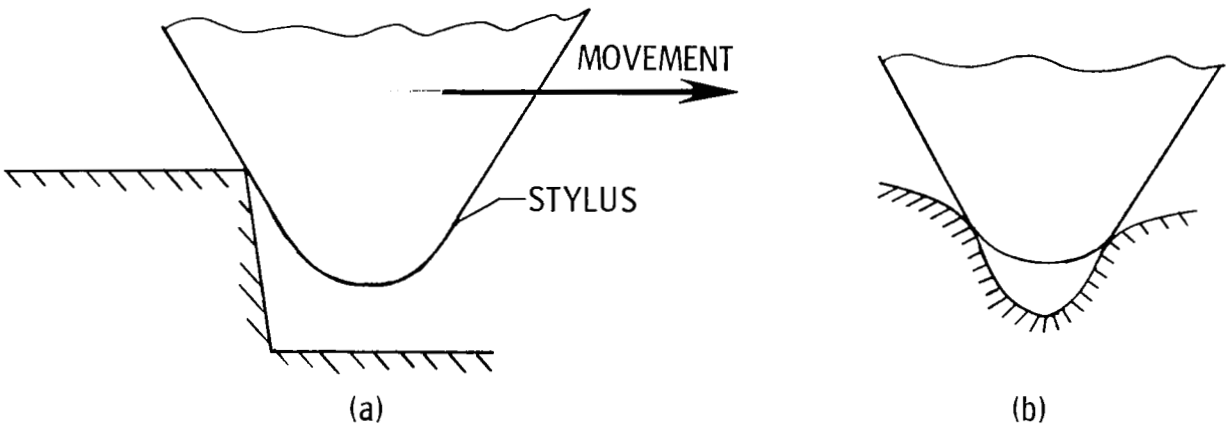


Figure 3.- Potential stylus profilometer problem areas.

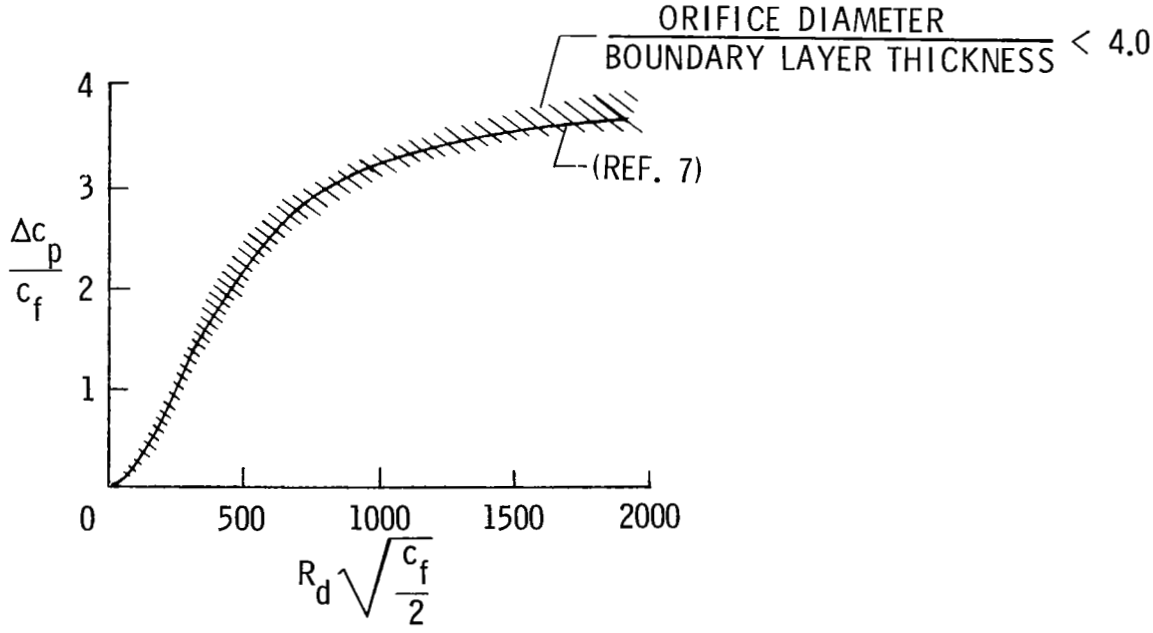


Figure 4.- Compilation of test results for orifice induced pressure error.

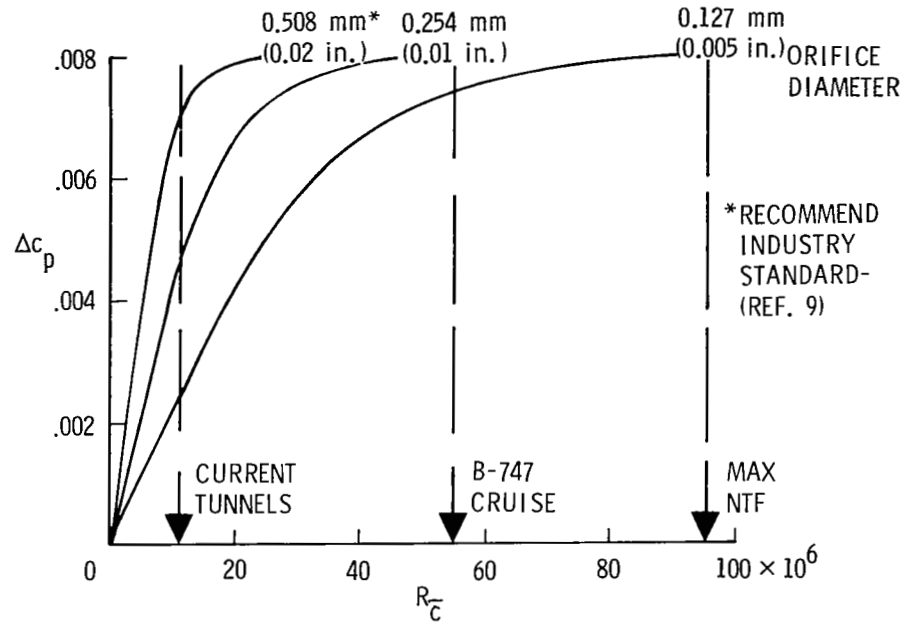


Figure 5.- Orifice induced pressure error. $c_f$ = 0.0022; $\bar{c}$ = 0.20 m (0.65 ft).

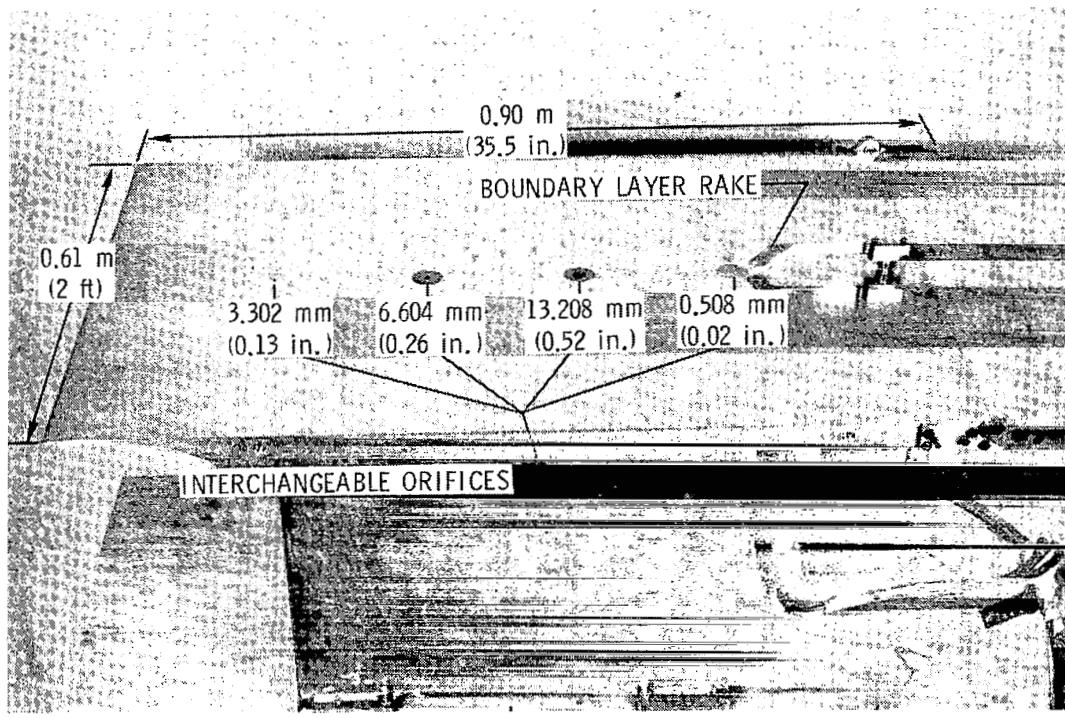


Figure 6.- Model setup for orifice induced pressure error studies.

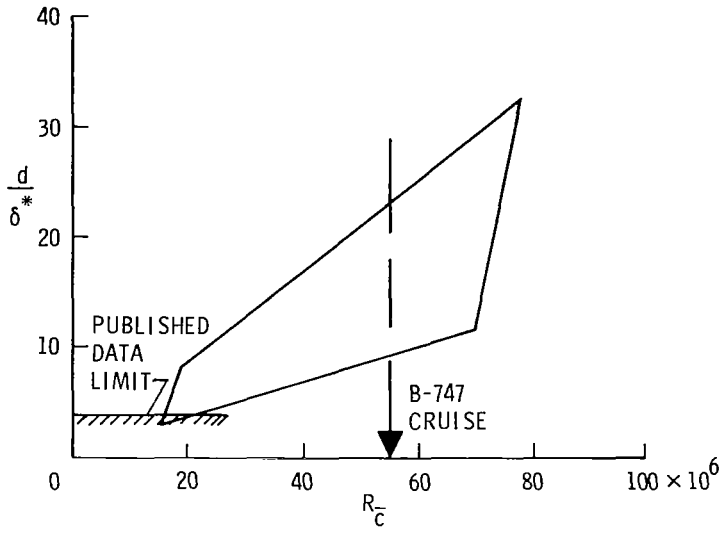


Figure 7.- Envelope of current pressure error experiment, $c_f = 0.0022$, $M_\infty = 0.85$, $\bar{c} = 0.20$ m (0.65 ft), $d = 0.508$ mm (0.020 in.).

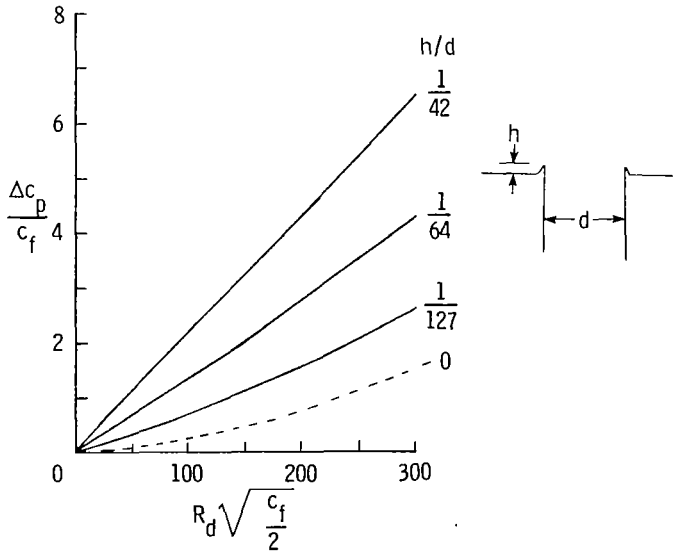


Figure 8.- Effect of hole imperfection on orifice induced pressure error (ref. 6).

# PATHFINDER I MODEL

James F. Bradshaw and Donald A. Lietzke
Langley Research Center

## SUMMARY

This paper describes the Pathfinder I Model that has been designed for testing in the National Transonic Facility. Unique considerations for the design of cryogenic models are discussed along with the particular design requirements for Pathfinder I. The geometric details of the model are provided and various features of the model components are discussed, along with a description of design validation test support activities. Also data are presented which emphasize the importance of material selection as it influences the model test program because of material property changes with temperature. It is found that good engineering practice with proper consideration given to the cryogenic environment and specific test requirements will produce a model acceptable to testing in the National Transonic Facility.

## INTRODUCTION

The National Transonic Facility (NTF) is being constructed at Langley Research Center as a research tool for testing models at Reynolds numbers to values comparable to those of full scale aircraft. Tests in the Langley .3-Meter Transonic Cryogenic Tunnel (TCT) have provided cryogenic research experience needed to initiate a cryo model program for the NTF. Two Pathfinder Models are being designed as an initial step in establishing criteria for the design, fabrication, inspection, and documentation of models to be tested in the NTF (see ref. 1). These criteria will become part of a tunnel operation manual. The Pathfinder models, a transport configuration and a high performance fighter configuration will be fabricated at Langley and will be the first models tested in the NTF. This paper presents the work that has been done in connection with the design of only the Pathfinder I Model.

## UNIQUE CONSIDERATIONS

There are two major differences that have to be considered in designing models for the NTF as compared to designing models for testing in conventional wind tunnels. The first of these is the cryogenic environment with temperatures as low as 78 K, and secondly, in order to utilize the full capability of the NTF for testing at high Reynolds number, some models will have to be designed for testing at much higher dynamic pressures. The cryogenic environment requires that particular attention be given to thermal considerations.

These include thermal stress, expansion and contraction, and the thermal compatibility of materials and joints. Also, a very critical aspect concerns the selection of materials, considering the wide variations in mechanical properties involved in the ambient to cryogenic temperature range. Although the strength of most materials increases as the temperature decreases, the toughness decreases. Therefore improper material selection or internal flaws may result in brittle failure. Thus the material for these models has to be characterized for cryogenic temperatures (see reference 2). Testing at high dynamic pressures will result in higher stresses than those typical for conventional tunnel models. In addition, factors associated with aeroelastic bending, potential flutter, and high dynamic response must be considered.

## MODEL DESCRIPTION

The NTF Pathfinder I Model is a representative wide-body transport configuration incorporating an advanced high aspect-ratio supercritical wing. It is a force and pressure model and will be instrumented with accelerometers, thermocouples, and buffet gages. The configuration has a low wing and tail and a design lift coefficient of approximately 0.55 at a cruise Mach number of 0.82.

The fuselage is .146 m (5.75 in.) in diameter and 1.27 m (50.0 in.) long (see figure 1). Its nose is an ogive shape that fairs into the body diameter. The center section is a cylinder and the aft end of the fuselage provides access and clearance for the sting.

The wing has a 9.8 aspect ratio based on the trapezoidal planform area of .183 $m^2$ (1.98 $ft^2$) (including fuselage intercept) and the 1.345 m (52.97 in.) span. The total area of the wing including the leading and trailing edge extensions is .214 $m^2$ (2.30 $ft^2$). The wing has 5° dihedral and the supercritical airfoil has a thickness to chord ratio of 0.145 at the side of the fuselage, 0.12 at the geometric break and 0.106 at the tip. The quarter chord line (C/4) of the trapezoidal planform has a sweep of 30°.

The horizontal tails have a 10 percent thick supercritical airfoil shape, are all moving, and are manually adjustable to +4°. The vertical tail has a 10 percent thick symmetrical supercritical airfoil shape. The detailed geometric characteristics of the model are given in table 1.

## DESIGN REQUIREMENTS

The Pathfinder I has the same aerodynamic configuration as a model that was tested in the Langley 8-ft transonic pressure tunnel and data from the 8-ft tunnel tests were used as a basis for calculating the aerodynamic design loads. This model will be tested in the NTF at a maximum dynamic pressure (q) of .134 x $10^6$ $N/m^2$ (2800 psf) and at temperatures ranging from 89 K to 339 K. The wing will have a maximum load of 24910 N (5600 lbs) at a lift coefficient

($C_L$) of 1.0. All model components have been designed and analyzed to have a minimum factor of safety of 1.5 on the yield at test temperatures. The aerodynamic loads on the tail section, the dimensional accuracy and surface finish requirements are given in table II.

## DESIGN

The basic approach in developing the mechanical configuration of the model was to use a minimum number of joints to reduce the effect of temperature gradients on the components. Additionally, this concept provides for convenient testing of the model in any configuration such as fuselage only, fuselage and wing, or fuselage, wing, and tails, (see figure 2).

The fuselage is designed in three sections, the nose, the center body which is also the model strongback, and the aft section. The nose section is .47 m (18.5 in.) long and is designed as a heavy wall shell. This design provides a large cavity for the model instrumentation and also provides for quick and easy access to this instrumentation. The heated instrumentation package will be isolated and insulated from the nose section and the cold environment. The fuselage center body is the structural section of the model which supports all of the model components and also provides the interface with the NTF-101 strain gage balance which has been specially designed for cryogenic service. This section is designed as a strongback to provide rigid mounting surfaces as well as passage for instrumentation. The nose and aft sections are mounted to cylindrical bosses on the center body and are retained by dowels equally spaced radially thru the mounting surface. The dowels connecting the aft section are designed to withstand the aerodynamic loads of the empennage.

The main impact of the cryogenic environment was in the design of the balance mount and the wing/centerbody attachment. The balance mount housing consists of two parts that are designed to clamp the balance and at the same time connect it to the strongback. There are two tunnel operation modes that influence the balance mount design in addition to the temperature at which the test will take place. The first mode is the cool down mode during which the model surface may be much colder than internal components such as the balance. To accommodate this mode the balance mount is a two piece split clamp with both components in turn being clamped to the strongback by the same bolts (see figure 3). These bolts are designed to be preloaded such that thermal gradients will not relieve the clamping forces either to the balance or to the strongback. The second mode involves the requirement that the model be heated to 278 K whenever any manual work is performed on it. In this case the balance and sting system may be several hundred degrees colder than the model surface. This mode also requires that the bolts be preloaded to maintain the desired clamping force.

The full span wing, designed as a single unit integral with the lower part of the center body, greatly simplified the connection of the wing to the strongback using only eight mounting screws. These screws are installed from the top

of the model and this design makes it easy to remove the wing and connect a balance calibration rig to the model.

The aft section of the model provides support for the horizontal and vertical tails. The fuselage in this area has been modified to allow for mounting the model on the sting with suitable clearance for deflection under load. This clearance was determined allowing for balance and sting deflection based on maximum loads of the NTF 101 balance. The vertical tail is mounted to this section by two rectangular bosses that are retained in the grooves by dowel pins. The horizontal tails are attached to this section by a modified breech lock type interrupted screw with square threads and zero lead as shown in figure 4. On the fuselage is a single thread with 90° segments at top and bottom which develop the strength necessary to withstand the aerodynamic loading of the tail. The butt end flange of the horizontal tail has a groove and also a single thread with corresponding vertically oriented 90° segments. The tail is positioned in proper attitude by a key plate mounted flush in the fuselage surface. Changes in the angle of incidence of the tail are accomplished by utilizing additional key plates with the key at different angular positions. The horizontal tail aerodynamic loads will produce a maximum 226 N-m (2000 in-lb) moment about the pivot axis; therefore, the key plate will have three keys (or teeth) to reduce the bearing stresses to an acceptable level. These changes, as well as disassembly of the nose and aft sections from the strongback, may be accomplished without contacting any surface still at cryogenic temperature.

The wing is designed as a full span wing and is instrumented with pressure orifices located on the upper surface of the left wing and the lower surface of the right wing at six spanwise stations. To locate all tubes internally, the wing is designed with a spanwise parting line along the 57 percent chord line (see figure 5). After evaluation of several joint designs the tongue and groove joint was selected. The leading and trailing edge sections are connected by a tongue and groove joint, the groove of which is enlarged to provide a spanwise tube passage (see figure 6). Analysis of the wing structure indicated that location of the tube passage in this position near the elastic axis reduced the strength of the wing by only 2 percent. The joint was stressed assuming that the loads on the wing trailing section are transmitted to the forward section. The analysis indicated that the pins should be designed for both shear and tensile loads to prevent distortion of the airfoil surface. At each spanwise location of pressure orifices, feeder passages and holes through the surface were designed and analyzed for minimum reduction of inertia and maximum strength of the section. Prior to final machining, with the wing .005m (.020 in.) oversize, the pressure tubes with plugs attached are inserted in the holes, and the plugs furnace brazed in place, as indicated in figure 7. After assembly of the wing sections, pinning of the joint, and final machining, the .00025m (.010 in.) diameter orifice holes are drilled through the plugs into the tubes.

As previously mentioned the wing strength design is based on a lift coefficient of 1. However the shape is designed to match the airplane at the cruise condition which is a $C_L$ of 0.55. To accomplish this, the wing is designed to a jig shape such that it will deflect and twist to the desired aerodynamic

shape under load. The magnitudes of the deflection and twist changes were calculated by the beam method discussed in reference 3 and are shown on figure 8. This analysis is based on the material stiffness characteristics at 89 K.

Spanwise bending stress profiles of the wing for a lift coefficient of 1 and a dynamic pressure of .134 x $10^6$ N/$m^2$ (2800 psf) are given in figure 9. The results using three methods to determine stresses in the wing are illustrated. The first method utilizes the spanwise loading of the wing and uses the streamwise moment of inertia, taking into consideration the reduction of inertia due to tube passages. This bending stress distribution, curve (A) of figure 9, shows the impact of the streamwise feeder passages and holes in the wing at each instrumented station. This method of analysis, however, does not take into consideration the torsion effect due to the offset loading resulting from the sweepback of the wing. Curve (B) of figure 9 is a spanwise distribution of bending stress along the elastic axis with section inertias taken normal to the elastic axis. In this case there is no offset loading since the chordwise center of pressure is coincident with the elastic axis. Curve (C) in figure 9 represents the wing stress distribution determined by using moment of inertias calculated from deflection data obtained by load testing a wing of exactly the same aerodynamic configuration (see reference 3). The effect of the streamwise tube passages (feeder passages) and orifice holes is illustrated by applying a stress concentration factor of 2 to the maximum stress distribution (peak values). These points are shown at the instrumented spanwise stations only and indicate that the maximum stress in the wing is about 689 x $10^6$ N/$m^2$ (100 KSI).

The selection of Nitronic 40 stainless steel for the model material (reference 2) allows a factor of safety of 1.5 on the yield strength at a temperature of 89 K and a dynamic pressure of .134 x $10^6$ N/$m^2$ (2800 psf.). Maintaining this factor of safety and accounting for variation in yield strength with temperature, the test envelope for the model based on a lift coefficient of 1 can be developed for all planned test temperatures and is presented in figure 10.

## TEST SUPPORT ACTIVITIES

The design of the Pathfinder I Model is being supported by test activities necessary to evaluate the component designs and also to provide additional experience with cryo model testing.

Figure 11 shows an example of the application of a filler material to repair an undercut model surface. After an evaluation of several materials, an aluminum filled epoxy was selected (see Appendix A). Satisfactory performance was obtained in the cryo environment of the 0.3 m TCT.

A 2-D wing model with the SC(2)-0510 airfoil shape has been designed using the same methods selected for the pathfinder wing and is illustrated in figure 12. This wing is under construction for testing in the .3 meter Transonic

APPENDIX A (Cont'd)

RESULTS OF MATERIALS TEST

| MATERIAL | ADHERE TO S.S. AND ALUMINUM | EASILY WORKED BY HAND | THERMOCYCLE 89 K-278 K | CURE AT 278 K OVERNIGHT | STAY UNDER MODEL UNTIL CURED | ACCEPT PAINT | SMOOTH SURFACE |
|---|---|---|---|---|---|---|---|
| A | | | | X | | | X |
| B | | | X | X | | | X |
| C | | | X | X | | | X |
| D | | | X | X | | | |
| E | | | | X | | | X |
| F | | | | X | | | X |
| G | | | X | | | | |
| H | | | | | | | |
| I | | | | | | | X |

X denotes unsatisfactory performance

TABLE I - GEOMETRIC CHARACTERISTICS

| | |
|---|---|
| **Fuselage:** | |
| Length, m | 1.27 |
| Diameter, m | .146 |
| **Wing:** | |
| Trapezoidal Planform | |
| Area (including fuselage intercept), $m^2$ | .183 |
| Span, m | 1.344 |
| Aspect ratio | 9.8 |
| Mean aerodynamic chord, m | .146 |
| Root chord, m | .196 |
| Tip chord, m | .078 |
| Sweep 0.25c, deg | 35 |
| Incidence, deg | -1 |
| Dihedral, deg | 5 |
| Area, Leading edge extension (including fuselage intercept), $m^2$ | .10 |
| Area, Trailing edge extension (including fuselage intercept), $m^2$ | .30 |
| Airfoil shape-Supercritical airfoil | |
| Side fuselage: Thickness/chord | .145 |
| Section incidence, deg | 1.0 |
| Planform break: Thickness/chord | .120 |
| Section incidence, deg | -.50 |
| Tip: Thickness/chord | .106 |
| Section incidence, deg | -5.10 |
| **Horizontal Tail:** | |
| Area (including fuselage intercept), $m^2$ | .065 |
| Span, m | .498 |
| Aspect ratio | 3.82 |
| Mean aerodynamic chord, m | .744 |
| Root chord, m | .198 |
| Tip chord, m | .062 |
| Sweep 0.25c, deg | 32.5 |
| Dihedral, deg | 10 |
| Tail arm, m | .467 |
| Tail volume | 1.12 |
| Airfoil shape 10 percent supercritical design lift coefficient | 0.4 |
| Control all moving manually set $\pm 4°$ at 1° increments | |
| **Vertical Tail:** | |
| Area, $m^2$ | .039 |
| Span, m | .254 |
| Aspect ratio | 1.65 |
| Mean aerodynamic chord, m | .166 |
| Root chord, m | .229 |
| Tip chord, m | .080 |
| Sweep 0.25c, deg | 35 |
| Tail arm, m | .461 |
| Tail volume | .67 |
| Airfoil shape 10% supercritical, sym. | |

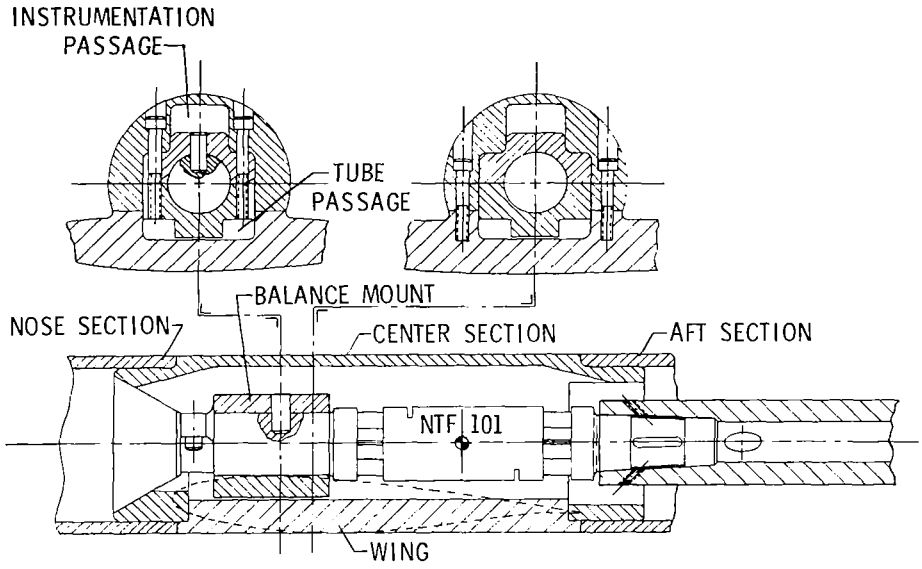


Figure 3.- Pathfinder I model to balance interface.

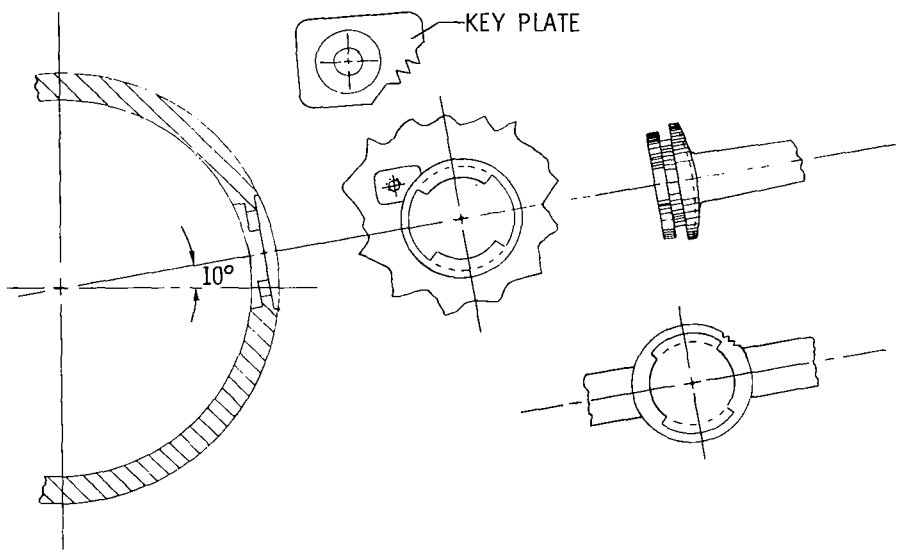


Figure 4.- Pathfinder I horizontal tail connection.

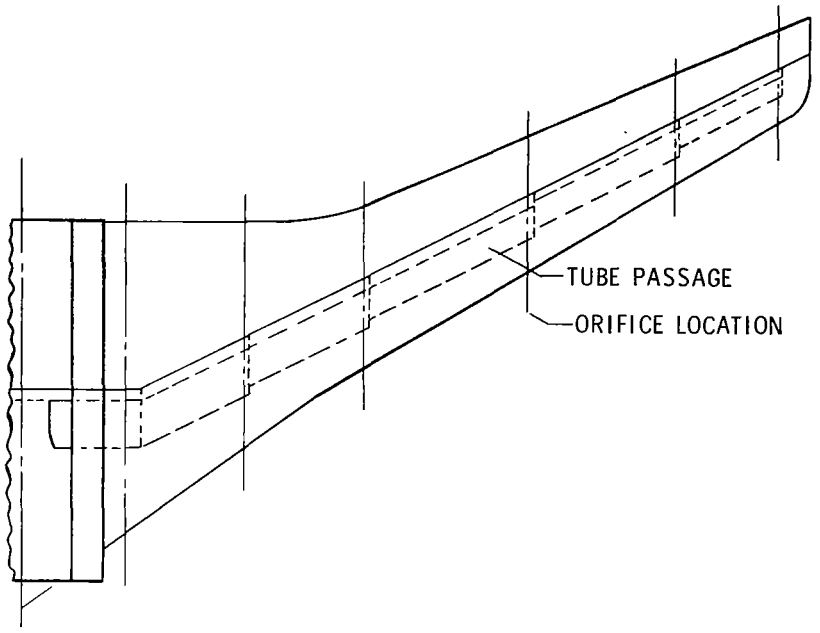


Figure 5.- Pathfinder I wing.

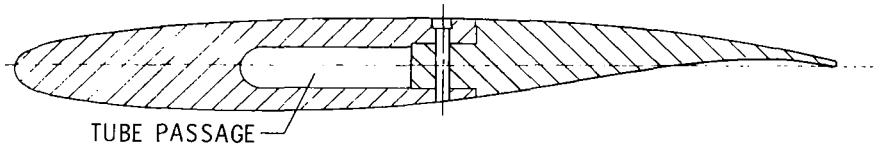


TONGUE AND GROOVE JOINT

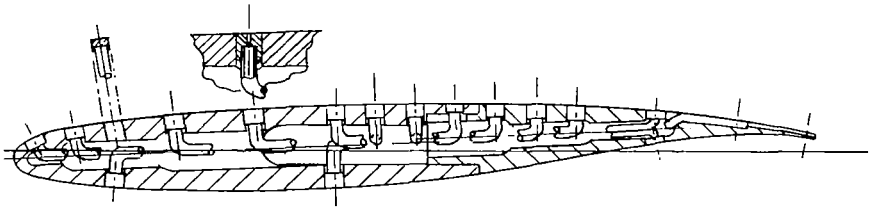

ORIFICE INSTALLATION

Figure 6.- Pathfinder I wing sections.

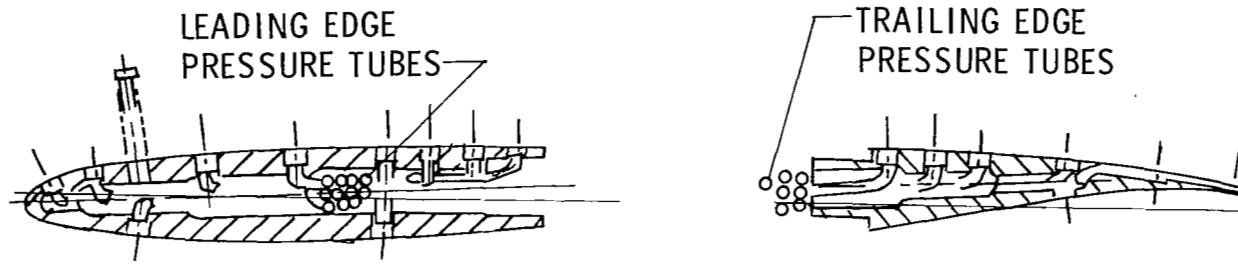


Figure 7.- Pathfinder I wing sections (rough machined and instrumented).

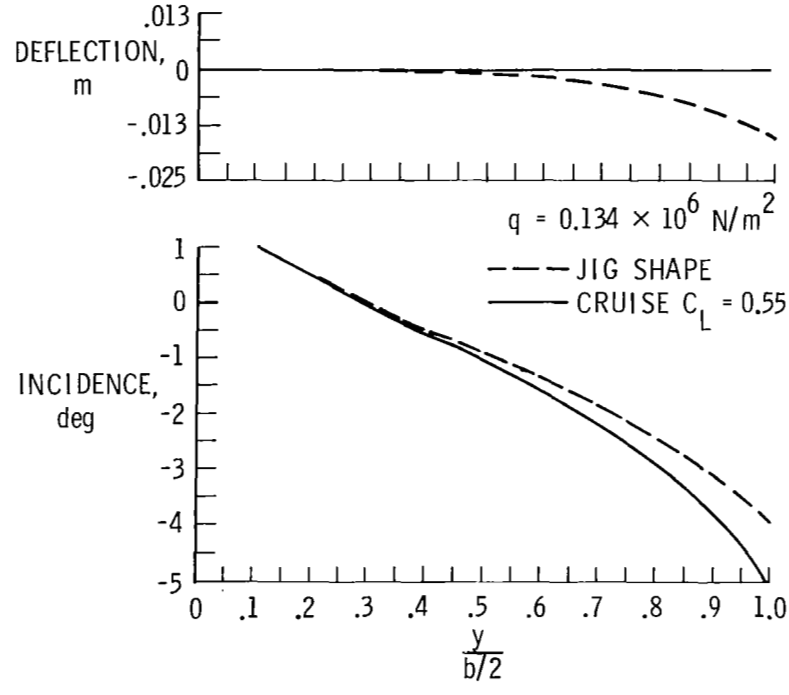


Figure 8.- Pathfinder I wing deflection and incidence, streamwise.

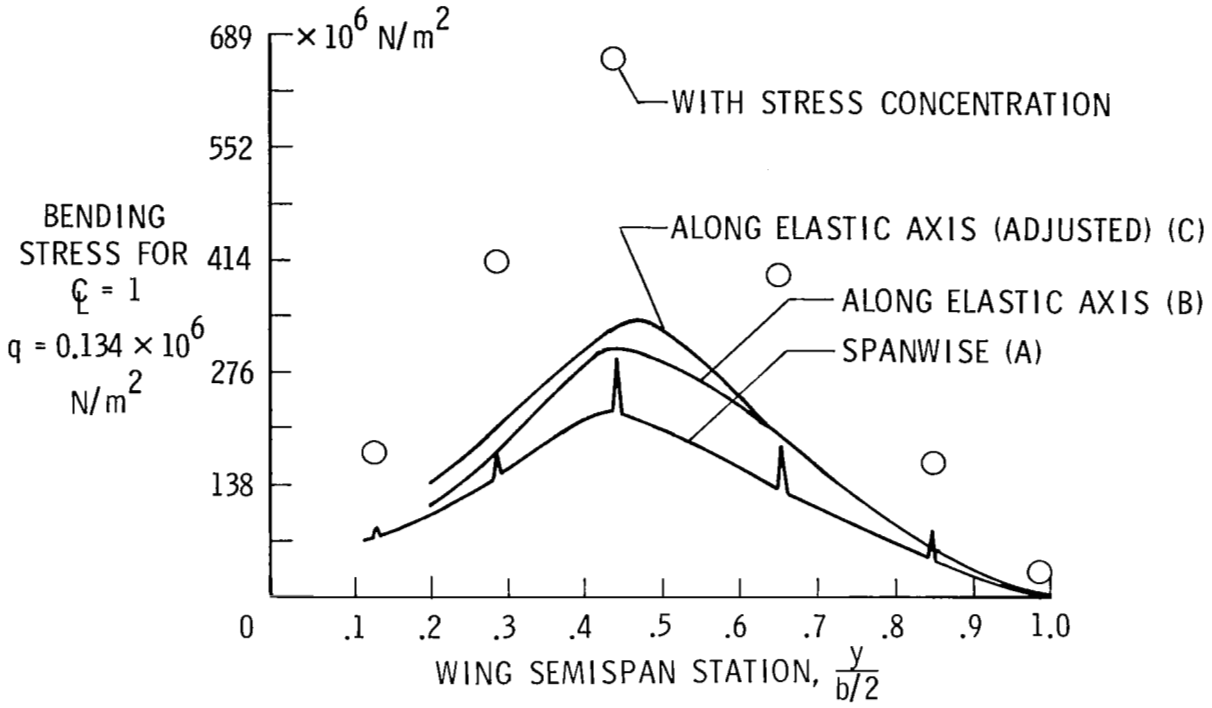


Figure 9.- Pathfinder I model wing stresses.

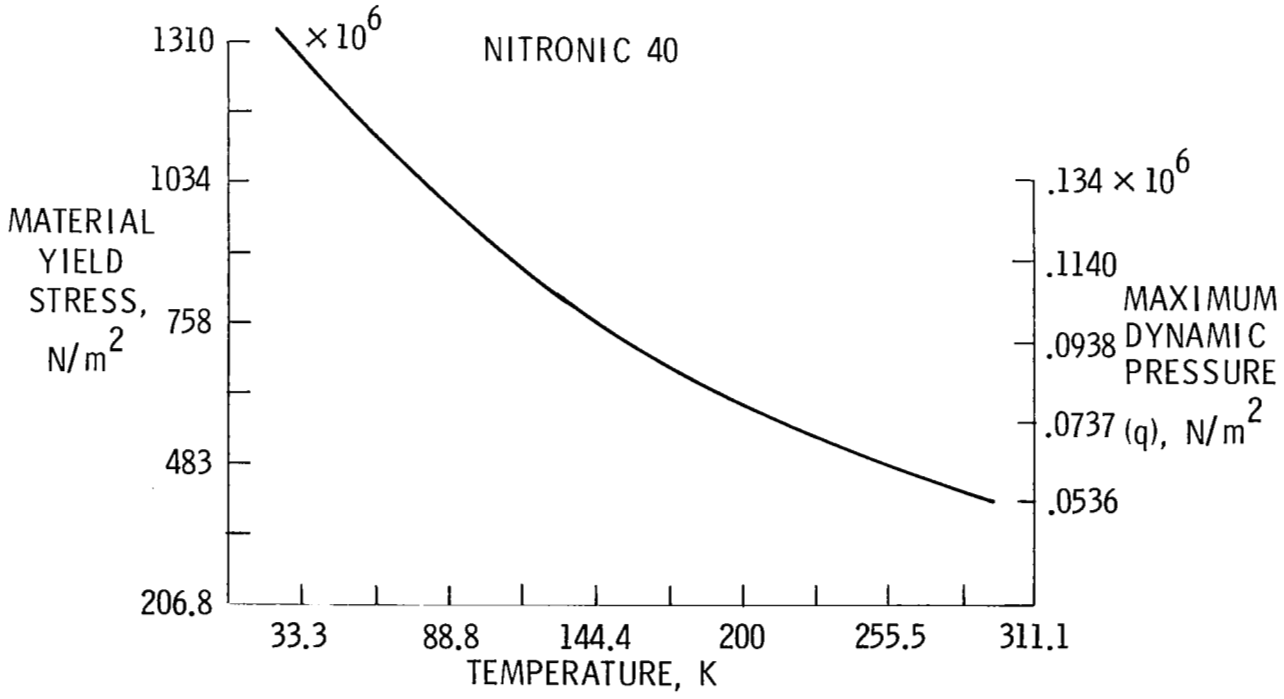


Figure 10.- Pathfinder I model test envelope for $C_L = 1$.

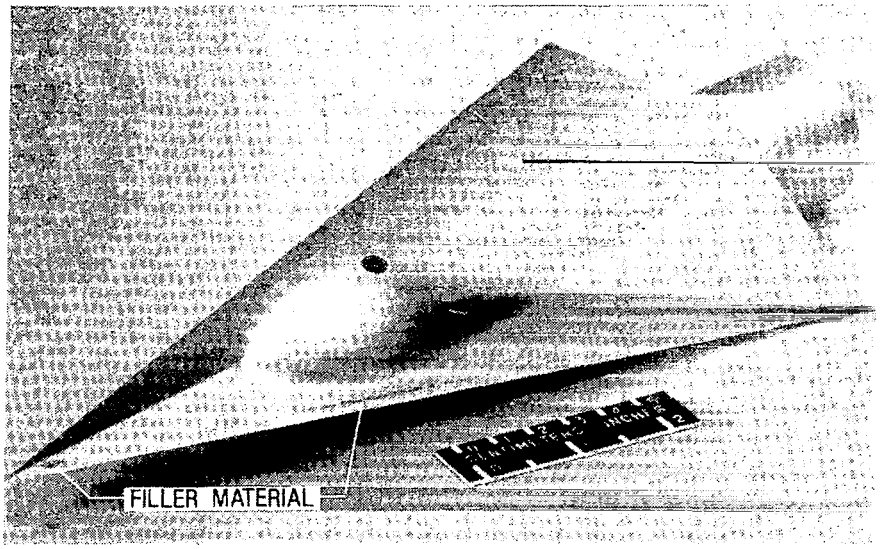


Figure 11.- Langley 0.3-Meter Transonic Cryogenic Tunnel model.

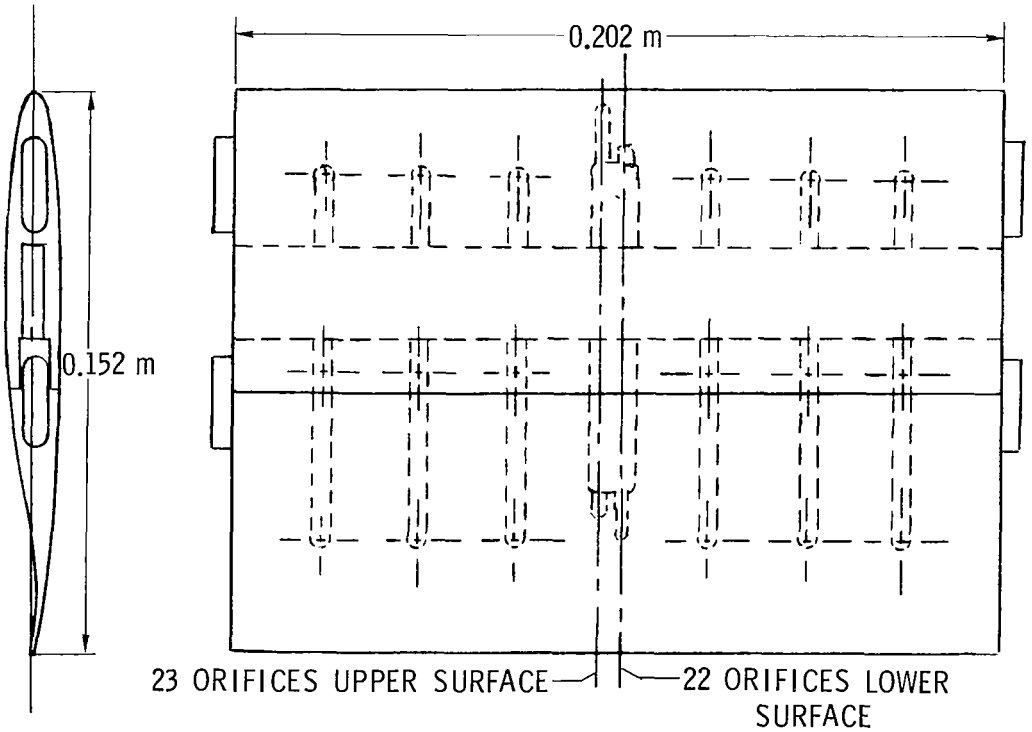


Figure 12.- SC(2)-0510 2-D wing.

# ANALYSIS AND TESTING OF

# MODEL/STING SYSTEMS

William F. Hunter
Langley Research Center

## SUMMARY

The analysis and testing approach for model/sting systems being designed for the National Transonic Facility at Langley Research Center is presented in this paper. Principal areas of analysis are discussed along with the development of mathematical models that are being employed for various analyses. The interrelation and importance of rigorous analysis and verification testing in the design of model/sting systems for cryogenic, high Reynolds Number testing are emphasized. The ongoing analysis and verification testing applications to the design of the first developmental model, Pathfinder I, are described and some preliminary results are given.

## INTRODUCTION

The utilization of the high Reynolds Number test capability provided by the National Transonic Facility (NTF) requires that models/stings be designed and analyzed for operation in a cryogenic environment and in some cases at high dynamic pressures. The combination of high aerodynamic loads and strength limitations on cryogenically acceptable materials will necessitate that model/sting systems be designed to lower safety factors than those which have been used for conventional wind tunnel model/sting systems. This will necessitate that more rigorous, and in some cases highly sophisticated analyses be performed along with math model verification tests. Also, proof testing may be required for critical applications.

This paper outlines the approach that is being used at the Langley Research Center for analyzing the initial developmental models and stings that will be tested in the NTF. Principal aspects of the thermal, stress, deformation, and aeroelastic analyses considerations are presented. Also the development of math models needed to perform the various analyses is discussed along with test activities that are being used to verify the math models. Some results of the current analysis and verification testing applications to the Pathfinder I model are presented.

## ANALYSIS OF NTF MODELS

Because of the cryogenic and possible high dynamic pressure test environment of the NTF, models such as Pathfinder I will require more extensive analyses than conventional wind tunnel models.

### Design By Analysis Approach

In view of material strength limitations, large aerodynamic loads will necessitate that many models for the NTF be designed to small safety factors. To insure that such a design is adequate, various detailed analyses and tests must be performed as the design progresses. This approach is referred to in this paper as Design by Analysis. The designer and the analyst must work closely in developing a suitable design. The flow chart of figure 1 shows how the various analyses and the design process are interrelated. Each element of the analysis process can influence the design.

Thermal Analysis. - The importance of the thermal analysis for NTF models should not be underestimated. Because of the tunnel transients there will be thermal gradients in the various system components and temperature differences between mating parts. These effects must be evaluated since they can lead to high stresses or loose structural joints.

The cryogenic models will be subjected to various thermal transients. First, there is the initial cooldown period. Also, there will be changes in the tunnel test conditions. In order to make alterations to the models, the tunnel has been designed such that the model and a portion of the sting can be isolated from the cryogenic environment. This is done by enclosing the model in a moveable tube-like structure which passes across the test section. Before model changes can be made, the model must be heated. After model changes are made, the model will be subjected almost instantaneously to the cryogenic environment. This thermal shock will probably be the most severe transient for the model.

The effects of these transient conditions on the entire model, balance, and sting system must be examined. This means that several thermal math models may need to be developed in order to determine the time-dependent temperature distributions in the various parts. An evaluation of resulting gradients may show the existence of large thermal stresses. For example, the thermal shock that can occur after a model change will certainly cause a high surface stress on the model.

The effects of thermal gradients and temperature changes on the numerous structural joints in the system must be investigated. Since a loss of joint stiffness could lead to divergence or flutter problems, special attention should be given to the model-to-balance joint and to the balance-to-sting joint. For these and other joints, appreciable preloads may be needed in order to avoid joint looseness. When preloading, consideration should be

given to both the positive and negative temperature swings so as to avoid over-stressing the joint.

For models having a tongue and groove wing design such as Pathfinder I (see reference 1), there is concern that slight temperature differences may develop between the leading and trailing edge portions of the wing. Any tendency for the two parts to contract differently spanwise could cause large shear stresses in the dowels which pass through the tongue and groove joint.

In many cases it is likely that instrumentation packages inside cryogenic models will be heated. Studies are needed to insure that such packages are properly insulated such that the gradient does not create a thermal stress problem.

Also, studies may be needed to determine the time required for the balance to reach thermal equilibrium. The present plans are that the initial NTF models will not be loaded aerodynamically until after thermal equilibrium is obtained within the model. However, the effect of combining the stresses due to aerodynamic loads with thermal stresses caused by a step change in the flow temperature will be examined.

Stress Analysis. - In view of the potentially high aerodynamic loadings and large thermal gradients, a very thorough stress analysis is required for the model and sting system. The stresses in the various components of the system will probably be evaluated using both finite element and strength of material approaches. The thermal stresses will be studied using finite element models except in instances where the geometry and temperature distribution can be represented by a classical Theory of Elasticity problem whose solution is known.

Since many models will be designed with small safety factors, much emphasis must be given to stress concentrations. There are numerous reports and handbooks available for determining stress concentration factors. Also, if necessary, stress concentrations can be evaluated by making detailed finite element models of the highly stressed regions.

For the Pathfinder I model, the highest stress is due to the stress concentration around the orifice plugs in the wings. The orifice plugs are normally circular and this causes a stress concentration factor of three. By designing the plugs to have an elliptical shape with the elongated dimension aligned with the bending stress, the stress concentration factor can be reduced to two or less.

Other sources of stress concentrations are dowels or shear pins such as those incorporated in the Pathfinder I wing. Whenever possible, care should be taken to avoid placement of pins in highly stressed regions. Also, consideration should be given to designing pins to have slight interference fits since this can increase the fatigue life.

Fatigue and Fracture Mechanics Analyses. - After determining the stress levels, the model design should be examined from fatigue and fracture mechanics viewpoints to insure adequate life. Reference 2 discusses the fracture mechanics aspects as well as other factors that influence material selection.

Development of Elastic Math Models. - The aeroelastic and deformation analyses are dependent upon the development of accurate elastic math models of the model and sting system. For the Pathfinder I model, two different types of math models are being used in the analysis: one is a beam representation of the wing and the other is a finite element approach. The math models being used in the analysis of the Pathfinder I model are presented in a subsequent section of this paper.

Verification Testing. - It is important that the elastic math models used in the analyses be verified by testing of the actual hardware. This is especially true if the design is marginal. The math models can be confirmed by performing load/displacement tests, measuring natural frequencies, and by strain gage data. Also, joint effects, which are often unpredictable, can be evaluated by testing. In support of the analysis of the Pathfinder I model, verification tests have been conducted on a supercritical wing which is very similar to the Pathfinder I wing. These tests, along with comparisons of measured and calculated deformations are presented in later sections of this paper.

Aeroelastic Analyses. - The aeroelastic analyses require the development of a math model of the entire model, balance, and sting system. The aeroelastic analyses consist of determining the natural vibration modes, using these modes as displacement functions in the flutter and divergence studies, and performing any needed dynamic response analyses.

It is thought that the flutter analysis, as well as the divergence analysis, must treat the entire system. As might be expected, recent vibration tests at Langley Research Center have shown appreciable differences in the modes and frequencies of the aforementioned supercritical wing mounted on and off of the balance/sting support. These differences reflect the influence of balance/sting flexibility effects on the system modal characteristics. Also, since aeroelastic divergence and flutter are of great concern for models that may be tested at high dynamic pressures in the NTF, the analyses must give particular attention to the stiffness of structural joints.

There are various computer codes available at Langley for performing flutter analyses. A system of programs called FAST for Flutter Analysis System (see reference 3) will be used in the initial studies of the Pathfinder I model. The unsteady aerodynamics programs in FAST are based on the subsonic kernel function lifting-surface theory. In order to adequately treat the unsteady aerodynamics in the transonic regime, it may be necessary to develop additional aerodynamic programs.

Deformation Analysis. - The deformation analysis is essential to the design of highly loaded models. Because of the large deformations, many models will be built with a jig shape such that the model lifting surfaces

will have the proper shape when loaded. Thus, it is necessary to be able to predict accurately the deflections of wings under aerodynamic loads.

### Integrated Computer Program

It is planned that the various elements of the analysis discussed above will eventually be combined into an integrated computer program. Such a program is needed for efficient and systematic evaluation of model/sting systems for the NTF.

## APPLICATIONS TO PATHFINDER I

Although the Pathfinder I analysis is ongoing, results of some of the activities can be reported. These include the development of the beam and the finite element math models, the verification tests, and the stress and deformation analyses.

### Beam Model

It is believed that many high aspect ratio wings such as those of Pathfinder I can be analyzed by treating the wing as a beam. The deformations (bending in two planes, torsion, and extension) are described by twelve first-order differential equations. The static and natural vibration solutions to the equations are obtained using a transfer matrix approach that is based upon Runge-Kutta integration.

The beam approach is a quick and efficient method for calculating stresses, deflections, and frequencies. The solution method easily handles any discontinuities in the cross-sectional properties. Also, the formulation conveniently accommodates displacement dependent loads as well as direct loads.

Load/displacement tests have been conducted on the supercritical test wing mentioned earlier. A comparison of the test results with the calculated deformations (presented in a subsequent section) shows that the beam treatment is a valid approach for high aspect ratio wings.

### Finite Element Models

Two finite element models have been developed for analyzing Pathfinder I. One is a detailed model of the wing by itself and the other is a model of the system.

A SPAR (reference 4) finite element model of the wing is given in figure 2. SPAR is a general purpose finite element computer program for performing structural and thermal analyses. This model is made up of about 600 solid

## Jig Shape

As a result of the beam model verification, the Pathfinder I cruise condition loads ($C_L$ = 0.555 and q = 134,000 $N/m^2$) were applied to determine the jig shape. This data is presented in reference 1.

## CONCLUDING REMARKS

The Design by Analysis Approach being employed at the Langley Research Center for model/sting systems to be tested in the National Transonic Facility has been presented. Analyses and verification testing requirements were discussed along with a description of mathematical models being used for the various analyses. Preliminary results of the analyses and verification testing completed to date for the developmental Pathfinder I model were also presented.

Although the material presented in this paper is somewhat limited in application to date, it is expected that the extension of this work will form the basis for a systematic and integrated approach to the analysis and testing of future model/sting systems that will be designed for high Reynolds Number testing in the National Transonic Facility.

## REFERENCES


1. Bradshaw, James F.; and Lietzke, Donald A.: Pathfinder I Model. Cryogenic Technology, NASA CP-2122, 1980. (Paper 27 of this compilation.)

2. Hudson, C. Michael: Material Selection for the Pathfinder I Model. Cryogenic Technology, NASA CP-2122, 1980. (Paper 29 of this compilation.)

3. Desmarais, Robert N.; and Bennett, Robert M.: User's Guide for a Modular Flutter Analysis Software System (FAST Version 1.0). NASA TM-78720, May 1978.

4. Whetstone, W. D.: SPAR Structural Analysis System Reference Manual. NASA CR-158970-1, December 1978.

5. Young, Clarence P., Jr.: Cryogenic Models/Stings Technology Session. Cryogenic Technology, NASA CP-2122, 1980. (Paper 24 in this compilation.)

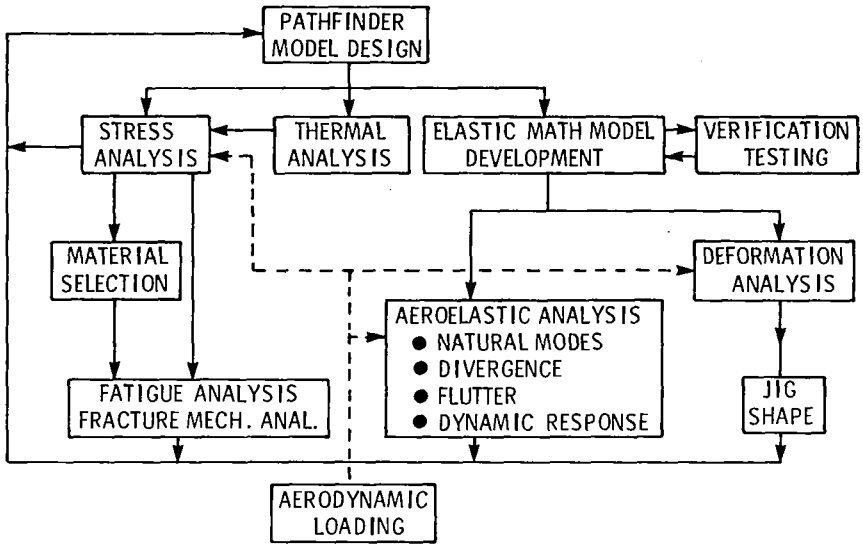


Figure 1.- Design by analysis flow diagram.

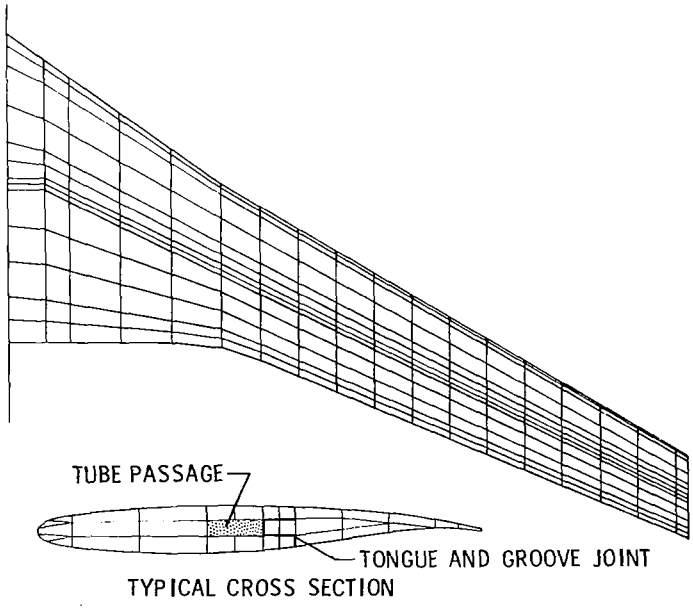


Figure 2.- SPAR finite element model of Pathfinder I wing.

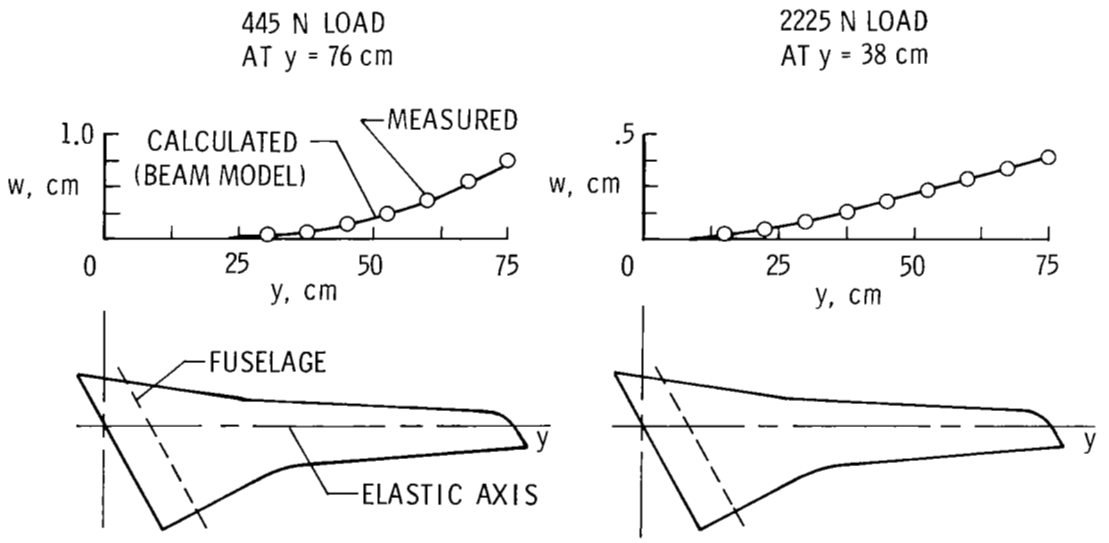


Figure 7.- Bending deformation comparison for supercritical test wing. w is deflection measured normal to wing reference plane.

# MATERIAL SELECTION FOR THE PATHFINDER I MODEL

C. Michael Hudson
Langley Research Center

## SUMMARY

The extremely low wind-stream temperatures (approximately 78 K (140° R)) in the National Transonic Facility (NTF) can significantly reduce the fracture toughness of many of the materials which might be used in constructing wind-tunnel models. Conversely, high fracture toughness is essential for the first model to be tested in the NTF (the so-called Pathfinder I model) because the stresses in the vicinity of structural discontinuities are quite high. These high stresses, if applied to relatively low toughness materials, would result in unacceptably small critical flaw sizes. To preclude the possibility of developing such small critical flaws (which would be difficult to detect), a materials survey was conducted to determine which materials possessed adequate strength and toughness at 78 K (140° R) to be considered for model construction. The Fracture and Deformation Division of the National Bureau of Standards developed a preliminary list of candidate materials. NASA-Langley personnel subsequently expanded this list to include several additional materials.

NASA-Langley personnel further developed a series of factors which governed the selection of the materials for model fabrication. These factors included: strength properties, fracture toughness, availability, corrosion resistance, machinability, cost, and delivery. The weldability of the material was not an important factor for this model since no structural welding will be done.

When the governing factors were applied to the list of candidate materials, Nitronic 40 stainless steel was judged to be the optimum material for fabricating Pathfinder I.

## INTRODUCTION

The extremely low wind-stream temperatures (approximately 78 K (140° R)) in the National Transonic Facility (NTF) can significantly reduce the fracture toughness of many of the materials which might be used in constructing wind-tunnel models. Conversely, high fracture toughness is essential for the first model to be tested in the NTF (the so-called Pathfinder I model) because the stresses in the vicinity of structural discontinuities are quite high. These high stresses, if applied to relatively low toughness materials, would result in unacceptably small critical flaw sizes. To preclude the possibility of developing such small critical flaws (which would be difficult to detect), a materials survey was conducted to identify which materials possessed adequate strength and toughness at 78 K (140° R) to be considered for model construction.

A series of criteria were then developed for selecting the optimum material for model fabrication. These criteria were applied to the materials identified in the survey.

This paper describes the candidate materials, the selection criteria, and the application of the criteria to the candidate materials.

## SYMBOLS

Values in this paper are given in both SI and U.S. Customary Units. The measurements and calculations were made in U.S. Customary Units.

| | |
|---|---|
| $C_{VN}$ | Charpy impact energy for vee-notched specimen |
| E | Young's modulus |
| ELI | extra low interstitials |
| $K_c$ | stress intensity factor at which unstable crack growth begins |
| $K_I$ | opening mode stress intensity factor |
| $K_{Ic}$ | plane strain fracture toughness |
| RT | room temperature |
| r | distance from the tip of a crack to the point at which stress is being calculated |
| S | applied, uniformly distributed stress |
| $\delta$ | angle between crack axis and r |
| $\sigma_u$ | ultimate tensile strength |
| $\sigma_x$ | stress in the long transverse direction |
| $\sigma_y$ | stress in the longitudinal direction |
| $\sigma_{yp}$ | yield strength (0.2% offset) |
| $\tau_{xy}$ | shear stress |

## SELECTION CRITERIA

The material selection criteria for the Pathfinder I model fell into primary and secondary categories. The primary criteria included the tensile

properties, fracture toughness and availability of the material. The secondary criteria included corrosion resistance, machinability, cost, and delivery. For this model, weldability was not an important factor since no structural welding will be permitted. The model design group invoked this prohibition because of the high stresses in the model, and the possibility of introducing defects during the welding process. A detailed discussion of the primary and secondary criteria follows.

## Primary Criteria

Tensile strength - A minimum tensile yield strength of nominally 1.03 GPa (150 ksi) at 78 K (140° R) was established for the Pathfinder I. This yield strength would yield a factor of safety of 1.5 on the peak stress in the model.

Fracture toughness - Fracture mechanics concepts were used in evaluating candidate materials for the Pathfinder I model. These concepts are reviewed briefly in the following paragraphs.

Irwin (ref. 1), among others, developed the stress solution for a transverse crack in an infinitely wide plate loaded in tension. This solution showed that the stresses near the tip of a crack were given by:

$$\sigma_y = \frac{K_I}{\sqrt{2\pi r}} \cos\frac{\delta}{2}\left[1 + \sin\frac{\delta}{2}\sin\frac{3\delta}{2}\right] \quad (1)$$

$$\sigma_x = \frac{K_I}{\sqrt{2\pi r}} \cos\frac{\delta}{2}\left[1 - \sin\frac{\delta}{2}\sin\frac{3\delta}{2}\right] \quad (2)$$

$$\tau_{xy} = \frac{K_I}{\sqrt{2\pi r}} \sin\frac{\delta}{2}\cos\frac{\delta}{2}\cos\frac{3\delta}{2} \quad (3)$$

where $\sigma_y$ is the stress in the longitudinal direction (see figure 1), $\sigma_x$ is the stress in the long transverse direction, $\tau_{xy}$ is the shear stress, $r$ is the distance from the tip of the crack to the point at which the stress is being calculated, $\delta$ is the angle between the crack axis and $r$, and $K_I$ is the stress intensity factor. This stress intensity factor is a local stress parameter which reflects the intensity of the stress at all points surrounding the tip of the crack.

The value of $K_I$ at which unstable crack growth begins is called the critical stress intensity factor $K_c$. The value of $K_c$ for a given material and temperature will vary with the stress state in the vicinity of the crack tip. The minimum value of $K_c$ occurs in a plane-strain stress state, and is referred to as the plane-strain fracture toughness of the material, $K_{Ic}$.

The plane-strain fracture toughness was one of the major criteria established for accepting materials for the Pathfinder I model. The nominal minimum value of $K_{Ic}$ considered acceptable for this model was 93.5 MPa-$m^{1/2}$ (85 ksi-$in^{1/2}$) at 78 K (140° R). This value would provide a conservative critical flaw size of approximately 6.4 mm (0.25 inch) at highly stressed regions of the model. Regular nondestructive examination of the model will identify flaws long before they approach this size.

The schedule for selecting the material for Pathfinder I did not permit a prolonged experimental program. Consequently, two approaches were adopted for screening potential model materials. These approaches are described as follows:

1. The technical literature was surveyed for fracture toughness data on candidate materials. An adequate quantity of data was located for most of the materials. These data were generated using either the procedures in reference 2 or reference 3.

2. The technical literature was also reviewed for Charpy impact data on candidate materials. Charpy impact energies, $C_{VN}$, are an indirect measure of material toughness. In fact, empirical relationships have been proposed which relate plane-strain fracture toughness and Charpy impact energies. Reference 4 proposes the following relationship between $K_{Ic}$ and $C_{VN}$

$$K_{Ic} = \left[ 2E \, (C_{VN})^{3/2} \right]^{1/2} \qquad (4)$$

for steels in the transition-temperature region. (The term E in equation (4) is Young's modulus.) Substituting values of 93.5 MPa-$m^{1/2}$ and 200 GPa (85 ksi-$in^{1/2}$ and 29 x $10^6$ psi) for $C_{VN}$ and E, respectively, one obtains a value of nominally 33.9 J (25 ft-lbs) as an acceptable Charpy impact energy at 78 K (140° R). Because Charpy impact specimens can be fabricated and tested quickly, a number of Charpy impact tests were conducted to supplement the data found in the literature.

Availability - Figure 2 shows side and front views of the proposed Pathfinder I model. Inspection of this figure shows (1) a fuselage length and diameter of 1.27 m and 146 mm (50 in. and 5.75 in.), respectively, and (2) a wing span of 1.345 m (52.97 in.). Discussions within the model design group indicated the optimum material blanks for the model components are (1) a 152 mm (6 in.) diameter bar approximately 1.8 m (6 ft.) long for the fuselage and (2) a 114 mm thick by 610 mm wide by 1.5 m long ( 4 1/2 in. thick by 24 in. wide by 60 in. long) plate for the wings and empennage. Thus, the material for model fabrication had to be available in these section sizes in order to be considered for use.

## Secondary Criteria

The secondary criteria included corrosion resistance, machinability, cost and delivery. The model design group set no specific guidelines for these

criteria. Consequently, the materials were compared to one another when using these criteria.

## MATERIALS EVALUATION BASED ON PRIMARY CRITERIA

Initially, the Fracture and Deformation Division of the National Bureau of Standards (under contract to NASA-Langley) searched the technical literature and developed a list of candidate materials for the Pathfinder I model. Reference 5 presents the results of this search. NASA-Langley personnel subsequently expanded this list to include several additional materials. Table I presents this expanded list of materials along with their nominal tensile, Charpy impact and fracture toughness properties. Except for the special 9% Ni and AF 1410 steels, and the PH 13-8 Mo stainless steel listed in Table I, the technical literature provided the Charpy impact energies for the candidate materials. In-house tests provided the Charpy energies for the AF 1410 and PH 13-8 Mo materials, and mill test reports provided these energies for the special 9% Ni steel.

The literature search failed to locate any fracture toughness data for some materials listed in Table I, e.g., Invar and PH 13-8 Mo. In-house tests to provide the missing data would have been quite expensive and time consuming. Consequently, the decision was made to rely on Charpy impact energies as the indicator of these materials' toughness.

A number of suppliers were queried in studying the availability of the various materials. However, all possible suppliers could not be located and queried. In that context, the following discussion on availability should be considered an indication, not an absolute determination, of the availability of the rod and plate required for Pathfinder I.

The following paragraphs present an evaluation of each material in Table I using the primary selection criteria as the evaluating guideline.

### 18 Ni, 250 Grade Steel

This material meets the yield strength criterion ($\sigma_{yp} \geq 1.03$ GPa at 78 K (150 ksi at 140$^{o}$ R)) for the model.

Its Charpy impact energy and fracture toughness nominally meet the model toughness criteria (i.e., 33.9 J and 93.5 MPa-m$^{1/2}$ (25 ft-lb and 85 ksi-in$^{1/2}$)), respectively, at RT. However, both the Charpy impact energy and the fracture toughness are below the Pathfinder I toughness criteria at 78 K (140$^{o}$ R).

A source of the bar material required for the Pathfinder I was located. However, no source for the required plate material was.

Because the material did not meet the model toughness criteria and could not be located in the required plate section, it was dropped from further consideration.

## 18 Ni, 200 Grade Steel

This material meets the yield strength criterion for the model.

Its Charpy impact energies and fracture toughness nominally meet the model toughness criteria at both RT and 78 K (140° R).

No source for the required bar and plate material was located.

Because the material could not be located in the required bar and plate sections, it was dropped from further consideration.

## AF 1410 Steel

This material meets the yield strength criterion for the model.

Its Charpy impact energies meet the model toughness criteria at both RT and 78 K (140° R). Its fracture toughness meets the toughness criterion at RT. No fracture toughness data were located for 78 K (140° R). However, based on the high Charpy impact energy at 78 K (140° R) the fracture toughness at 78 K (140° R) is probably adequate.

A source of the required bar and plate material was located.

Because this material meets all of the primary selection criteria, it is judged acceptable for model fabrication.

## Special 9% Ni Steel

This material nominally meets the yield strength criterion for the model.

Its Charpy impact energy and fracture toughness meet the model toughness criteria at 78 K (140° R). No data were located on these two toughness properties at RT. This alloy was especially developed for the National Transonic Facility's fan disc. (See reference 6.) It has the same nominal chemical composition as ASTM A553 Type 1 steel. However, the chemical composition of this 9% Ni steel is more closely controlled. Table II presents a comparison of the specified chemical compositions of these two alloys. The heat treatment procedures are also different for the two alloys.

A source of the required bar and plate material was located.

Because this material meets all of the primary selection criteria, it is judged acceptable for model fabrication.

## A286 Stainless Steel

This material does not meet the yield strength criterion for the model.

Its Charpy impact energies and fracture toughnesses do meet the model toughness criteria at RT and 78 K ($140^{o}$ R).

No source for the required plate material was located.

Because this material did not meet the model yield strength criterion and could not be located in the required plate section, it was dropped from further consideration.

## Nitronic 40 Stainless Steel

This material meets the yield strength criterion for the model.

Its Charpy impact energies meet the Pathfinder I toughness criterion at RT and 78 K ($140^{o}$ R). Its fracture toughness meets the model toughness criterion at 78 K ($140^{o}$ R). No RT fracture toughness data were located.

A source for the required bar and plate material was located.

Because this material meets all of the primary selection criteria, it is judged acceptable for model fabrication.

## PH 13-8 Mo H1150M Stainless Steel

This material nominally meets the yield strength criterion for the model.

Its Charpy impact energies meet the model criterion at both RT and 78 K ($140^{o}$ R). The survey of the technical literature located no fracture toughness data on this material.

A source for the required bar and plate material was located.

Because this material meets all of the primary selection criteria, it is judged acceptable for model fabrication.

## Invar

This material does not meet the yield strength criterion for the model.

Its Charpy impact energies meet the model criterion at both RT and 78 K ($140^{o}$ R). The survey of the technical literature located no fracture toughness data on this material.

A source of the required bar material was located, however, no source of the required plate was.

Because this material did not meet the model yield strength criterion and could not be located in the required plate section, it was dropped from further consideration.

## Inconel 718

This material meets the yield strength criterion for the model.

Its Charpy impact energies at both RT and 78 K ($140^{o}$ R) were slightly below the model criterion. Its fracture toughnesses were slightly above the Pathfinder I criterion at RT and 78 K ($140^{o}$ R).

A source of the required bar and plate material was located.

Because this material meets the yield strength, fracture toughness and availability criteria for the model and closely approached the Charpy impact criterion, it is judged acceptable for model fabrication.

## Inconel X750

This material does not meet the yield strength criterion (by nominally 172 MPa (25 ksi)) for the model.

Its Charpy impact energies meet the model criterion at RT and 78 K ($140^{o}$ R). Its fracture toughness meets the model criterion at 78 K ($140^{o}$ R). The literature search located no fracture toughness data for RT.

A source of the required bar and plate material was located.

Because this material meets the fracture toughness, Charpy impact and availability criteria for the model, the judgement was made to evaluate this material using the secondary criteria. This evaluation was made while keeping in mind that the nominal yield strength fell 172 MPa (25 ksi) below the yield strength criterion.

## Ti-6A1-4V ELI

This material meets the yield strength criterion for the model.

Its Charpy impact energy and fracture toughness do not meet the model criteria at 78 K ($140^{o}$ R).

A source of the required bar and plate material was located.

Because this material does not meet the Charpy impact and fracture toughness criteria for the model, it was dropped from further consideration.

## Ti-5A1-2.5Sn ELI

This material meets the yield strength criterion for the model.

Its Charpy impact energies meet the model criterion at RT but not at 78 K ($140^{o}$ R). Its fracture toughnesses also meet the criterion at RT but not at 78 K ($140^{o}$ R).

A source of the required bar and plate material was located.

Because this material does not meet the Charpy impact and fracture toughness criteria for the model, it was dropped from further consideration.

## MATERIALS EVALUATION BASED ON SECONDARY CRITERIA

As indicated in the foregoing section of this paper, six materials exhibited potential for use in model fabrication. (These materials were AF 1410 and 9% Ni steel, Nitronic 40 and PH 13-8 Mo (H 1150M) stainless steels, and Inconel 718 and possibly Inconel X750 nickel base alloys.) These six materials were subsequently evaluated using the secondary criteria, i.e., machinability, corrosion resistance, cost and delivery. Table III presents NASA-Langley's experience in machining the materials under consideration. The information listed in Table III is based on the experience of both NASA-Langley's in-house machine shops and several contractors who have built models for NASA-Langley.

Table IV presents information on the corrosion resistance, cost (per kg (lb)) and delivery of the six materials. A discussion of these secondary selection criteria follows. (In reading this discussion, the reader should bear in mind that the information presented is applicable for the fall of 1979.)

## Discussion

The relative humidity in the Hampton Roads area is frequently quite high. If a cooled model is exposed to this high humidity environment during, say, a model change, significant quantities of water can be expected to condense on the model surfaces. This water, if left in place for any significant amount of time, could corrode these surfaces. To minimize the possibility of corrosion damage, the model design group decided that the Pathfinder I model should be fabricated from an intrinsically corrosion resistant material. This decision eliminated the AF 1410 and 9% Ni steels from further consideration.

Table II indicates none of the four remaining materials are easy to machine. Consequently, machinability, which is a significant factor, could not be used to screen materials for the model.

Cost and delivery thus became the deciding factors in making the final selection among the four remaining materials. Table IV indicates the cost of Nitronic 40 stainless steel is nominally \$3/pound compared to nominally \$5-6/pound for the three remaining materials. Further, the delivery time for Nitronic 40 is nominally 3 months compared to nominally 5-6 months for the three remaining materials. Based on its lower cost and shorter delivery time, Nitronic 40 was selected as the model fabrication material.

## CONCLUDING REMARKS

The Fracture and Deformation Division of the National Bureau of Standards developed a preliminary list of candidate materials for fabricating the first model to be tested in the National Transonic Facility (NTF). NASA-Langley personnel subsequently expanded this list to include several additional materials.

NASA-Langley personnel further developed a series of factors which governed the material selection process for Pathfinder I. These factors included: strength properties, fracture toughness, availability, corrosion resistance, machinability, cost and delivery. The weldability of the material was not an important factor for this model since no structural welding will be done.

When the governing factors were applied to the list of candidate materials, Nitronic 40 stainless steel was judged to be the optimum material for fabricating the first model to go into the NTF.

## REFERENCES


1. Irwin, G. R.: Analysis of Stresses and Strains Near the End of a Crack Traversing a Plate. Trans. ASME, Volume 79, 1957, pp. 361-364.

2. Anon.: Standard Method of Test for Plane-Strain Fracture Toughness of Metallic Materials, ASTM Designation: E399-74, ASTM 1974 Annual Book of ASTM Standards, 1974, pp. 432-457.

3. Landes, J. D. and Begely, J. A.: Test Results from J-Tntegral Fracture Studies: An Attempt to Establish a $J_{Ic}$ Testing Procedure, Fracture Analysis, ASTM STP 560, 1974, pp. 170-186.

4. Barsom, J. M. and Rolfe, S. T.: Correlations Between $K_{Ic}$ and Charpy V-Notch Test Results in the Transition-Temperature Range. Impact Testing of Metals, ASTM STP 466 1970, pp. 281-302.

5. Tobler, R. L.: Materials Studies for Cryogenic Wind Tunnel Testing, National Bureau of Standards Report IR 79-1624, Boulder, CO, 1979.

6. Wingate, Robert T.: Design of Compressor Fan Disks for Large Cryogenic Wind Tunnels. Cryogenic Technology, NASA CP-2122, 1980. (Paper 9 of this compilation.)

TABLE II. COMPARISON OF SPECIFIED CHEMICAL COMPOSITIONS OF THE SPECIAL 9% Ni STEEL UNDER CONSIDERATION AND OF A553 TYPE 1 STEEL

| STEEL | ELEMENT, WEIGHT PERCENT | | | | | | | |
|---|---|---|---|---|---|---|---|---|
| | C | Si | Mn | P | S | Ni | Mo | Al |
| SPECIAL 9% Ni | 0.06 TO 0.12 | 0.05 TO 0.15 | 0.75 MAX | 0.015 MAX | 0.015 MAX | 8.50 TO 9.50 | 0.10 TO 0.20 | 0.050 MAX |
| A553 TYPE 1 | 0.13 MAX | 0.15 TO 0.30 | 0.90 MAX | 0.035 MAX | 0.040 MAX | 8.50 TO 9.50 | -- | -- |

TABLE III. NASA-LANGLEY EXPERIENCE WITH CANDIDATE MATERIALS FOR THE PATHFINDER MODEL

| MATERIAL | CONDITION | MACHINABILITY |
|---|---|---|
| AF 1410 STEEL | DOUBLE AUSTENITIZED AND AGED | 1. MACHINES WITH GREAT DIFFICULTY AFTER HEAT TREATMENT.<br>2. POSSESS LITTLE EXPERIENCE WITH THIS MATERIAL. |
| SPECIAL 9% Ni STEEL | NORMALIZED & TEMPERED<br>QUENCHED & TEMPERED<br>STRESS RELIEVED | POSSESS NO EXPERIENCE |
| NITRONIC 40 STAINLESS STEEL | ANNEALED | 1. MACHINES SIMILAR TO OTHER AUSTENITIC STAINLESS STEELS.<br>2. DEVELOPING EXPERIENCE IN MACHINING. |
| PH 13-8 Mo STAINLESS STEEL | H1150M | 1. ROUGH MACHINES SLOWLY IN CONDITION A WITH CONVENTIONAL TOOLING (LEAVE MODEL OVERSIZE BEFORE HEAT TREATMENT).<br>2. MAY WARP SLIGHTLY DURING HEAT TREATMENT.<br>3. DOES NOT WARP DURING MACHINING.<br>4. REQUIRES EXPENSIVE TOOLING (COBALT OR TUNGSTEN CARBIDE) AFTER HEAT TREATMENT. WEARS DOWN EVEN THIS EXPENSIVE TOOLING. |
| INCONEL 718 | SOLUTION TREATED AND AGED | 1. MACHINES WITH GREAT DIFFICULTY BECAUSE IT WORK HARDENS RAPIDLY.<br>2. MACHINES AT VERY SLOW SURFACE SPEEDS.<br>3. DISCOURAGES ACCURATE DRILLING OF DEEP HOLES. |
| INCONEL X750 | SOLUTION TREATED AND AGED | 1. MACHINES SAME AS INCONEL 718.<br>2. SURFACE IS VERY EASILY SCRATCHED. |

TABLE IV. DELIVERY, COST, AND CORROSION RESISTANCE OF AVAILABLE, ACCEPTABLE MATERIALS FOR PATHFINDER I

| MATERIALS | NOMINAL DELIVERY, MONTHS | NOMINAL COST | | CORROSION RESISTANCE |
|---|---|---|---|---|
| | | $/kg | $/lb | |
| AF 1410 | 4 - 5 | 20 | 9 | COULD CORRODE |
| SPECIAL 9% Ni | 4 | 9 | 4 | COULD CORRODE |
| NITRONIC 40 | 3 | 7 | 3 | CORROSION RESISTANT |
| PH 13-8 Mo | 8 - 9 | 11 | 5 | CORROSION RESISTANT |
| INCONEL 718 | 5 - 6 | 13 | 6 | CORROSION RESISTANT |
| INCONEL X750 | 5 - 6 | 11 | 5 | CORROSION RESISTANT |

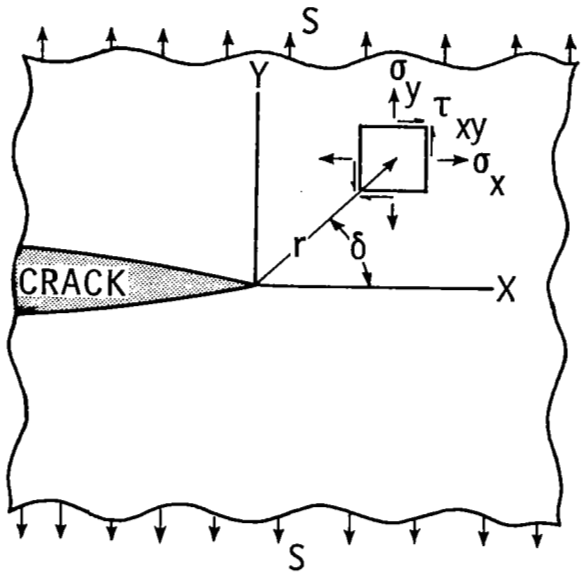


Figure 1.- Stress characterization in the vicinity of a crack tip.

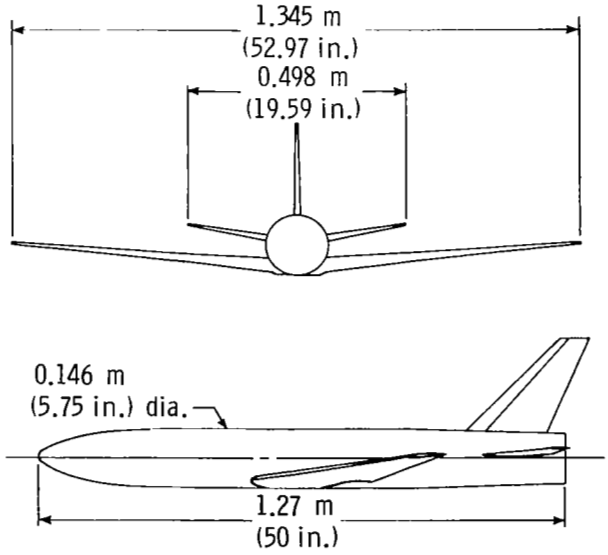


Figure 2.- Front and side views of the Pathfinder I model.

| 1. Report No. | 2. Government Accession No. | 3. Recipient's Catalog No. |
|---|---|---|
| NASA CP-2122, Part II | | |

| 4. Title and Subtitle | 5. Report Date |
|---|---|
| CRYOGENIC TECHNOLOGY | March 1980 |
| | 6. Performing Organization Code |
| 7. Author(s) | 8. Performing Organization Report No. L-13547 |
| | 10. Work Unit No. 505-31-53-01 |
| 9. Performing Organization Name and Address<br>NASA Langley Research Center<br>Hampton, VA 23665 | 11. Contract or Grant No. |
| | 13. Type of Report and Period Covered<br>Conference Publication |
| 12. Sponsoring Agency Name and Address<br>National Aeronautics and Space Administration<br>Washington, DC 20546 | 14. Sponsoring Agency Code |

15. Supplementary Notes

16. Abstract

The proceedings of the NASA Conference, Cryogenic Technology, held at the Langley Research Center on November 27-29, 1979, are reported in this NASA conference proceedings. The proceedings contain 29 papers which address different engineering problems associated with the design of mechanisms and systems to operate in a cryogenic environment. The focal point for entire engineering effort was the design of the National Transonic Facility, which is a closed-circuit cryogenic wind tunnel. The papers covered a variety of subjects including thermal structures insulation systems, noise, seals, controls, instrumentation, and materials. Papers also addressed design, fabrication, and instrumentation problems for models to be tested in a cryogenic medium.

| 17. Key Words (Suggested by Author(s)) | 18. Distribution Statement |
|---|---|
| Cryogenic technology<br>Cryogenic wind tunnel<br>Cryogenic seals<br>Cryogenic insulation<br>Cryogenic wind-tunnel models | FEDD Distribution<br>Subject Category 31 |

| 19. Security Classif. (of this report) | 20. Security Classif. (of this page) | 21. No. of Pages | 22. Price* |
|---|---|---|---|
| Unclassified | Unclassified | 169 | $8.00 |



NASA-Langley, 1980

National Aeronautics and Space Administration

Washington, D.C.
20546

Official Business
Penalty for Private Use, $300

SPECIAL FOURTH CLASS MAIL
BOOK

Postage and Fees Paid
National Aeronautics and
Space Administration
NASA-451


NASA

POSTMASTER: If Undeliverable (Section 158 Postal Manual) Do Not Return